

Frequency-based decay electron spectroscopy to probe the neutrino mass scale and chirality-flipping interactions

Martin Fertl

Physics of Fundamental Symmetries and Interactions 2016



Outline

- Neutrino mass
- The tritium endpoint measurement scheme
- Project 8: A frequency based neutrino mass measurement
- ${}^6\text{He}$ decay: CRES using highly relativistic electrons!?
- Summary

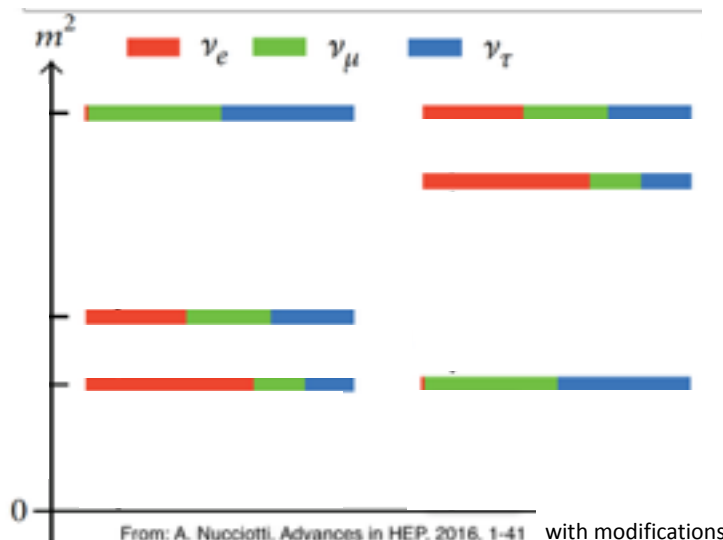
Non-zero, but small neutrino masses



From oscillation experiments:
normal hierarchy inverted hierarchy

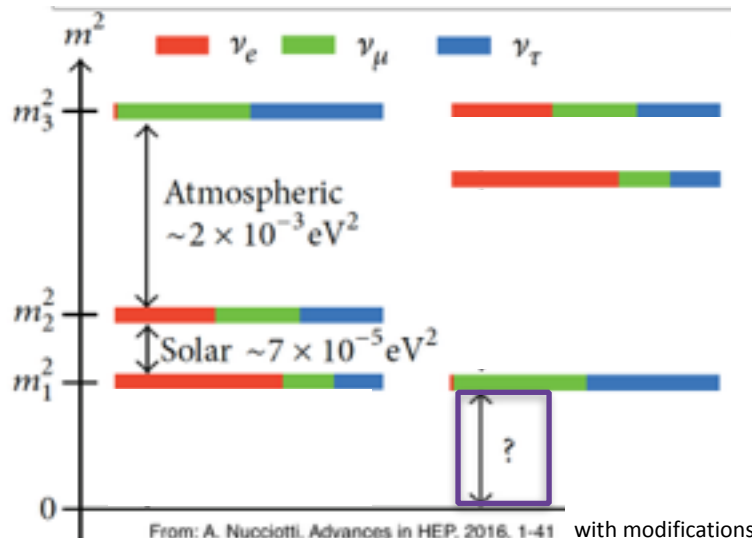
Non-zero, but small neutrino masses

From oscillation experiments:
normal hierarchy inverted hierarchy



Non-zero, but small neutrino masses

From oscillation experiments:
normal hierarchy inverted hierarchy



LARGE mixing angles

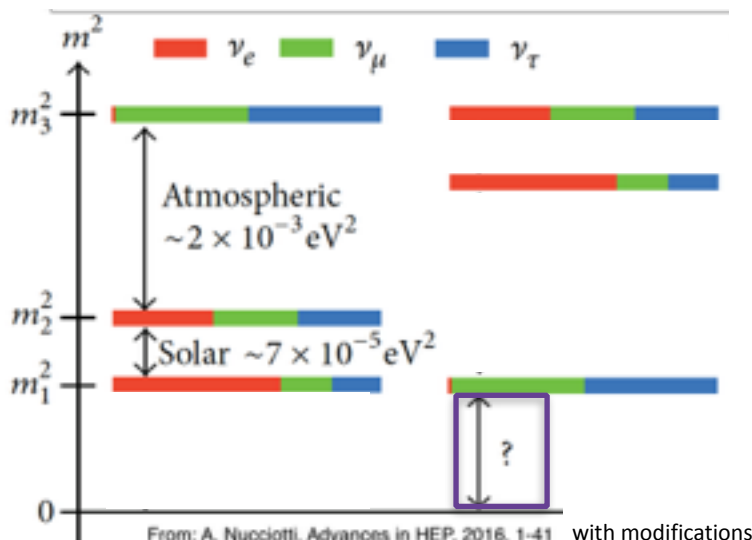
TINY mass differences

NH or IH? → G. Brunetti, Tue 4:20 pm

No absolute mass scale sensitivity!

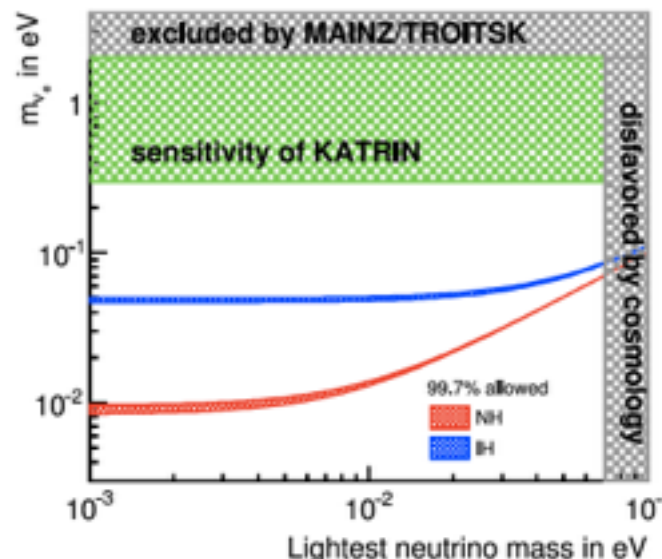
Non-zero, but small neutrino masses

From oscillation experiments:
normal hierarchy inverted hierarchy



From: A. Nucciotti, Advances in HEP, 2016, 1-41 with modifications

From tritium decay and cosmology:



Qian and Vogel, Progress in Particle
And Nuclear Physics 83 (2015), 1-30

LARGE mixing angles

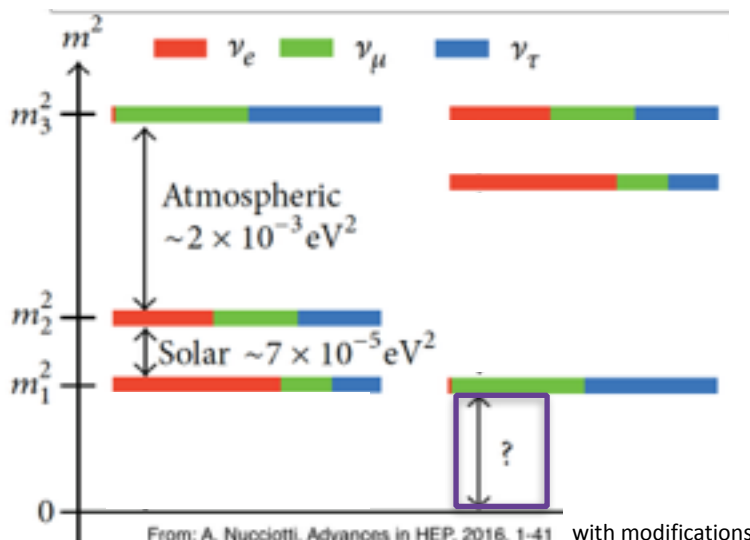
TINY mass differences

NH or IH? → G. Brunetti, Tue 4:20 pm

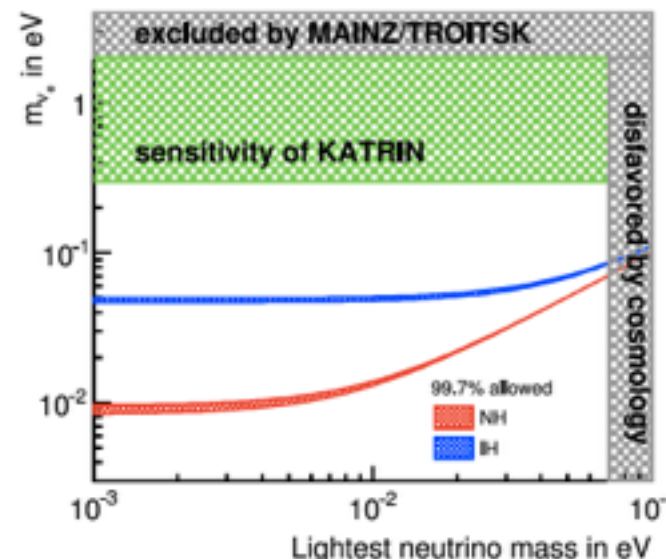
No absolute mass scale sensitivity!

Non-zero, but small neutrino masses

From oscillation experiments:
normal hierarchy inverted hierarchy



From tritium decay and cosmology:



Qian and Vogel, Progress in Particle
And Nuclear Physics 83 (2015), 1-30

LARGE mixing angles

TINY mass differences

NH or IH? → G. Brunetti, Tue 4:20 pm

No absolute mass scale sensitivity!

KATRIN exp. probes degenerate mass region!

Now disfavored by cosmology.

Direct limits $m(\nu_e) < 2 \text{ eV}/c^2$

Goal: Probe the complete IH allowed region!

The β^- -spectrum of tritium decay

PHYSIQUE NUCLÉAIRE. — Possibilité d'émission de particules neutres de masse intrinsèque nulle dans les radioactivités β . Note de M. FRANCIS Perrin, présenté par M. Jean Perrin.

SÉANCE DU 18 DÉCEMBRE 1933.



Versuch einer Theorie der β -Strahlen. I^{1).}

Von E. Fermi in Rom.

Mit 3 Abbildungen. (Eingegangen am 16. Januar 1934.)

Zeitschrift für Physik, Vol. 88, p. 161

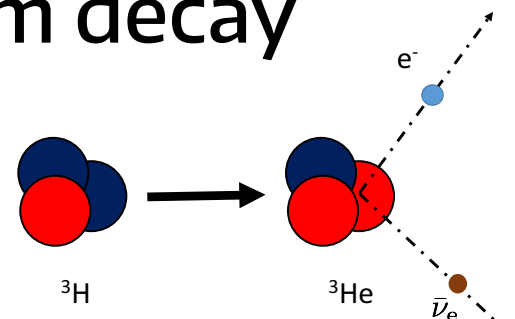
The β^- -spectrum of tritium decay

PHYSIQUE NUCLÉAIRE. — Possibilité d'émission de particules neutres de masse intrinsèque nulle dans les radioactivités β . Note de M. FRANCIS Perrin, présenté par M. Jean Perrin.

SÉANCE DU 18 DÉCEMBRE 1933.



The simple picture:



Versuch einer Theorie der β -Strahlen. I¹⁾.

Von E. Fermi in Rom.

Mit 3 Abbildungen. (Eingegangen am 16. Januar 1934.)

Zeitschrift für Physik, Vol. 88, p. 161

The β^- -spectrum of tritium decay

PHYSIQUE NUCLÉAIRE. — Possibilité d'émission de particules neutres de masse intrinsèque nulle dans les radioactivités β . Note de M. FRANCIS Perrin, présenté par M. Jean Perrin.

SÉANCE DU 18 DÉCEMBRE 1933.

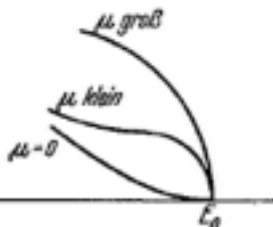


Fig. 1.

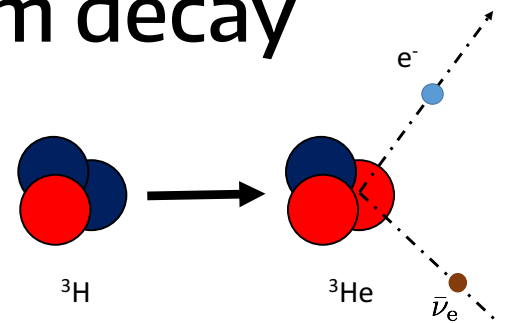
Versuch einer Theorie der β -Strahlen. I¹⁾.

Von E. Fermi in Rom.

Mit 3 Abbildungen. (Eingegangen am 16. Januar 1934.)

Zeitschrift für Physik, Vol. 88, p. 161

The simple picture:



Finite neutrino mass modifies the decay electron spectrum (mainly around the endpoint)!

The β^- -spectrum of tritium decay

PHYSIQUE NUCLÉAIRE. — Possibilité d'émission de particules neutres de masse intrinsèque nulle dans les radioactivités β . Note de M. FRANCIS Perrin, présenté par M. Jean Perrin.

SÉANCE DU 18 DÉCEMBRE 1933.

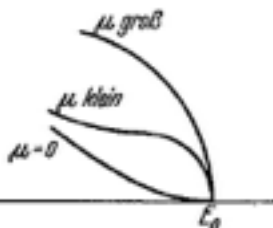


Fig. 1.

Versuch einer Theorie der β -Strahlen. I¹⁾.

Von E. Fermi in Rom.

Mit 3 Abbildungen. (Eingegangen am 16. Januar 1934.)

Zeitschrift für Physik, Vol. 88, p. 161

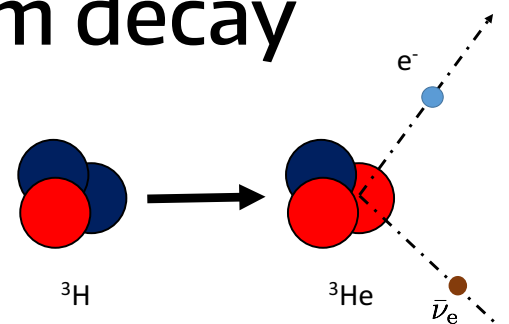
$$Q(T_A) = 18.59201(7) \text{ keV}$$

Myers et al, PRL 114, 013033, 2015

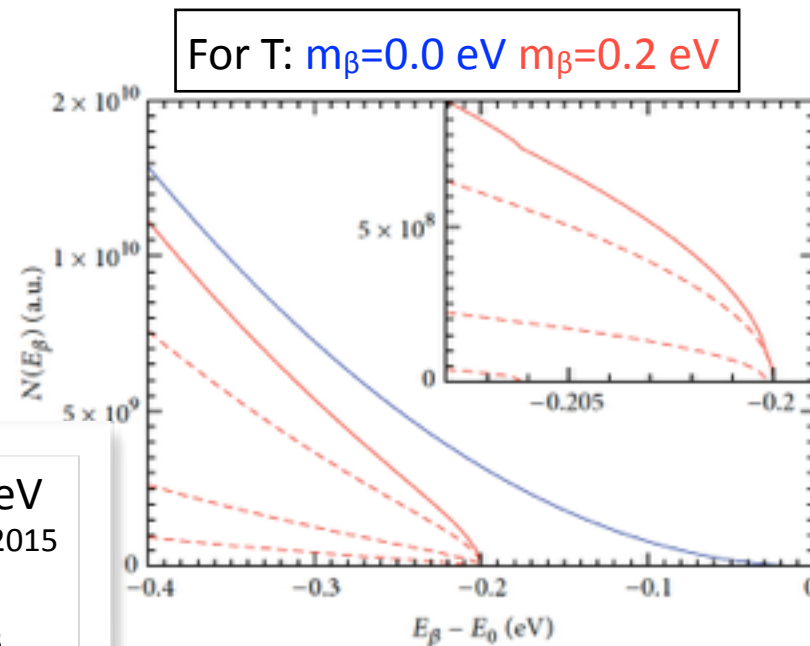
$$T_{1/2} = 12.32 \text{ y}$$

$$\text{BR}(1\text{eV}) = 2 \times 10^{-13}$$

The simple picture:



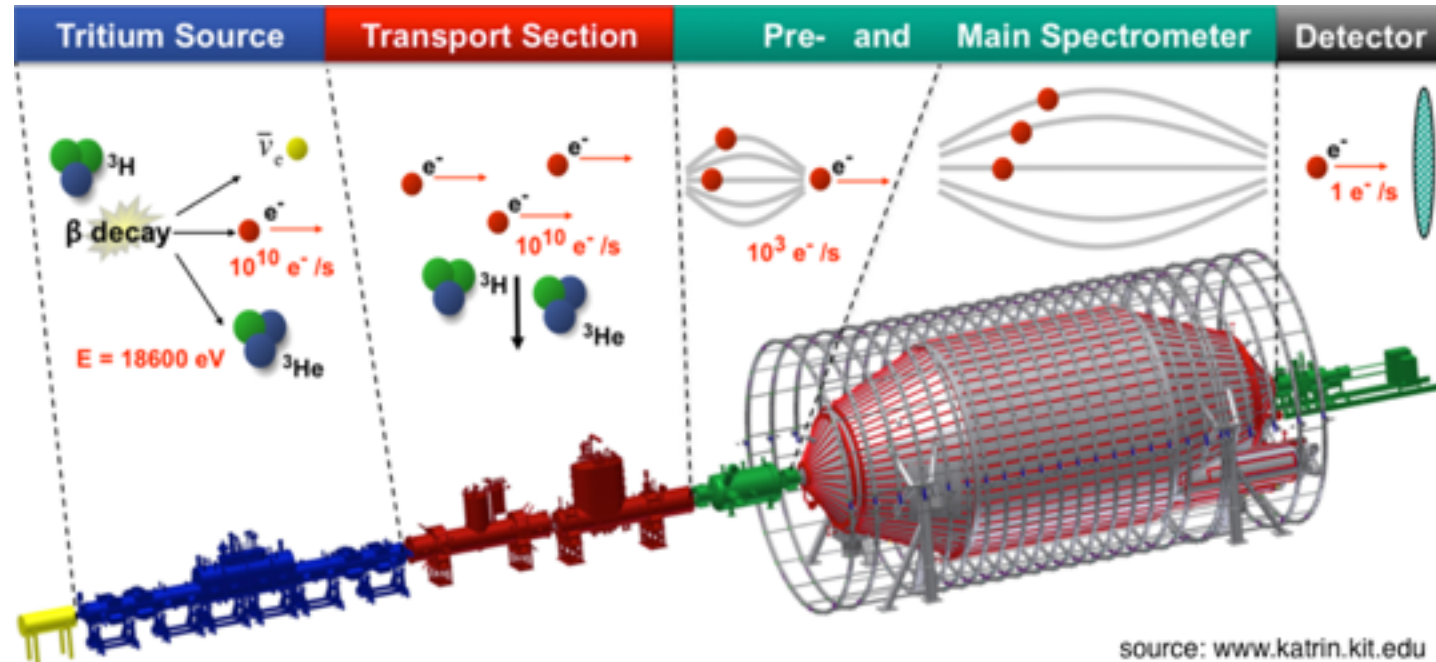
Finite neutrino mass modifies the decay electron spectrum (mainly around the endpoint)!



Nucciotti, Advances in High Energy Physics, Vol. 2016, 9153024

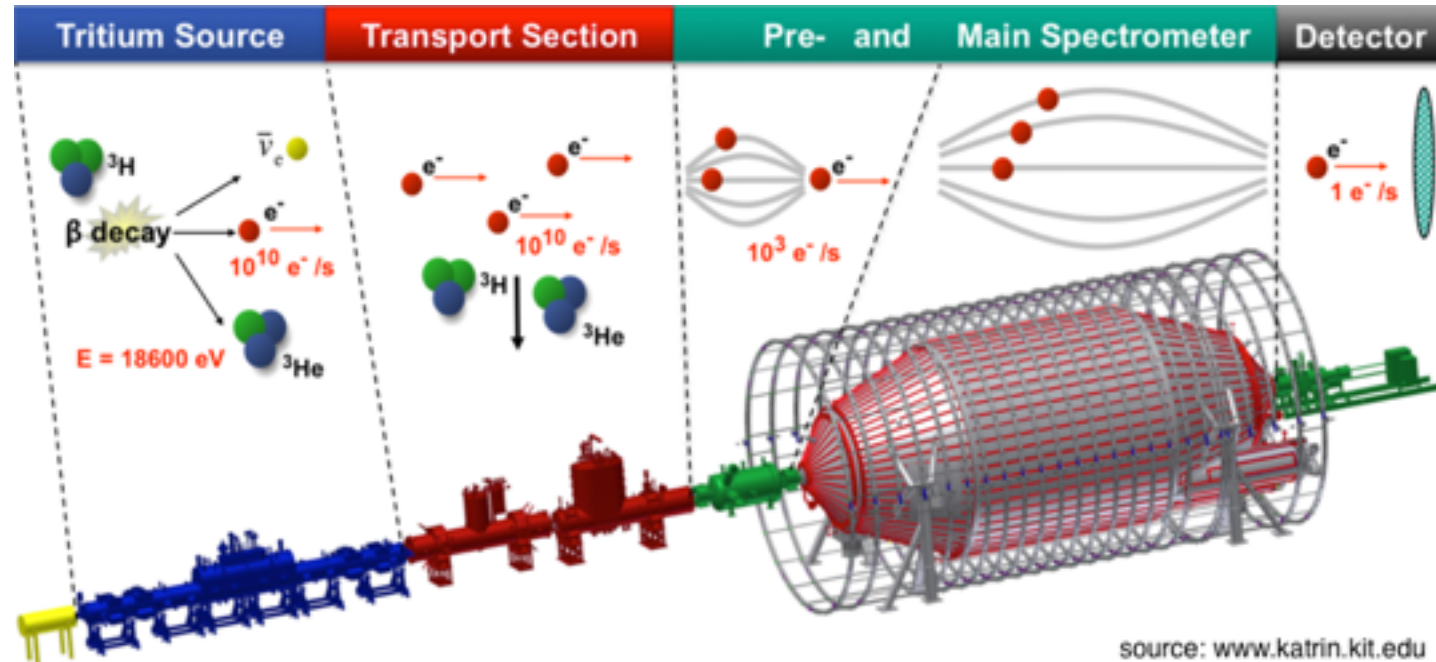
The current state of the art: MAC-E Filter

KATRIN: The largest MAC-E filter ever built pushes all boundaries to the extremes!



The current state of the art: MAC-E Filter

KATRIN: The largest MAC-E filter ever built pushes all boundaries to the extremes!



source: www.katrin.kit.edu

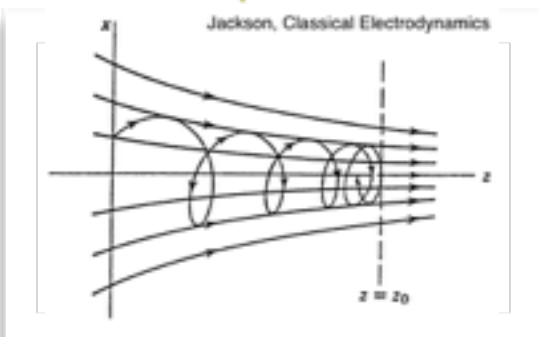
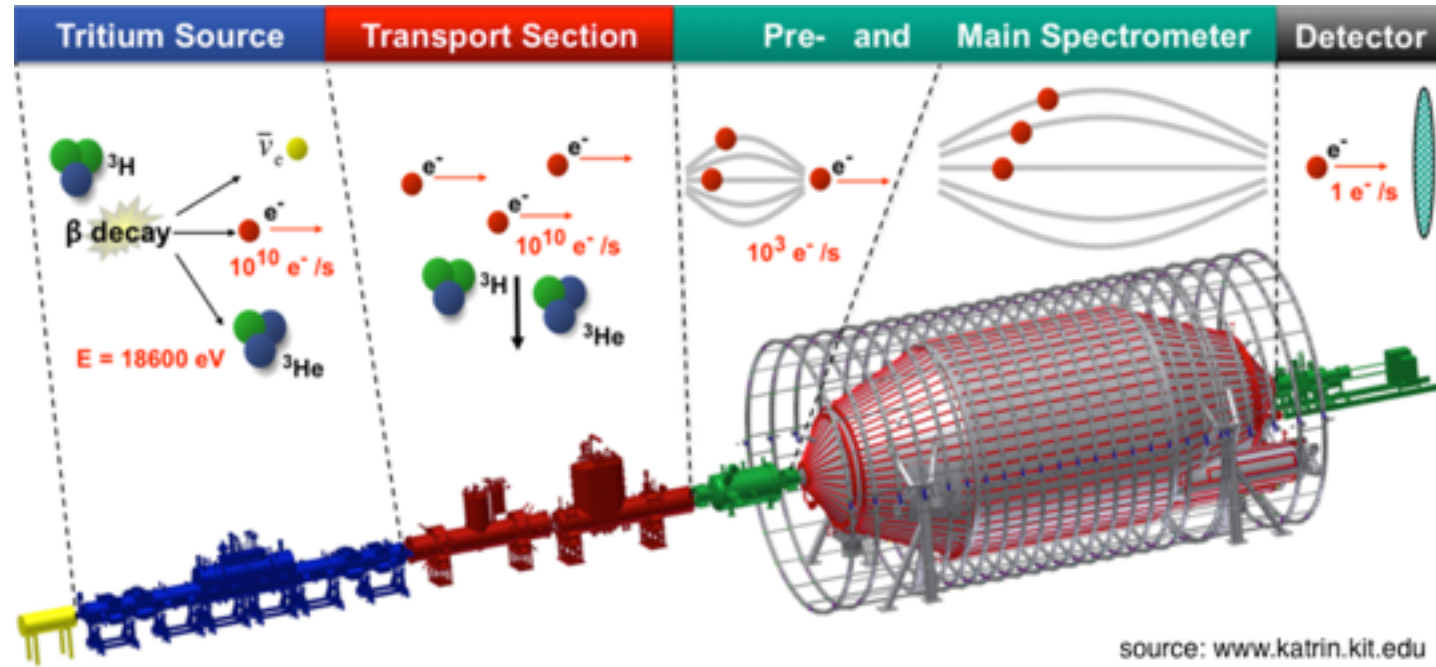
Highest statistics
Window less gaseous
 T_2 source (10^{11} Bq)
Column density limited

Tritium handling
 T_2 suppression by
more than 10^{14} !

Main spectrometer
Largest UHV tank ever built
(1500 m^3 , 10^{-11} mbar)!
Most precise high voltage divider!

The current state of the art: MAC-E Filter

KATRIN: The largest MAC-E filter ever built pushes all boundaries to the extremes!

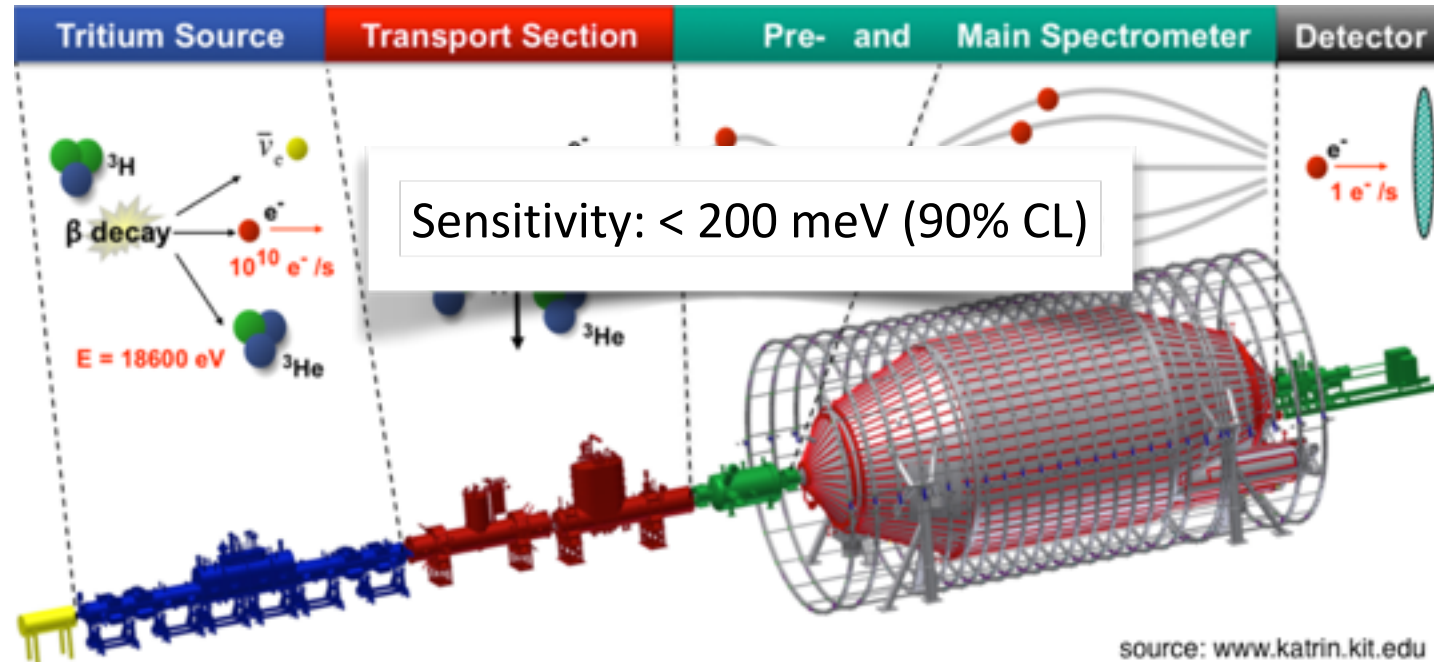


Tritium handling
T₂ suppression by
more than 10^{14} !

Main spectrometer
Largest UHV tank ever built
(1500 m³, 10⁻¹¹ mbar)!
Most precise high voltage divider!

The current state of the art: MAC-E Filter

KATRIN: The largest MAC-E filter ever built pushes all boundaries to the extremes!



source: www.katrin.kit.edu

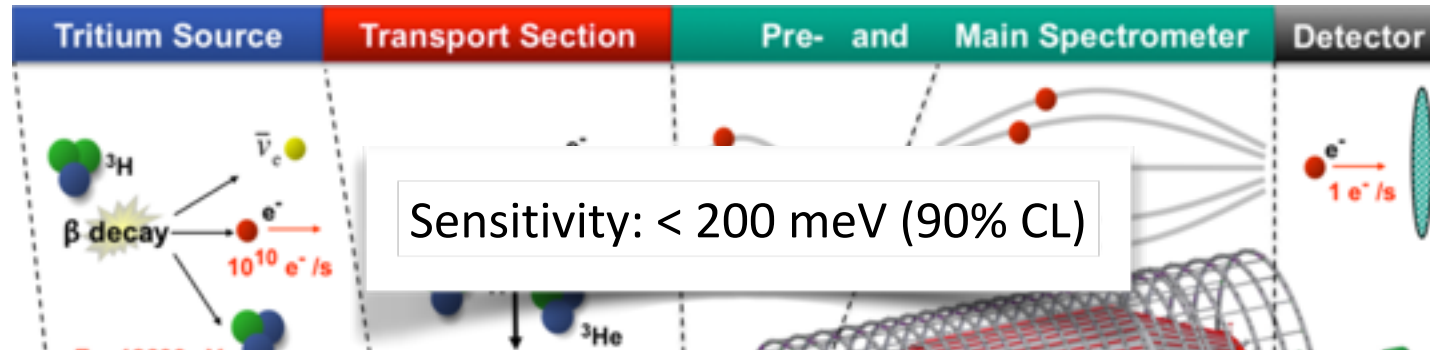
Highest statistics
Window less gaseous
 T_2 source (10^{11} Bq)
Column density limited

Tritium handling
 T_2 suppression by
more than 10^{14} !

Main spectrometer
Largest UHV tank ever built
(1500 m^3 , 10^{-11} mbar)!
Most precise high voltage divider!

The current state of the art: MAC-E Filter

KATRIN: The largest MAC-E filter ever built pushes all boundaries to the extremes!



First light on 10/14/2016! Tritium operation starts in 2017!



source: www.katrin.kit.edu

Highest statistics

Window less gaseous
T₂ source (10^{11} Bq)
Column density limited

Tritium handling

T₂ suppression by
more than 10^{14} !

Main spectrometer

Largest UHV tank ever built
(1500 m^3 , 10^{-11} mbar)!

Most precise high voltage divider!

New techniques and isotopes beyond KATRIN

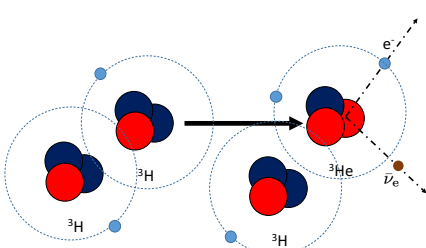
MAC-E resolution scales
with $B_{\min} \propto \text{area}$

Irreducible final state
distribution in ${}^3\text{HeT}^+$

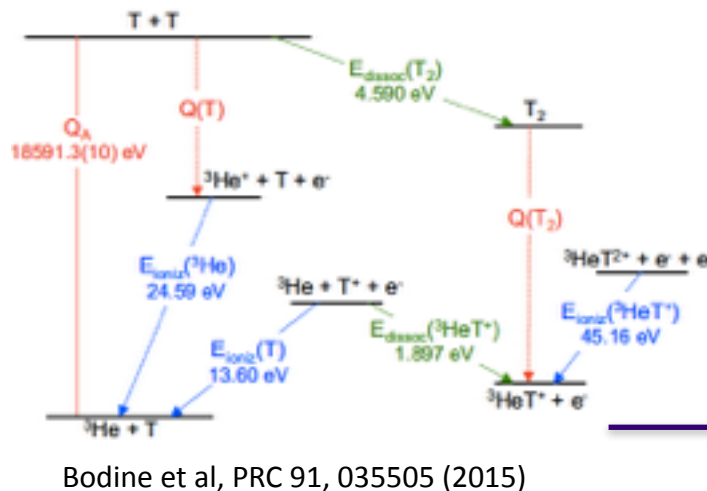
Electron transport:
source \neq detector

New techniques and isotopes beyond KATRIN

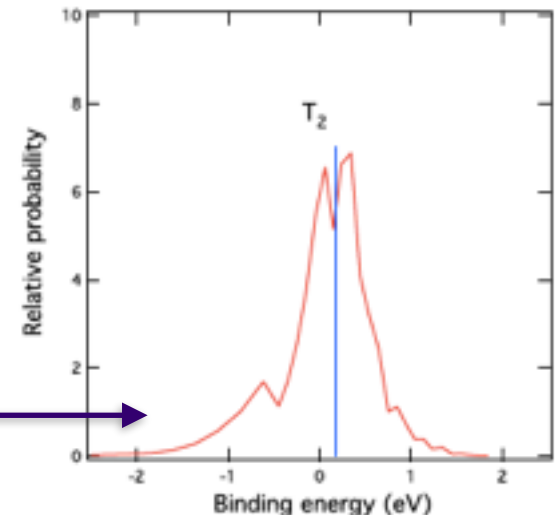
MAC-E resolution scales
with $B_{\min} \propto \text{area}$



Irreducible final state
distribution in $^3\text{HeT}^+$



Electron transport:
source \neq detector



New techniques and isotopes beyond KATRIN

MAC-E resolution scales
with $B_{\min} \propto \text{area}$

Irreducible final state
distribution in ${}^3\text{HeT}^+$

Electron transport:
source \neq detector

New techniques across field boundaries are needed!

New techniques and isotopes beyond KATRIN

MAC-E resolution scales
with $B_{\min} \propto \text{area}$

Irreducible final state
distribution in ${}^3\text{HeT}^+$

Electron transport:
source \neq detector

New techniques across field boundaries are needed!

New isotopes: ${}^{187}\text{Re}$, ${}^{163}\text{Ho}$

${}^{163}\text{Ho}$ microcalorimeter



NuMECS

New techniques and isotopes beyond KATRIN

MAC-E resolution scales
with $B_{\min} \propto \text{area}$

Irreducible final state
distribution in ${}^3\text{HeT}^+$

Electron transport:
source \neq detector

New techniques across field boundaries are needed!

New isotopes: ${}^{187}\text{Re}$, ${}^{163}\text{Ho}$

${}^{163}\text{Ho}$ microcalorimeter

K. Blaum, Tue 11:00 AM
A. Rischka and R. Schüssler, Tue 5:40 PM

NuMECS

New techniques and isotopes beyond KATRIN

MAC-E resolution scales
with $B_{\min} \propto \text{area}$

Irreducible final state
distribution in ${}^3\text{HeT}^+$

Electron transport:
source \neq detector

New techniques across field boundaries are needed!

New isotopes: ${}^{187}\text{Re}$, ${}^{163}\text{Ho}$

Tritium

${}^{163}\text{Ho}$ microcalorimeter

K. Blaum, Tue 11:00 AM
A. Rischka and R. Schüssler, Tue 5:40 PM

NuMECS

Project 8: Cyclotron radiation
emission spectroscopy with
(atomic) tritium

New techniques and isotopes beyond KATRIN

MAC-E resolution scales
with $B_{\min} \propto \text{area}$

Irreducible final state
distribution in ${}^3\text{HeT}^+$

Electron transport:
source \neq detector

New techniques across field boundaries are needed!

New isotopes: ${}^{187}\text{Re}$, ${}^{163}\text{Ho}$

${}^{163}\text{Ho}$ microcalorimeter

K. Blaum, Tue 11:00 AM
A. Rischka and R. Schüssler, Tue 5:40 PM

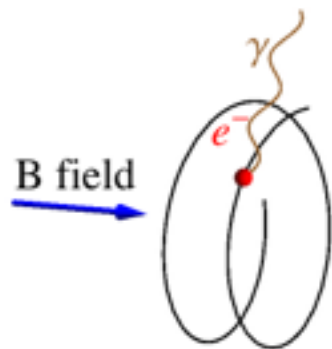
NuMECS

Tritium

PROJECT 8

“Never measure anything but frequency”
A. Schawlow

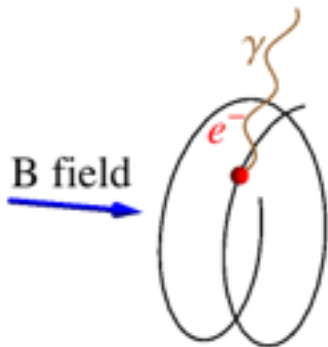
Cyclotron radiation emission spectroscopy



Cyclotron radiation emission spectroscopy

Novel approach: J. Formaggio and B. Monreal, Phys. Rev D 80:051301 (2009)

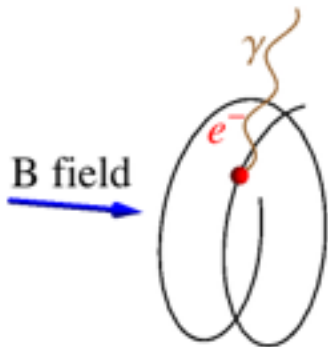
- Cyclotron radiation from single e^- in magnetic field
- Source gas transparent to microwave radiation
- No e^- transport from source to detector (gas scattering)



Cyclotron radiation emission spectroscopy

Novel approach: J. Formaggio and B. Monreal, Phys. Rev D 80:051301 (2009)

- Cyclotron radiation from single e^- in magnetic field
- Source gas transparent to microwave radiation
- No e^- transport from source to detector (gas scattering)
- Highly precise frequency measurement

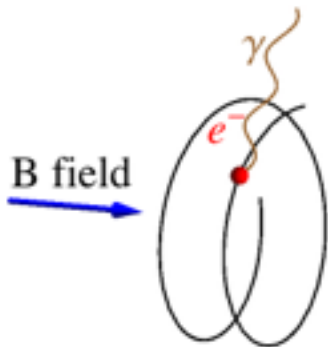


$$f_c = \frac{f_{c,0}}{\gamma} = \frac{1}{2\pi} \frac{eB}{m_e + E_{\text{kin}}/c^2} \approx \frac{1}{2\pi} \frac{eB}{m_e} \left(1 - \underbrace{\frac{E_{\text{kin}}}{m_e c^2} + \left(\frac{E_{\text{kin}}}{m_e c^2} \right)^2}_{0.13\% \text{ for } \Delta E_{\text{kin}}=18.6 \text{ keV}} + \dots \right)$$

Cyclotron radiation emission spectroscopy

Novel approach: J. Formaggio and B. Monreal, Phys. Rev D 80:051301 (2009)

- Cyclotron radiation from single e^- in magnetic field
- Source gas transparent to microwave radiation
- No e^- transport from source to detector (gas scattering)
- Highly precise frequency measurement

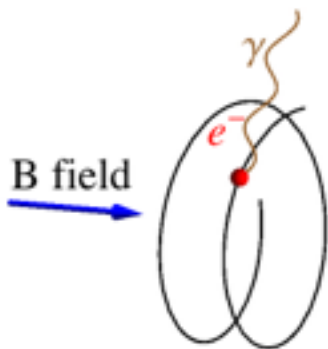


$$f_c = \frac{f_{c,0}}{\gamma} = \frac{1}{2\pi} \frac{eB}{m_e + E_{\text{kin}}/c^2} \approx \frac{1}{2\pi} \frac{eB}{m_e} \left(1 - \frac{E_{\text{kin}}}{m_e c^2} + \underbrace{\left(\frac{E_{\text{kin}}}{m_e c^2} \right)^2}_{4 \times 10^{-8} \text{ for } \Delta E_{\text{kin}}=100 \text{ eV}} + \dots \right)$$

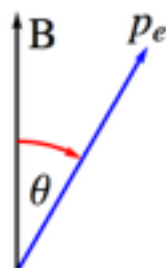
Cyclotron radiation emission spectroscopy

Novel approach: J. Formaggio and B. Monreal, Phys. Rev D 80:051301 (2009)

- Cyclotron radiation from single e^- in magnetic field
- Source gas transparent to microwave radiation
- No e^- transport from source to detector (gas scattering)
- Highly precise frequency measurement



$$f_c = \frac{f_{c,0}}{\gamma} = \frac{1}{2\pi} \frac{eB}{m_e + E_{\text{kin}}/c^2} \approx \frac{1}{2\pi} \frac{eB}{m_e} \left(1 - \frac{E_{\text{kin}}}{m_e c^2} + \underbrace{\left(\frac{E_{\text{kin}}}{m_e c^2} \right)^2}_{4 \times 10^{-8} \text{ for } \Delta E_{\text{kin}}=100 \text{ eV}} + \dots \right)$$



$$P(E_{\text{kin}}, m, \theta) = \frac{1}{4\pi\epsilon_0} \frac{2}{3} \frac{e^4}{m^4 c^5} B^2 (E_{\text{kin}}^2 + 2 E_{\text{kin}} m c^2) \sin^2 \theta$$

$$P(17.8 \text{ keV}, 90^\circ, 1 \text{ T}) = 1 \text{ fW}$$

Small but readily detectable

$$P(30.2 \text{ keV}, 90^\circ, 1 \text{ T}) = 1.7 \text{ fW}$$

with state of the art detectors

Frequency and energy resolution of CRES

Energy vs. frequency resolution:

$$\frac{\Delta E_{\text{kin}}}{E_{\text{kin}}} = \left(1 + \frac{m_e c^2}{E_{\text{kin}}}\right) \frac{\Delta \nu_c}{\nu_c}$$

Frequency and energy resolution of CRES

Energy vs. frequency resolution:

$$\frac{\Delta E_{\text{kin}}}{E_{\text{kin}}} = \left(1 + \frac{m_e c^2}{E_{\text{kin}}} \right) \frac{\Delta \nu_c}{\nu_c}$$

≈ 28 for e^- at T_2 endpoint 18.6 keV

Frequency and energy resolution of CRES

Energy vs. frequency resolution:

$$\frac{\Delta E_{\text{kin}}}{E_{\text{kin}}} = \left(1 + \frac{m_e c^2}{E_{\text{kin}}}\right) \frac{\Delta \nu_c}{\nu_c}$$

≈ 28 for e^- at T_2 endpoint 18.6 keV

$$\Delta E_{\text{kin}} \approx 0.2 \text{ eV} \rightarrow \frac{\Delta \nu_c}{\nu_c} \approx 4 \times 10^{-7}$$

$$\nu_c \approx 27 \text{ GHz} \rightarrow \Delta \nu_c \approx 11 \text{ kHz}$$

Frequency and energy resolution of CRES

Energy vs. frequency resolution:

$$\frac{\Delta E_{\text{kin}}}{E_{\text{kin}}} = \left(1 + \frac{m_e c^2}{E_{\text{kin}}}\right) \frac{\Delta \nu_c}{\nu_c}$$

≈ 28 for e⁻ at T₂ endpoint 18.6 keV

$$\Delta E_{\text{kin}} \approx 0.2 \text{ eV} \rightarrow \frac{\Delta \nu_c}{\nu_c} \approx 4 \times 10^{-7}$$

$$\nu_c \approx 27 \text{ GHz} \rightarrow \Delta \nu_c \approx 11 \text{ kHz}$$

Frequency resolution vs. observation time:

$$\Delta \nu_c \times t_{\text{obs}} \geq \frac{1}{2\pi} \rightarrow t_{\text{obs}} \geq 14 \mu\text{s}$$

Frequency and energy resolution of CRES

Energy vs. frequency resolution:

$$\frac{\Delta E_{\text{kin}}}{E_{\text{kin}}} = \left(1 + \frac{m_e c^2}{E_{\text{kin}}}\right) \frac{\Delta \nu_c}{\nu_c}$$

≈ 28 for e⁻ at T₂ endpoint 18.6 keV

$$\Delta E_{\text{kin}} \approx 0.2 \text{ eV} \rightarrow \frac{\Delta \nu_c}{\nu_c} \approx 4 \times 10^{-7}$$

$$\nu_c \approx 27 \text{ GHz} \rightarrow \Delta \nu_c \approx 11 \text{ kHz}$$

Frequency resolution vs. observation time:

$$\Delta \nu_c \times t_{\text{obs}} \geq \frac{1}{2\pi} \rightarrow t_{\text{obs}} \geq 14 \mu\text{s}$$

$\beta t_{\text{obs}} \cos \theta \approx 20 \text{ m}$ for a 18.6 keV electron
and 89° pitch angle

Frequency and energy resolution of CRES

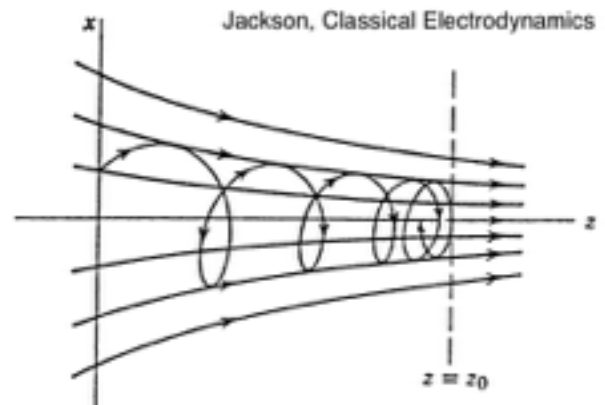
Energy vs. frequency resolution:

$$\frac{\Delta E_{\text{kin}}}{E_{\text{kin}}} = \left(1 + \frac{m_e c^2}{E_{\text{kin}}}\right) \frac{\Delta \nu_c}{\nu_c}$$

≈ 28 for e⁻ at T₂ endpoint 18.6 keV

$$\Delta E_{\text{kin}} \approx 0.2 \text{ eV} \rightarrow \frac{\Delta \nu_c}{\nu_c} \approx 4 \times 10^{-7}$$

$$\nu_c \approx 27 \text{ GHz} \rightarrow \Delta \nu_c \approx 11 \text{ kHz}$$



Frequency resolution vs. observation time:

$$\Delta \nu_c \times t_{\text{obs}} \geq \frac{1}{2\pi} \rightarrow t_{\text{obs}} \geq 14 \mu\text{s}$$

$\beta t_{\text{obs}} \cos \theta \approx 20 \text{ m}$ for a 18.6 keV electron
and 89° pitch angle

Frequency and energy resolution of CRES

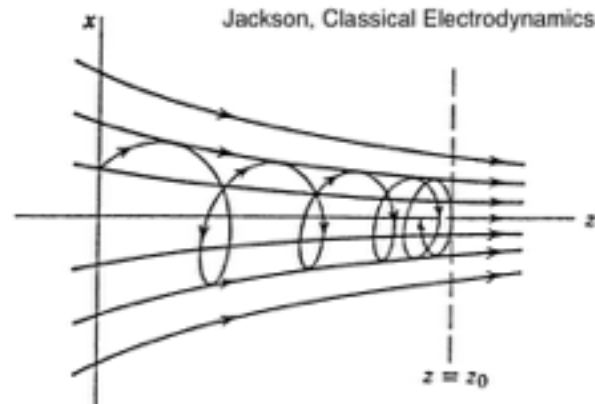
Energy vs. frequency resolution:

$$\frac{\Delta E_{\text{kin}}}{E_{\text{kin}}} = \left(1 + \frac{m_e c^2}{E_{\text{kin}}}\right) \frac{\Delta \nu_c}{\nu_c}$$

≈ 28 for e⁻ at T₂ endpoint 18.6 keV

$$\Delta E_{\text{kin}} \approx 0.2 \text{ eV} \rightarrow \frac{\Delta \nu_c}{\nu_c} \approx 4 \times 10^{-7}$$

$$\nu_c \approx 27 \text{ GHz} \rightarrow \Delta \nu_c \approx 11 \text{ kHz}$$



$$\text{P8 typical: } \sin \theta_{\min} = \sqrt{\frac{B_{\min}}{B_{\max}}} \rightarrow 85^\circ$$

Frequency resolution vs. observation time:

$$\Delta \nu_c \times t_{\text{obs}} \geq \frac{1}{2\pi} \rightarrow t_{\text{obs}} \geq 14 \mu\text{s}$$

$\beta t_{\text{obs}} \cos \theta \approx 20 \text{ m}$ for a 18.6 keV electron
and 89° pitch angle

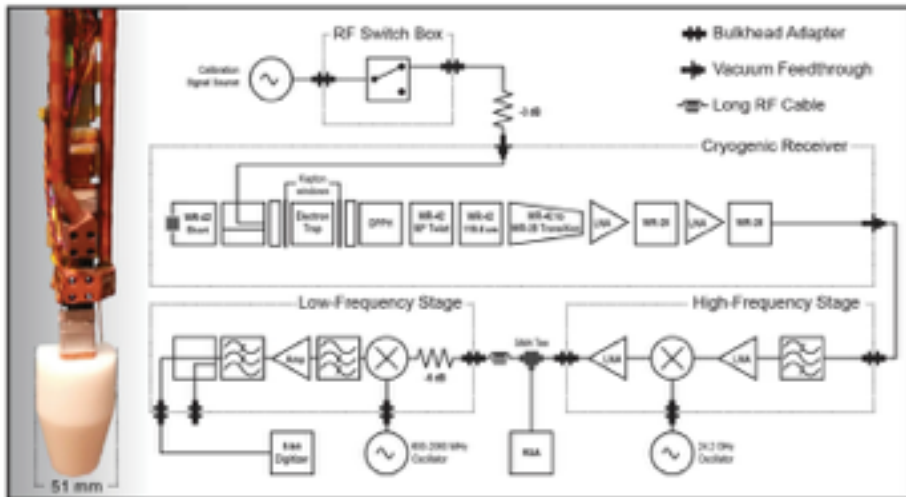


harmonic trap

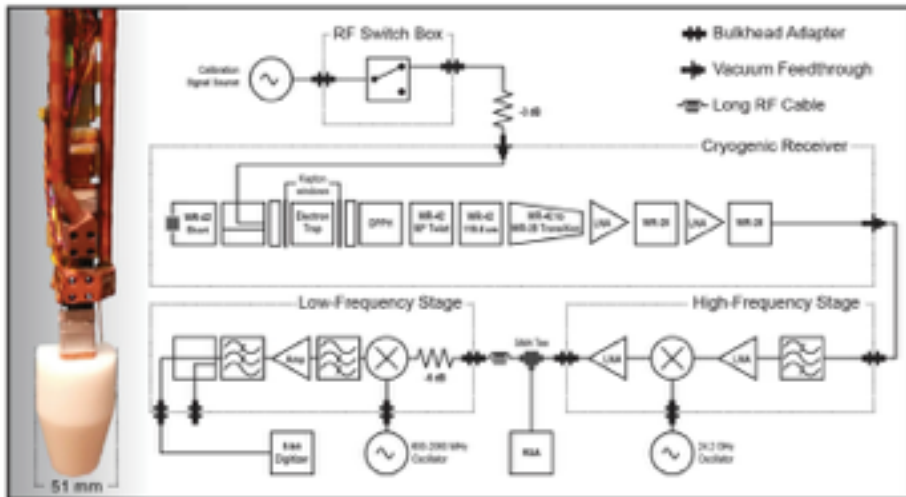


bath tub trap

Phase I setup and results



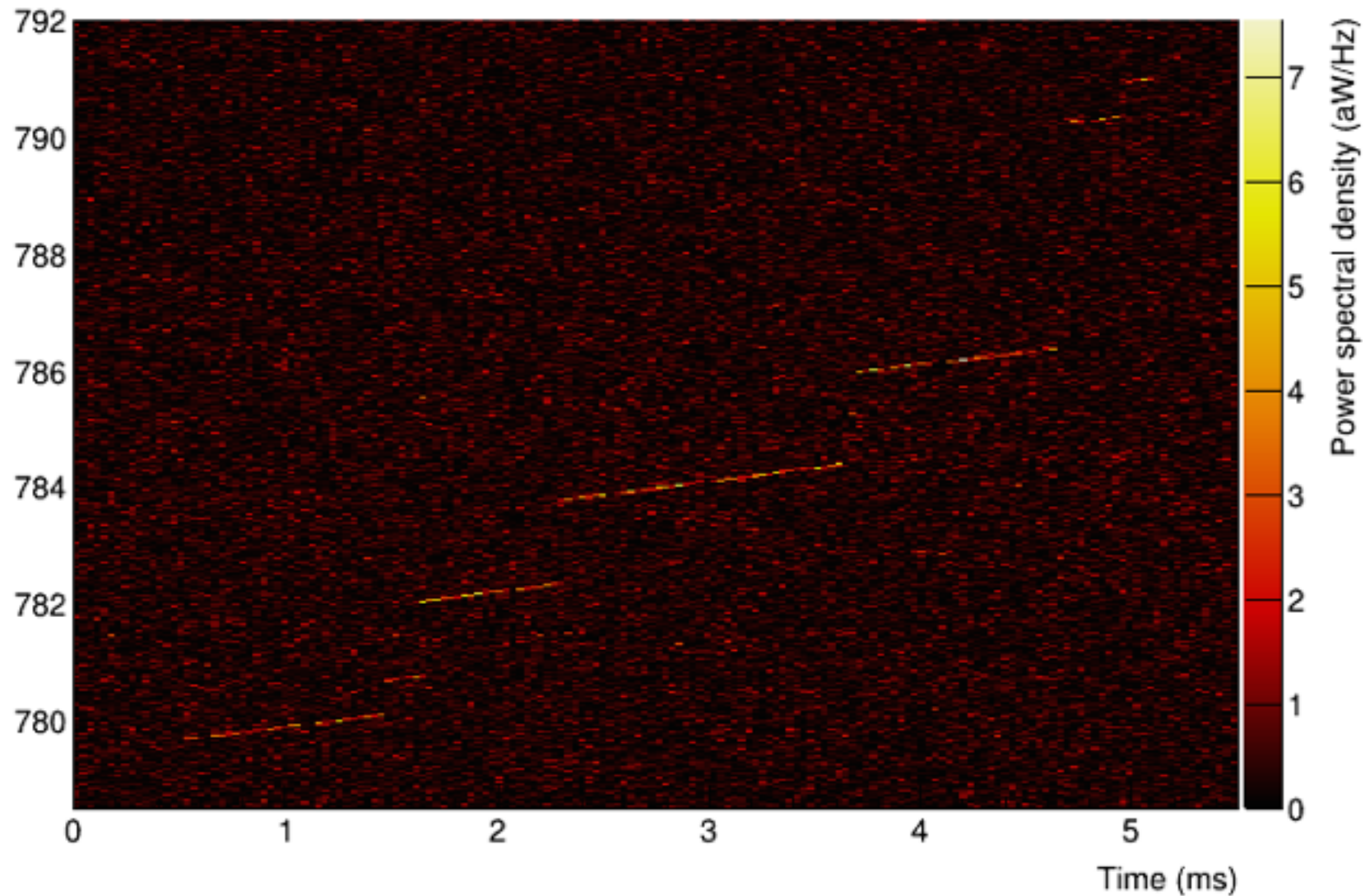
Phase I setup and results



- Cryogenic waveguide cell and amplifiers
- RT heterodyne double mixing stage

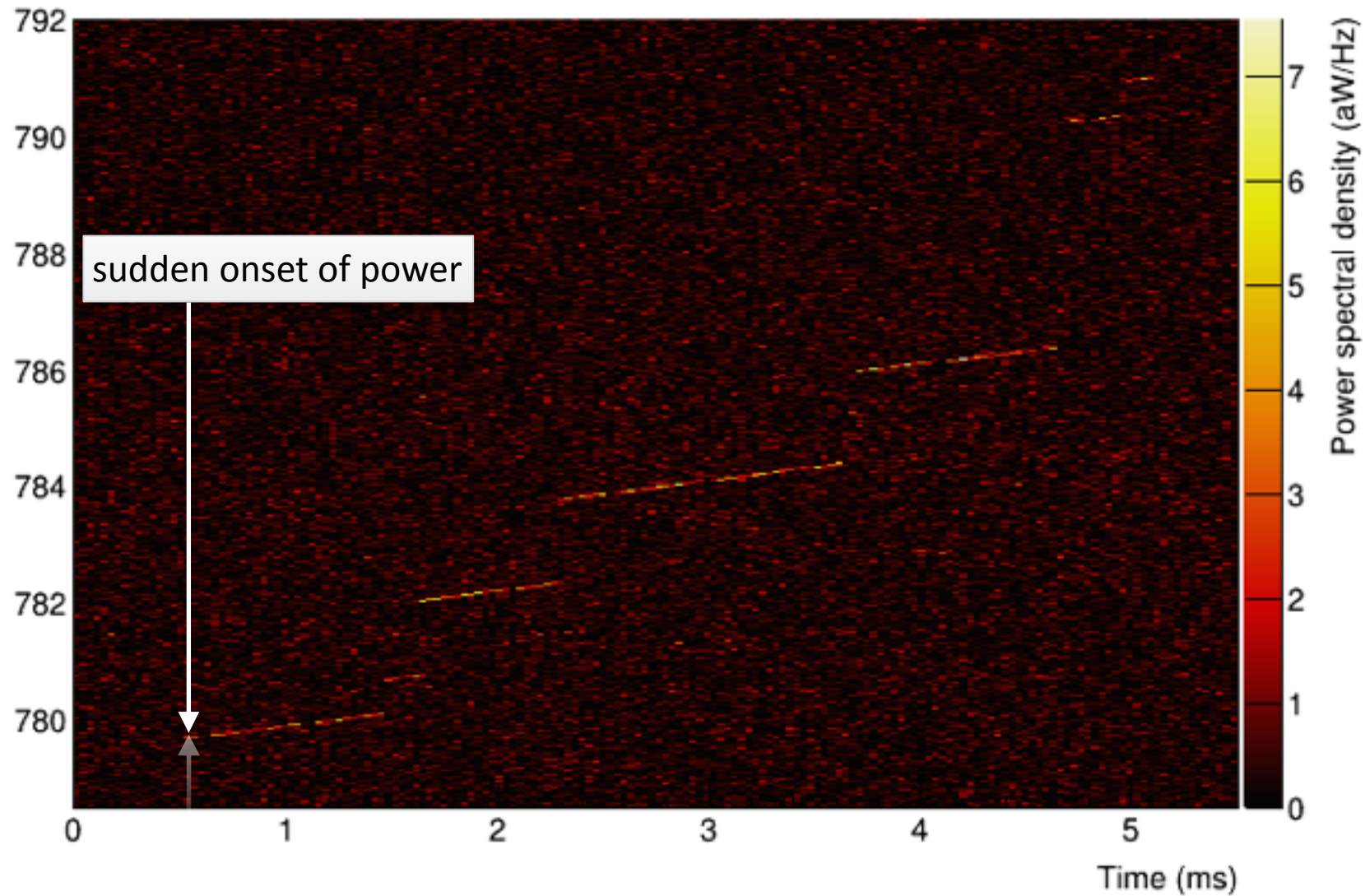
Phase I setup and results

Output of heterodyne mixing stage

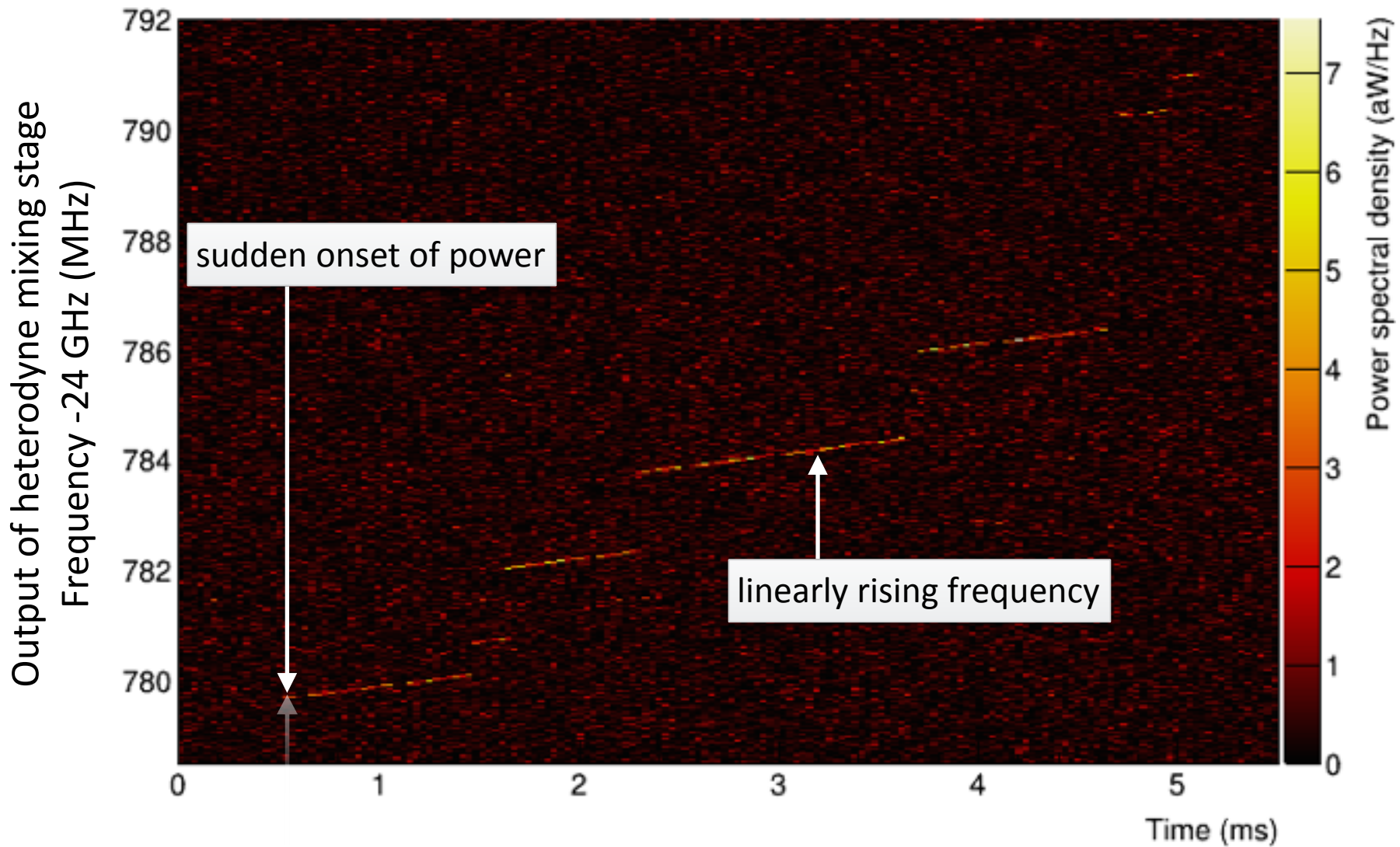


Phase I setup and results

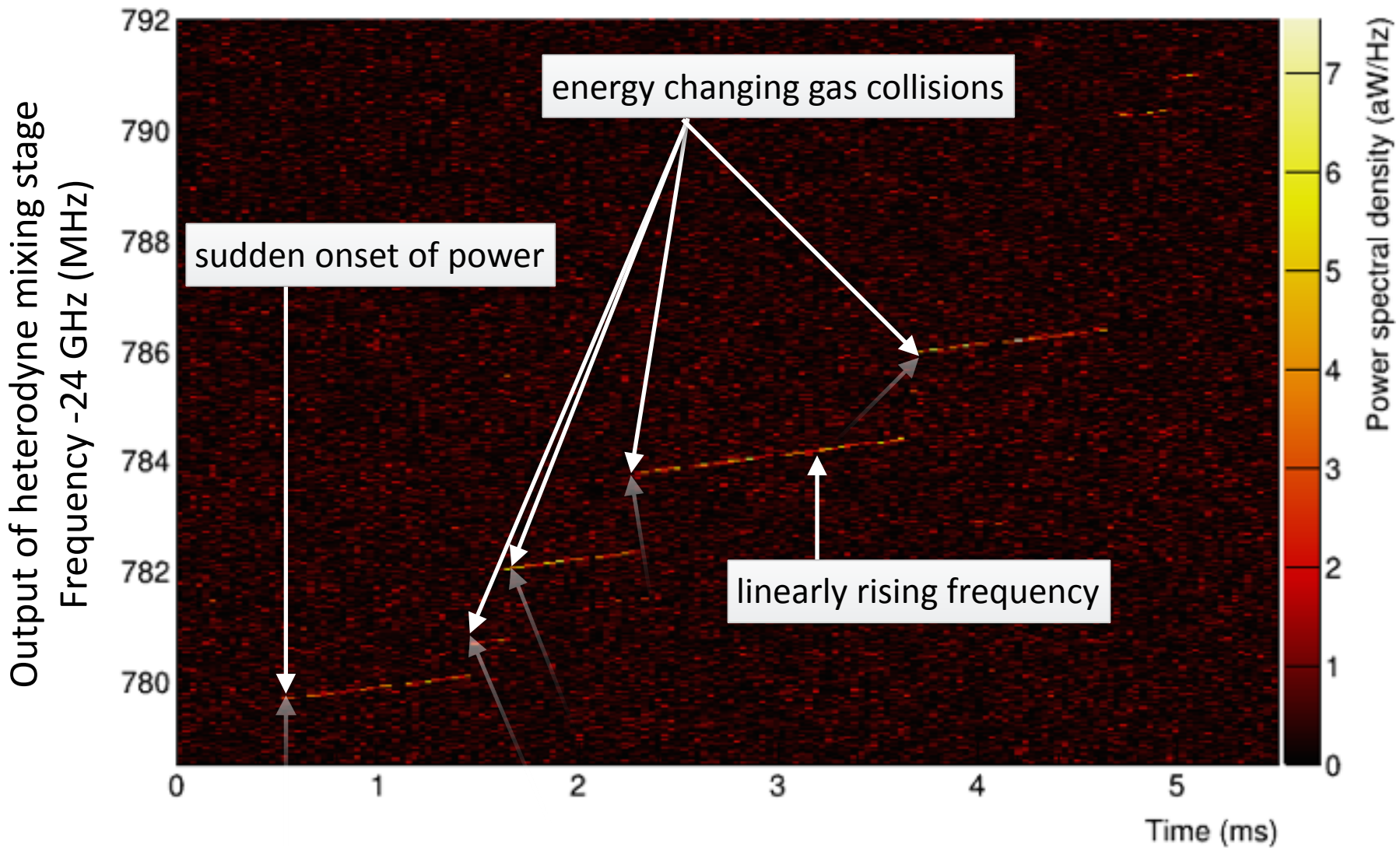
Output of heterodyne mixing stage



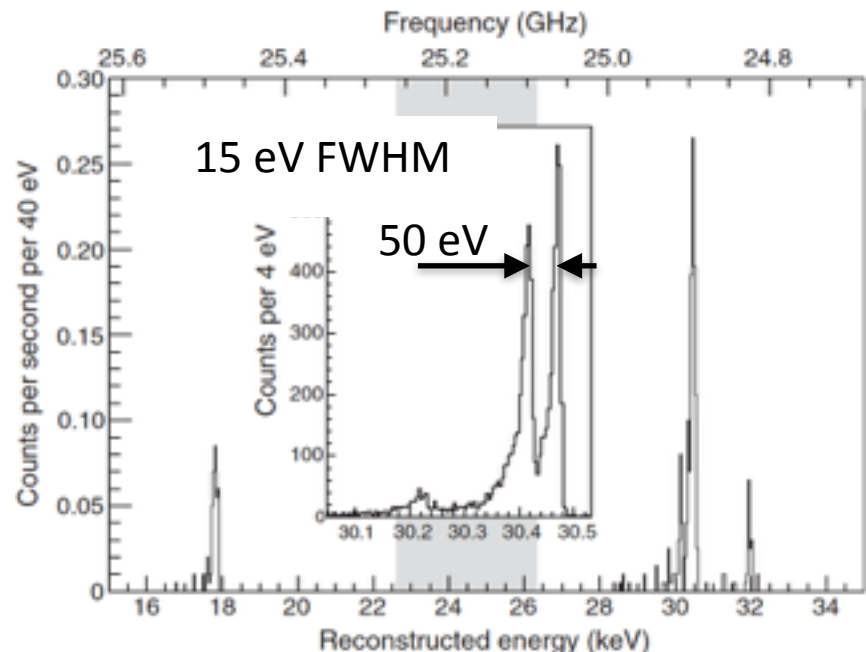
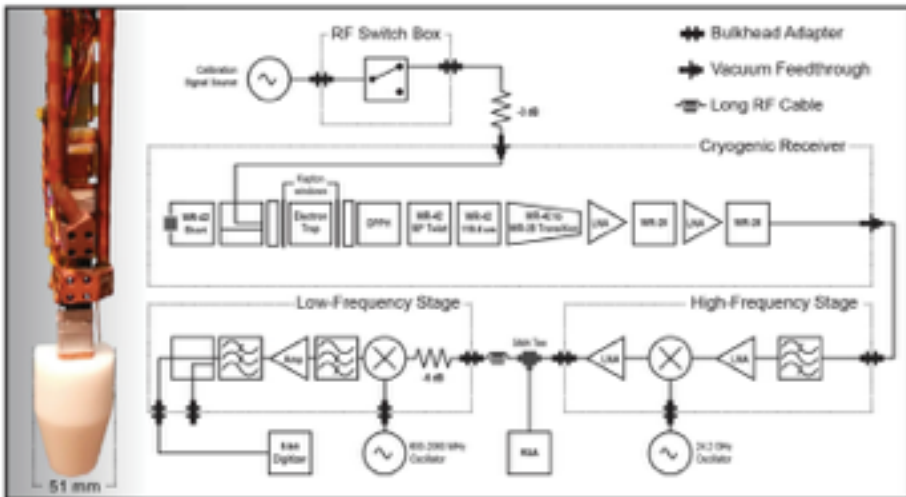
Phase I setup and results



Phase I setup and results



Phase I setup and results

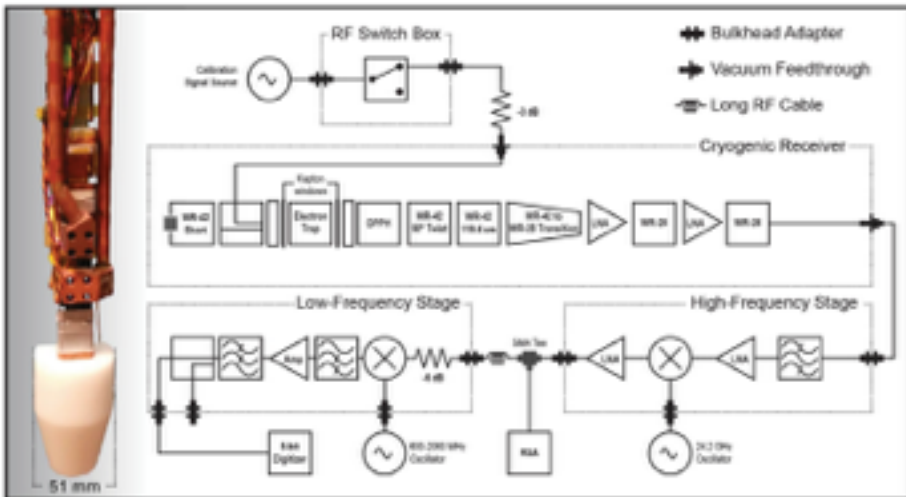


Asner et al., Physical Review Letters, 114, 162501 (2015)

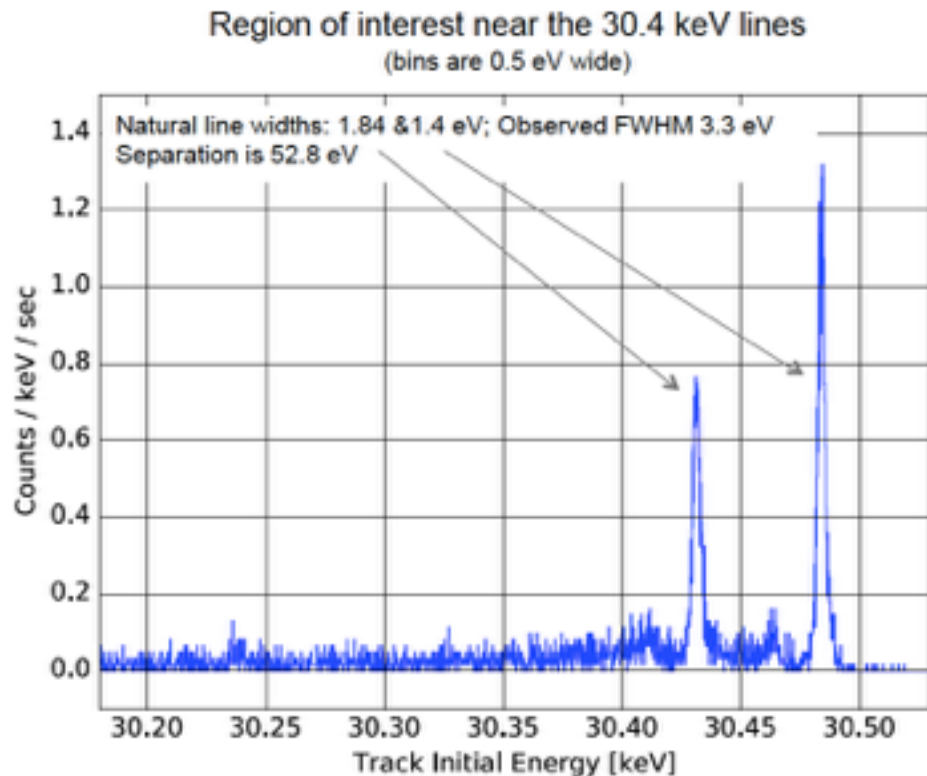
- Cryogenic waveguide cell and amplifiers
- RT heterodyne double mixing stage
- Initial resolution: 15 eV in harmonic trap



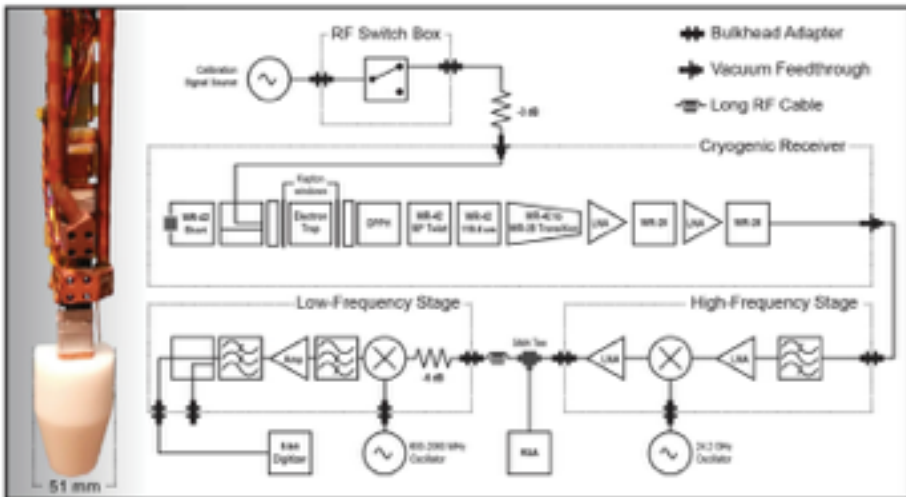
Phase I setup and results



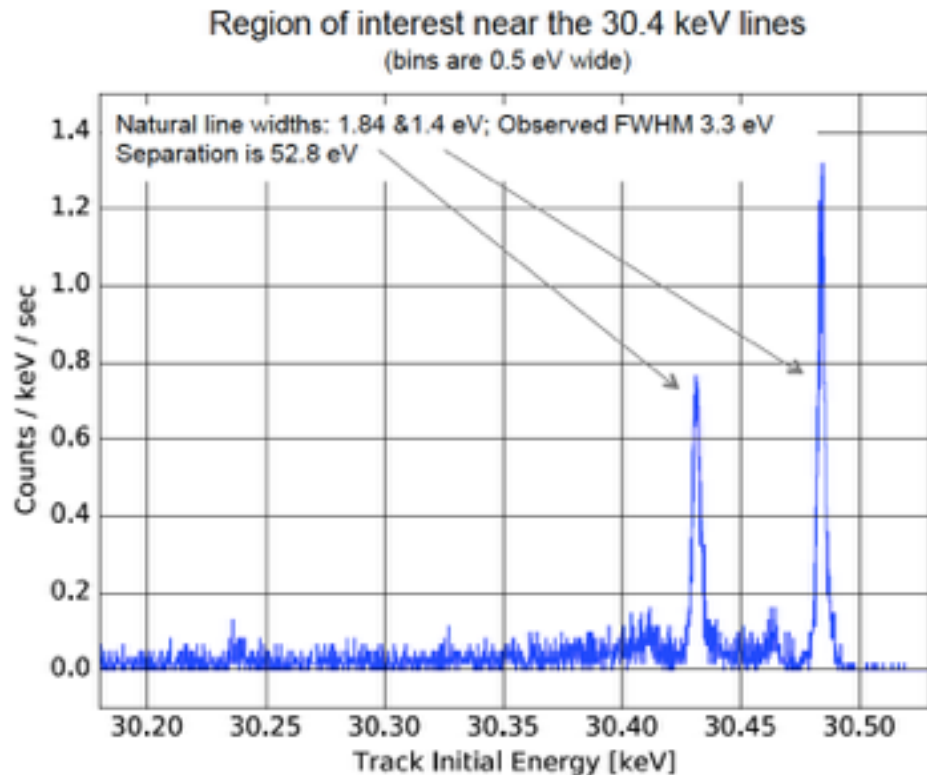
- Cryogenic waveguide cell and amplifiers
- RT heterodyne double mixing stage
- Initial resolution: 15 eV in harmonic trap
- Bathtub trap: 3.3 eV resolution



Phase I setup and results



- Cryogenic waveguide cell and amplifiers
- RT heterodyne double mixing stage
- Initial resolution: 15 eV in harmonic trap
- Bathtub trap: 3.3 eV resolution
- With power cut under investigation:
2.2 eV FWHM

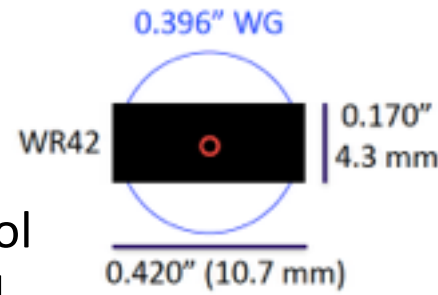


The Project 8 Phase II waveguide cell



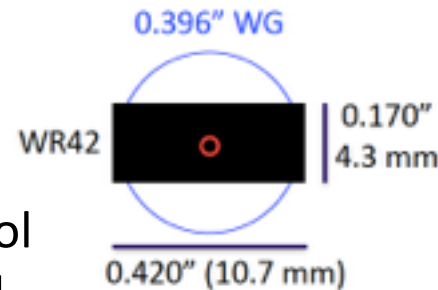
The Project 8 Phase II waveguide cell

- Tritium compatible waveguide cell → CaF₂ windows
- Circular waveguide → Larger active volume
- Circulator and cryo termination → 3dB more signal, better control of the microwave background



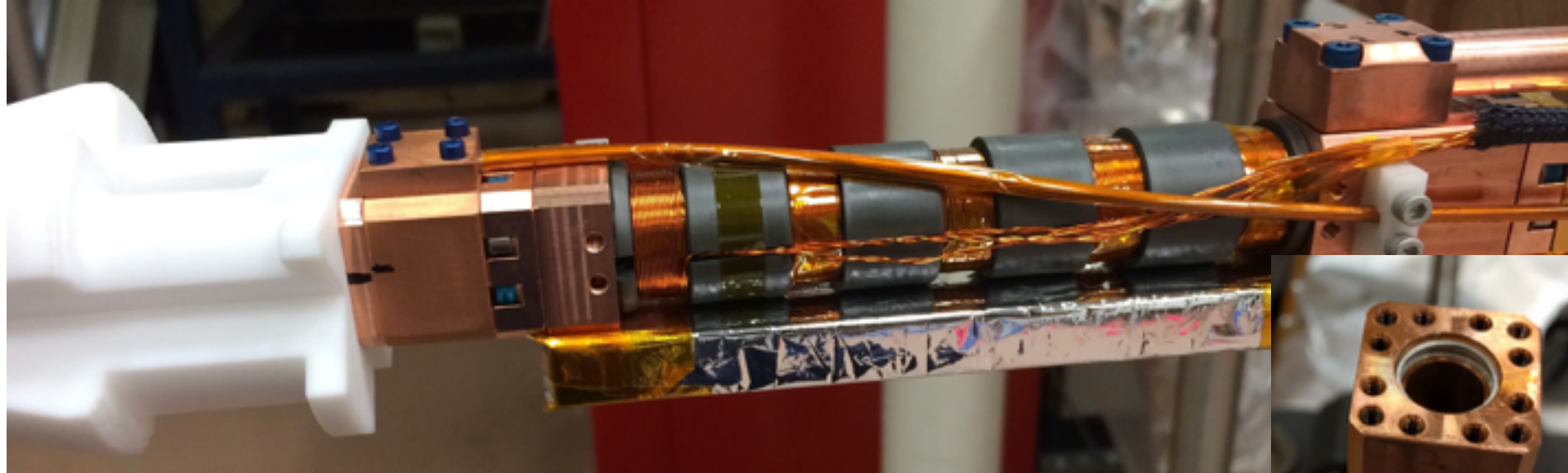
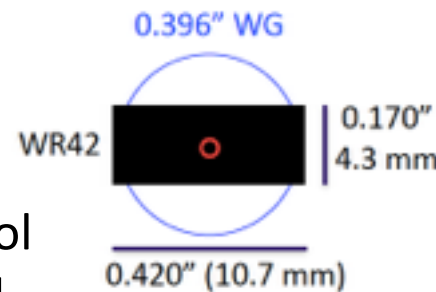
The Project 8 Phase II waveguide cell

- Tritium compatible waveguide cell → CaF₂ windows
- Circular waveguide → Larger active volume
- Circulator and cryo termination → 3dB more signal, better control of the microwave background
- Study optimal shape of magnetic trap → 5 instead of 3 traps

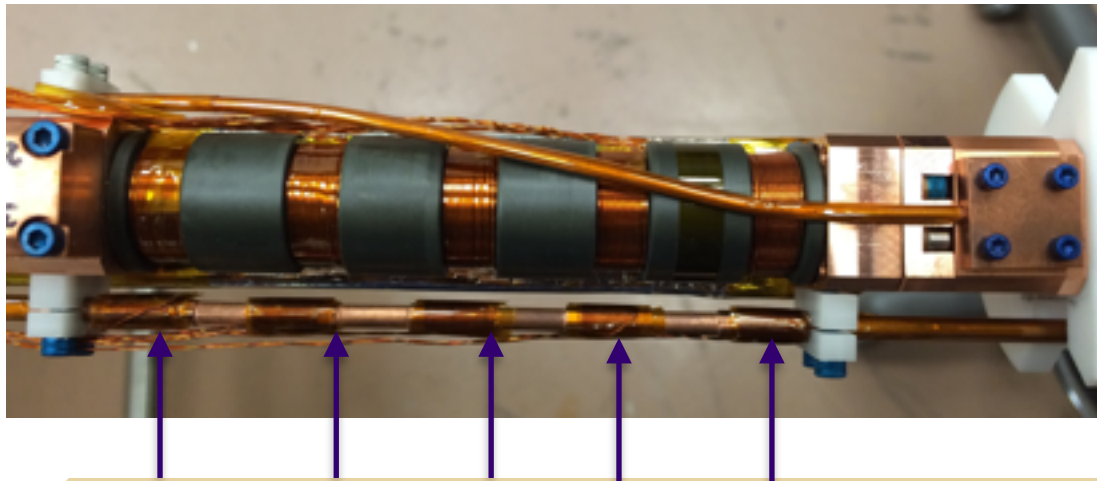


The Project 8 Phase II waveguide cell

- Tritium compatible waveguide cell → CaF₂ windows
- Circular waveguide → Larger active volume
- Circulator and cryo termination → 3dB more signal, better control of the microwave background
- Study optimal shape of magnetic trap → 5 instead of 3 traps
- 5 off-axis ESR magnetometers → B field stability measurements

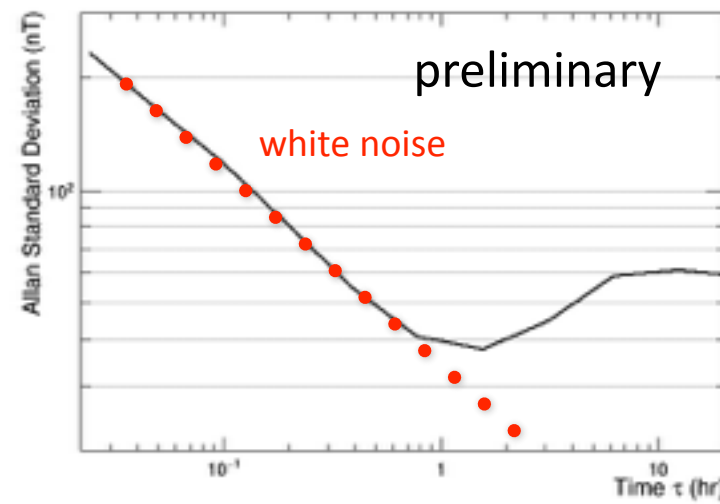
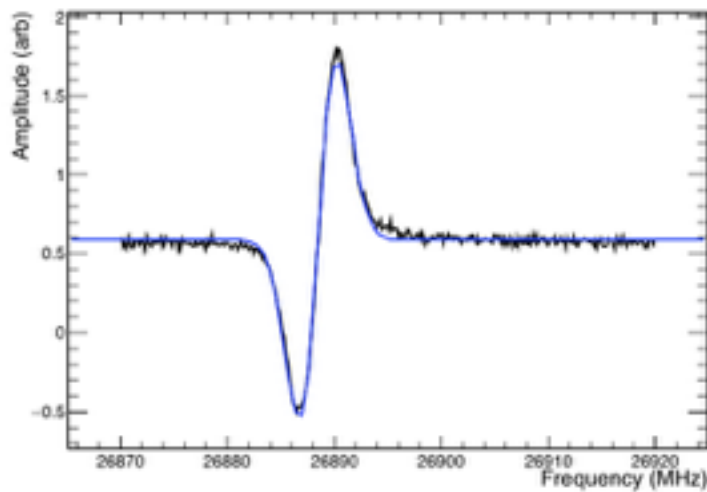


ESR magnetometer



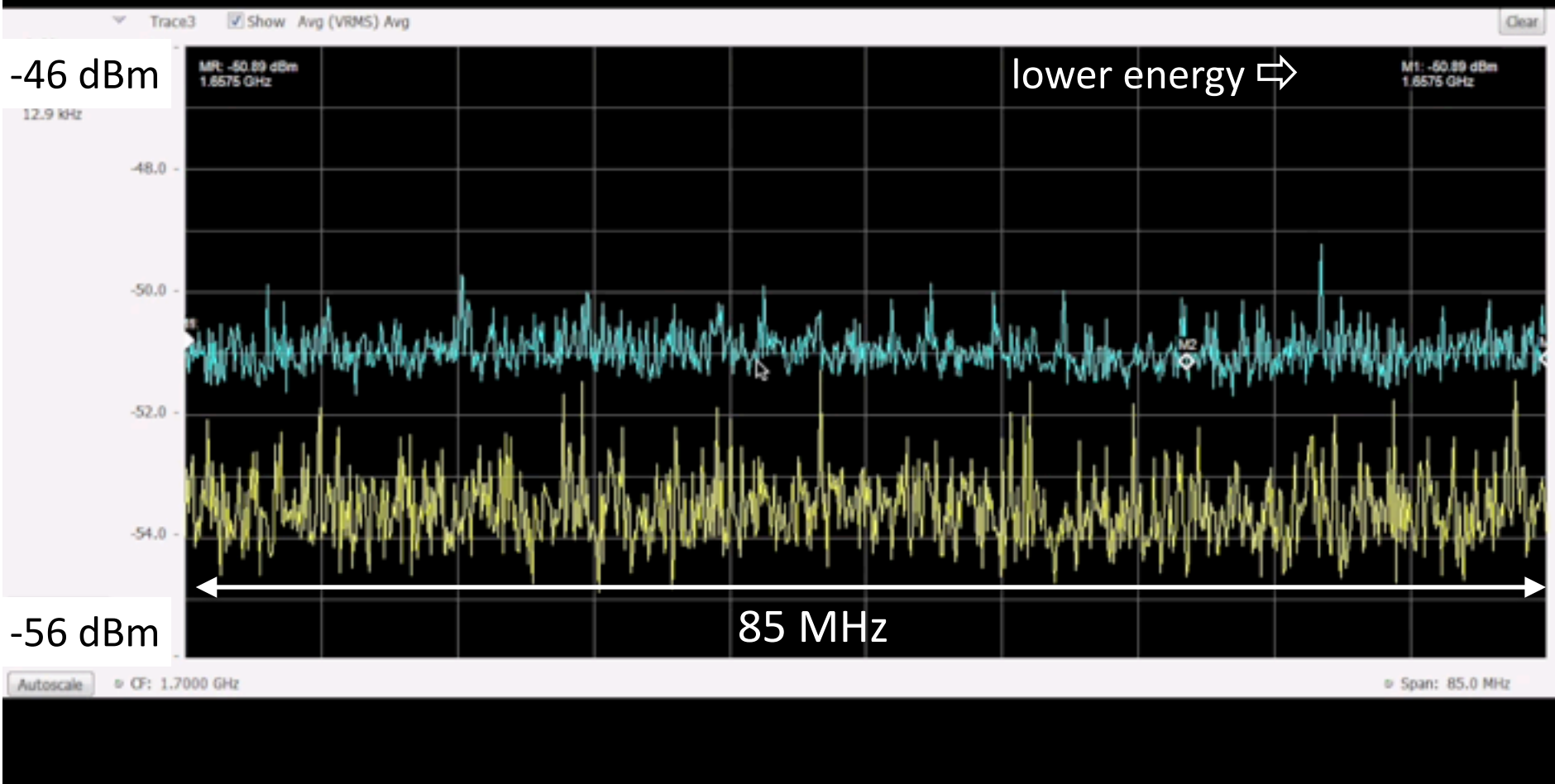
- New diagnostics tool for Project 8
- Rel. B precision 0.3 ppm measured
- Rel. B stability 40 ppb/hr measured
- B field drift has negligible influence on Phase II energy resolution

5 sample ESR magnetometer with BDPA (thanks to P. Hautle)



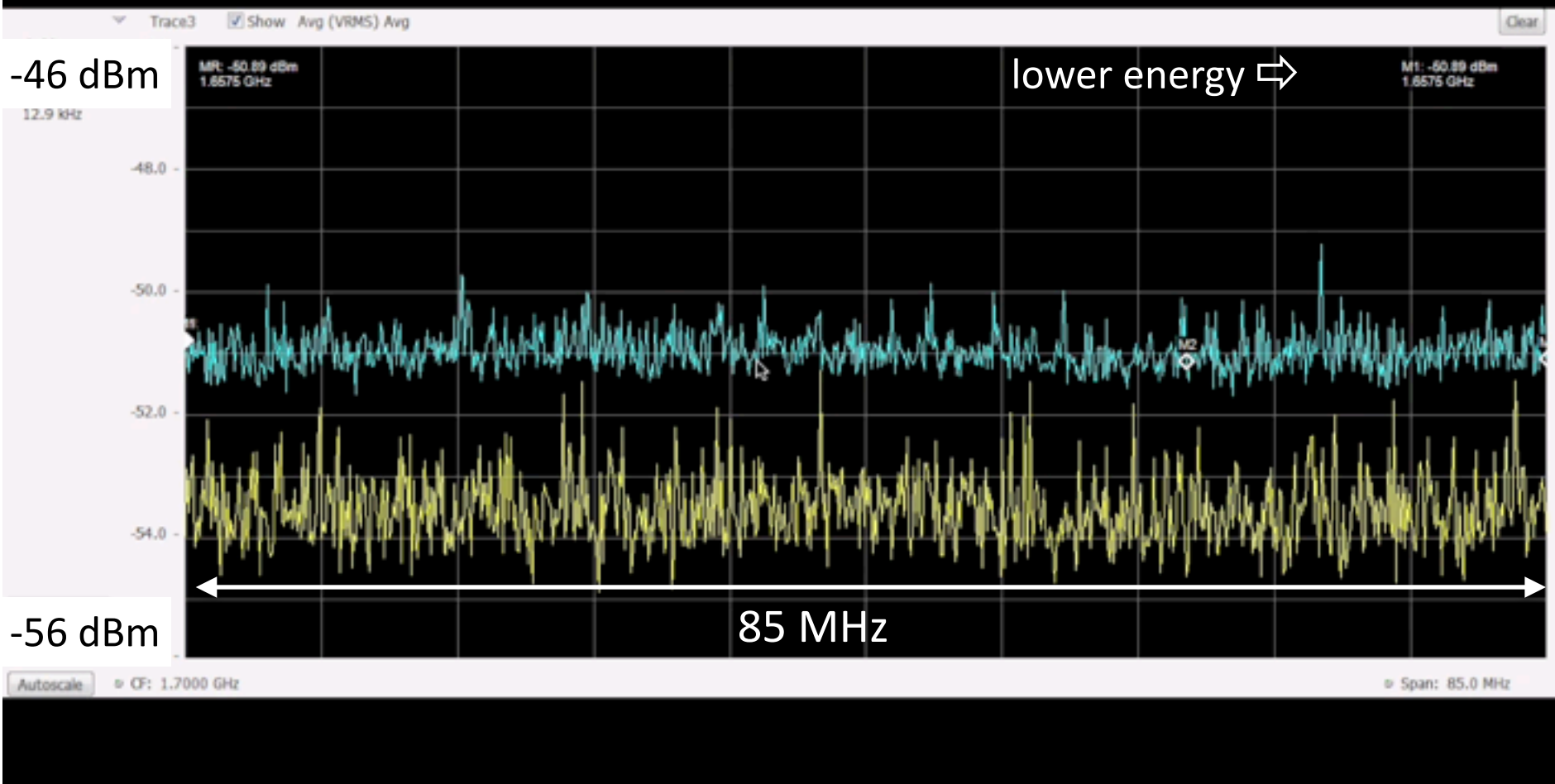
^{83m}Kr conversion electrons in Phase II

17.6 keV electrons, realtime x20



^{83m}Kr conversion electrons in Phase II

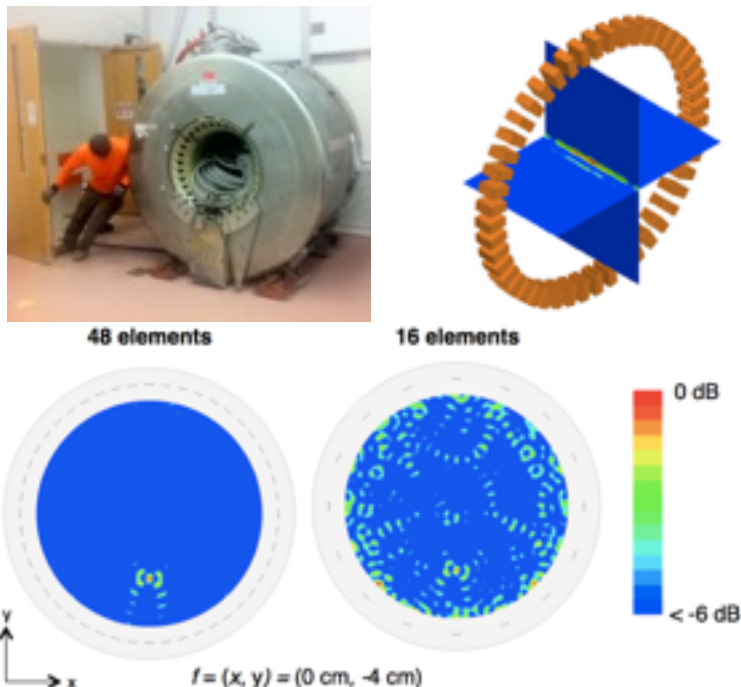
17.6 keV electrons, realtime x20



Project 8 Phase III+IV: Free space radiation

Phase III (2016-2020)

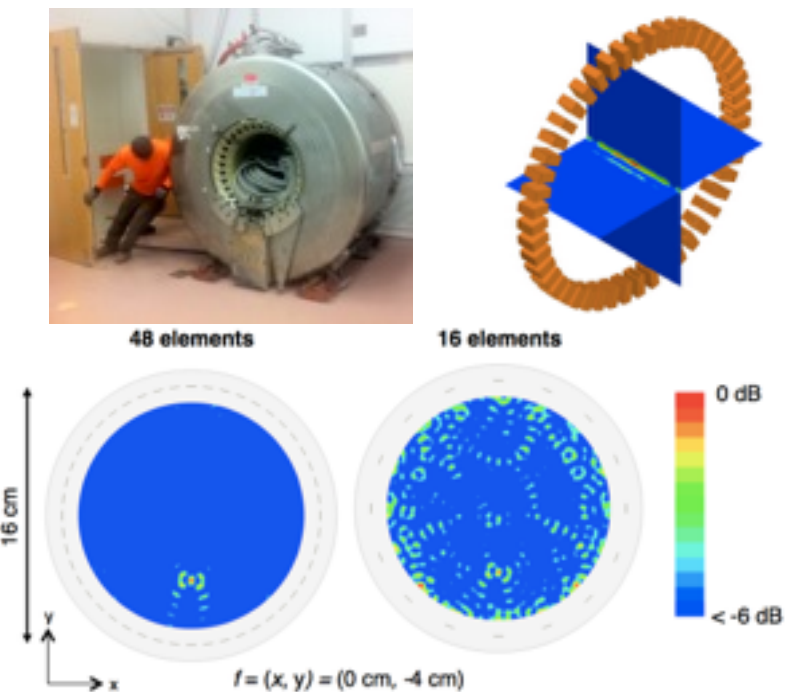
- 10 cm³ eff. T₂ source volume (1 yr)
- Sensitivity goal: 2 eV (90% CL)
- Study of phased antenna array
- Commissioning MRI magnet



Project 8 Phase III+IV: Free space radiation

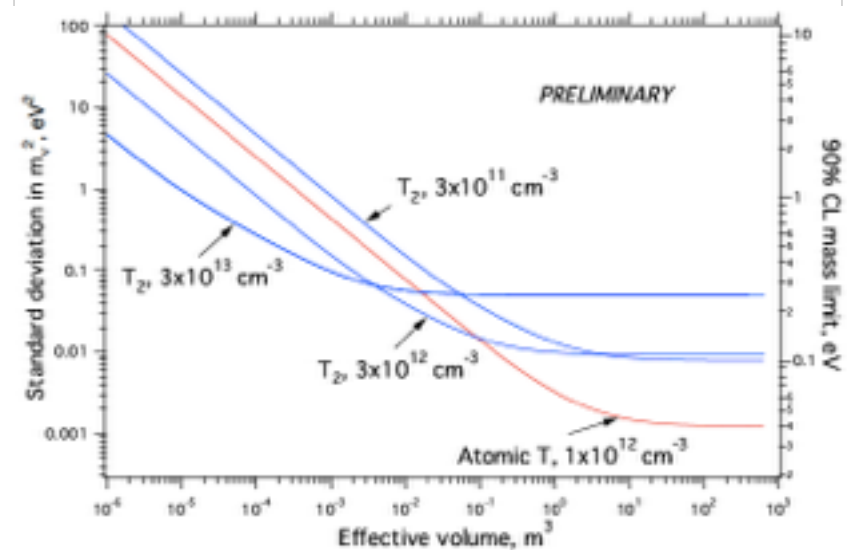
Phase III (2016-2020)

- 10 cm³ eff. T₂ source volume (1 yr)
- Sensitivity goal: 2 eV (90% CL)
- Study of phased antenna array
- Commissioning MRI magnet



Phase IV (2017-2022+)

- Large-scale experiment
- Atomic tritium source
- IH, sub-eV sensitivity
- Trapped atomic tritium



${}^6\text{He}$: High energy CRES for chirality flipping interactions

Goal: Measure Fierz interference term “b” in ${}^6\text{He}$ decay to better than 10^{-3} !

$$dw = dw_0 \left(1 + a \frac{\vec{p}_e}{E_e} \cdot \frac{\vec{p}_\nu}{E_\nu} + b_{\text{Fierz}} \frac{m_e}{E_e} \right) \quad a \approx -\frac{1}{3} \frac{2|C_A|^2 - |C_T|^2 + |C'_T|^2}{2|C_A|^2 + |C_T|^2 + |C'_T|^2} \quad b \approx \frac{\Re(2C_A(C_T + C'_T))}{2|C_A|^2 + |C_T|^2 + |C'_T|^2}$$

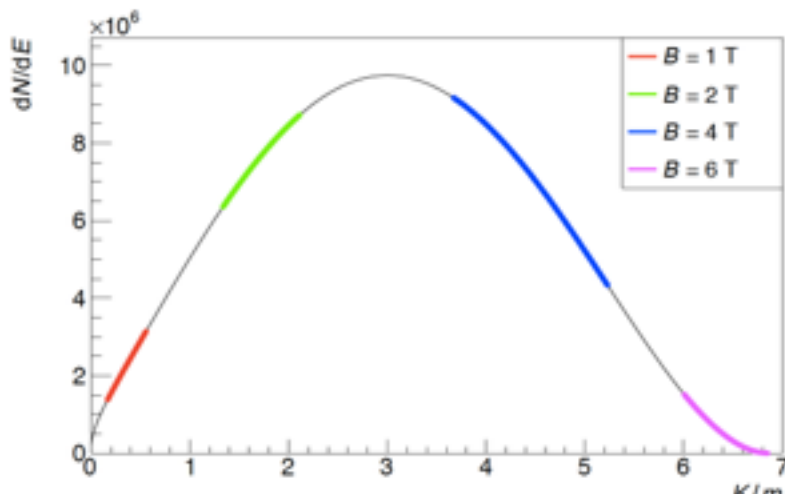
“Fierz” measurements: X. Huyan, J. Wexler, E. Scott

^6He : High energy CRES for chirality flipping interactions

Goal: Measure Fierz interference term “b” in ^6He decay to better than 10^{-3} !

$$dw = dw_0 \left(1 + a \frac{\vec{p}_e}{E_e} \cdot \frac{\vec{p}_\nu}{E_\nu} + b_{\text{Fierz}} \frac{m_e}{E_e} \right) \quad a \approx -\frac{1}{3} \frac{2|C_A|^2 - |C_T|^2 + |C'_T|^2}{2|C_A|^2 + |C_T|^2 + |C'_T|^2} \quad b \approx \frac{\Re(2C_A(C_T + C'_T))}{2|C_A|^2 + |C_T|^2 + |C'_T|^2}$$

Fixed frequency range 18-24 GHZ → Scan B field to scan e^- energy



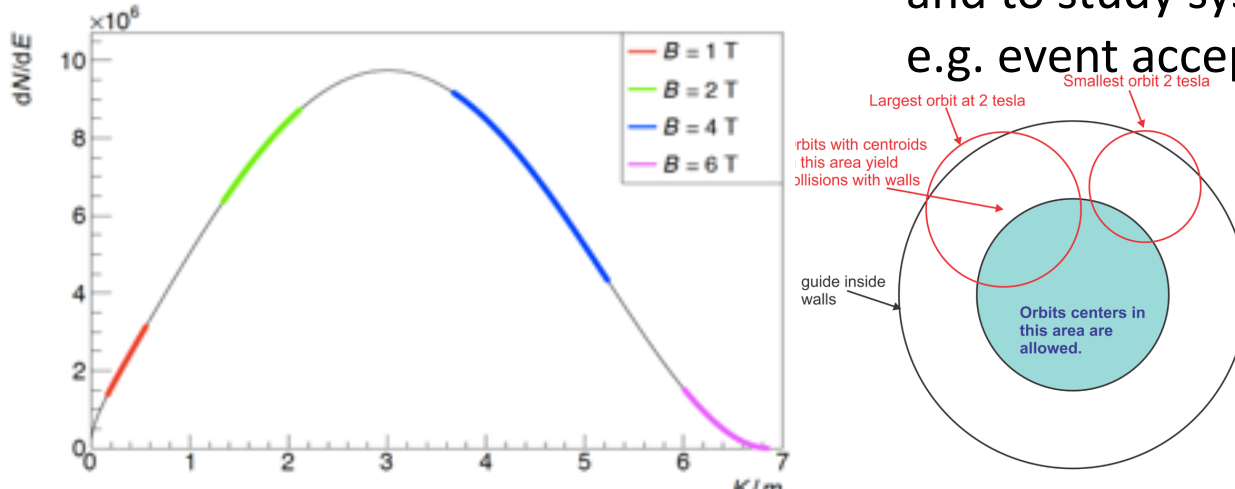
“Fierz” measurements: X. Huyan, J. Wexler, E. Scott

^6He : High energy CRES for chirality flipping interactions

Goal: Measure Fierz interference term “b” in ^6He decay to better than 10^{-3} !

$$dw = dw_0 \left(1 + a \frac{\vec{p}_e}{E_e} \cdot \frac{\vec{p}_\nu}{E_\nu} + b_{\text{Fierz}} \frac{m_e}{E_e} \right) \quad a \approx -\frac{1}{3} \frac{2|C_A|^2 - |C_T|^2 + |C'_T|^2}{2|C_A|^2 + |C_T|^2 + |C'_T|^2} \quad b \approx \frac{\Re(2C_A(C_T + C'_T))}{2|C_A|^2 + |C_T|^2 + |C'_T|^2}$$

Fixed frequency range 18-24 GHZ → Scan B field to scan e^- energy
and to study systematic effects:
e.g. event acceptance vs energy



“Fierz” measurements: X. Huyan, J. Wexler, E. Scott

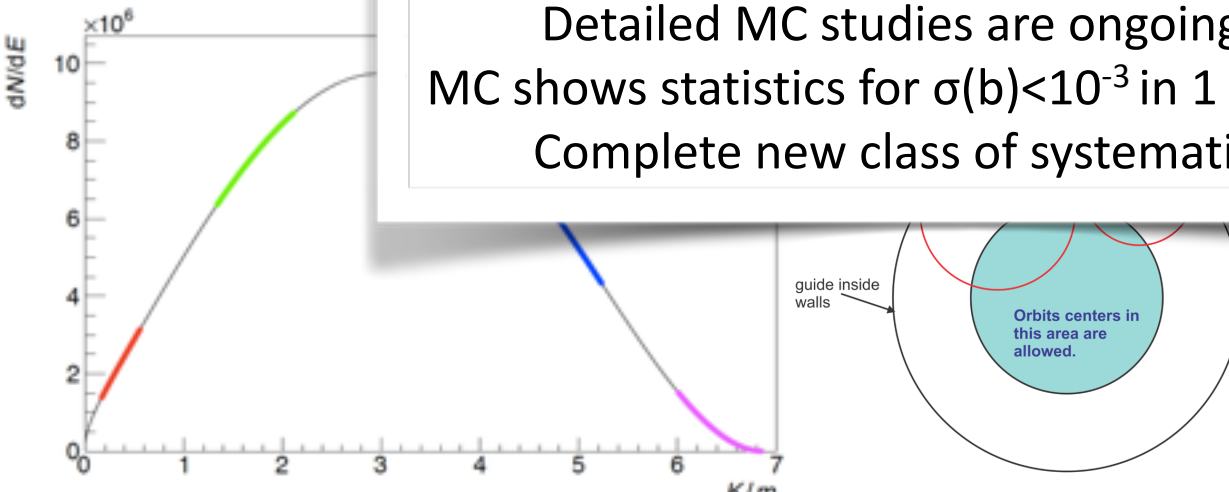
^6He : High energy CRES for chirality flipping interactions

Goal: Measure Fierz interference term “b” in ^6He decay to better than 10^{-3} !

$$dw = dw_0 \left(1 + a \frac{\vec{p}_e}{E_e} \cdot \frac{\vec{p}_\nu}{E_\nu} + b_{\text{Fierz}} \frac{m_e}{E_e} \right) \quad a \approx -\frac{1}{3} \frac{2|C_A|^2 - |C_T|^2 + |C'_T|^2}{2|C_A|^2 + |C_T|^2 + |C'_T|^2} \quad b \approx \frac{\Re(2C_A(C_T + C'_T))}{2|C_A|^2 + |C_T|^2 + |C'_T|^2}$$

Fixed frequency

Expand CRES to high energy range.
Detailed MC studies are ongoing for ^6He .
MC shows statistics for $\sigma(b) < 10^{-3}$ in 1 day @ CENPA.
Complete new class of systematic effects!



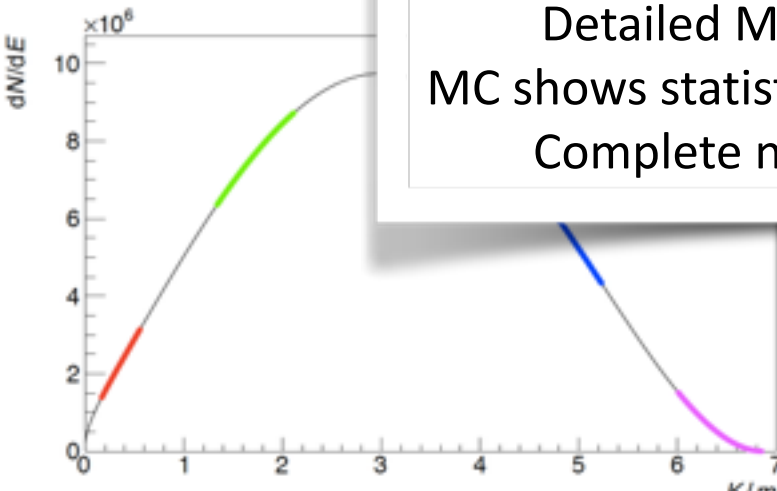
“Fierz” measurements: X. Huyan, J. Wexler, E. Scott

^6He : High energy CRES for chirality flipping interactions

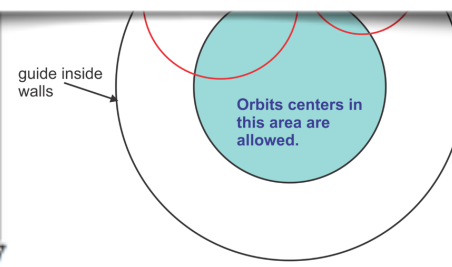
Goal: Measure Fierz interference term “b” in ^6He decay to better than 10^{-3} !

$$dw = dw_0 \left(1 + a \frac{\vec{p}_e}{E_e} \cdot \frac{\vec{p}_\nu}{E_\nu} + b_{\text{Fierz}} \frac{m_e}{E_e} \right) \quad a \approx -\frac{1}{3} \frac{2|C_A|^2 - |C_T|^2 + |C'_T|^2}{2|C_A|^2 + |C_T|^2 + |C'_T|^2} \quad b \approx \frac{\Re(2C_A(C_T + C'_T))}{2|C_A|^2 + |C_T|^2 + |C'_T|^2}$$

Fixed frequency



Expand CRES to high energy range.
Detailed MC studies are ongoing for ^6He .
MC shows statistics for $\sigma(b) < 10^{-3}$ in 1 day @ CENPA.
Complete new class of systematic effects!



“Fierz” measurements: X. Huyan, J. Wexler, E. Scott



The Project 8 collaboration

E.C. Finn, M. Guigue, A. M.Jones, N. S. Oblath, J. R. Tedeschi, B. A. VanDevender

Pacific Northwest National Laboratory, Richland, WA

A. Asthari, R. Cervantes, P. J. Doe, M. Fertl, E. Machado, W. Pettus, R. G. H. Robertson, L. J. Rosenberg, G. Rybka, M. Wachtendonk,

University of Washington, Seattle, WA

J.A. Formaggio, E. M. Zyas

Massachusetts Institute of Technology, Cambridge, MA

L. de Viveiros, B. H. Laroque, B. Monreal

University of California, Santa Barbara, CA

K. M. Heeger, J.A. Nikkel, L. Saldaña, P. Slocum

Yale University , New Haven , CT

Th. Thümmler

Karlsruher Institut fuer Technologie, Karlsruhe, Germany

S. Böser, Ch. Claessens,

Universität Mainz, Mainz, Germany

S. Doeleman, J. Weintraub, A. Young

Harvard-Smithsonian Center for Astrophysics,

K.Kazkaz, Lawrence Livermore National Laboratory

The Project 8 collaboration is supported by:

- U.S. Department of Energy, Office of Science, Office of Nuclear Physics
- National Science Foundation
- Institutional Computing at Pacific Northwest National Laboratory
- University of Washington Royalty Research Foundation
- Massachusetts Institute of Technology Wade Fellowship
- Laboratory Directed Research and Development Program
Pacific Northwest National Laboratory

The collaborations

Project 8



M. Fertl

PSI 10/18/2016

CRES on ${}^6\text{He}$
collaboration forming



UNIVERSITY of WASHINGTON 16

Summary and Outlook

Project 8

- Phase I: 1st observation of cyclotron radiation from a single electron
- Phase I: Successfully measured ^{83m}Kr spectrum using CRES
- Phase II: Taking commissioning data with ^{83m}Kr to prepare for molecular tritium gas
- Phase III and IV: planning and design ongoing in parallel

CRES on ^6He : Fierz interference term “b” beyond 10^{-3} seems promising

Thank you!

CENPA is hiring post docs

<https://www.npl.washington.edu/cenpa-jobs>

Post Doc positions open for

^6He CRES spectroscopy

$^{10}\text{v}\beta\beta$ decay with Majorana

RF axion search with ADMX

The University of Washington Center for Experimental Nuclear Physics and Astrophysics (CENPA) has immediate openings for postdoctoral appointments for work on one or more of the following experiments: the Axion Dark-Matter eXperiment (ADMX), which is a RF-cavity search for axion dark matter in our galactic halo; a ^6He beta decay experiment that is searching for non-standard-model currents in weak decays; and the Majorana Demonstrator, which is testing the Majorana nature of the neutrino.

Back up slides



The PMNS matrix elements

Oscillation experiments depend on PNMS matrix and mass differences:

“solar” mixing angle

$$\begin{pmatrix} 1 & 0 & 0 \\ 0 & \cos \theta_{23} & \sin \theta_{23} \\ 0 & -\sin \theta_{23} & \cos \theta_{23} \end{pmatrix}$$

“atmospheric” mixing angle

$$\begin{pmatrix} \cos \theta_{13} & 0 & \sin \theta_{13} e^{-i\delta_{CP}} \\ 0 & 1 & 0 \\ -\sin \theta_{13} e^{i\delta_{CP}} & 0 & \cos \theta_{13} \end{pmatrix}$$

$$\begin{pmatrix} \cos \theta_{12} & \sin \theta_{12} & 0 \\ -\sin \theta_{12} & \cos \theta_{12} & 0 \\ 0 & 0 & 1 \end{pmatrix}$$

$$\begin{pmatrix} 1 & 0 & 0 \\ 0 & e^{i\frac{\alpha_{21}}{2}} & 0 \\ 0 & 0 & e^{i\frac{\alpha_{31}}{2}} \end{pmatrix}$$

The PMNS matrix elements

Oscillation experiments depend on PNMS matrix and mass differences:

“solar” mixing angle

$$\begin{pmatrix} 1 & 0 & 0 \\ 0 & \cos \theta_{23} & \sin \theta_{23} \\ 0 & -\sin \theta_{23} & \cos \theta_{23} \end{pmatrix}$$

$$\begin{pmatrix} \cos \theta_{13} & 0 & \sin \theta_{13} e^{-i\delta_{CP}} \\ 0 & 1 & 0 \\ -\sin \theta_{13} e^{i\delta_{CP}} & 0 & \cos \theta_{13} \end{pmatrix}$$

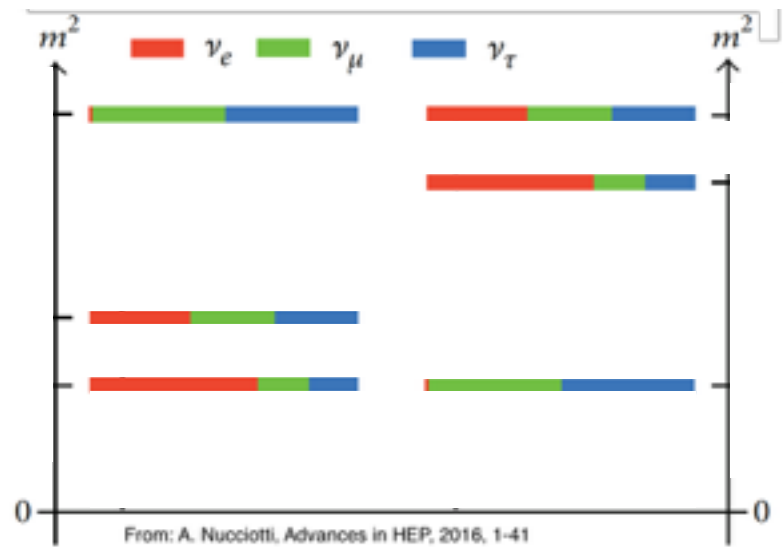
“atmospheric” mixing angle

$$\begin{pmatrix} \cos \theta_{12} & \sin \theta_{12} & 0 \\ -\sin \theta_{12} & \cos \theta_{12} & 0 \\ 0 & 0 & 1 \end{pmatrix}$$

$$\begin{pmatrix} 1 & 0 & 0 \\ 0 & e^{i\frac{\alpha_{21}}{2}} & 0 \\ 0 & 0 & e^{i\frac{\alpha_{31}}{2}} \end{pmatrix}$$

LARGE mixing angles

$$\theta_{23} \approx 45^\circ, \theta_{13} \approx 9^\circ, \theta_{12} \approx 34^\circ$$



The PMNS matrix elements

Oscillation experiments depend on PNMS matrix and mass differences:

“solar” mixing angle

$$\begin{pmatrix} 1 & 0 & 0 \\ 0 & \cos \theta_{23} & \sin \theta_{23} \\ 0 & -\sin \theta_{23} & \cos \theta_{23} \end{pmatrix}$$

$$\begin{pmatrix} \cos \theta_{13} & 0 & \sin \theta_{13} e^{-i\delta_{CP}} \\ 0 & 1 & 0 \\ -\sin \theta_{13} e^{i\delta_{CP}} & 0 & \cos \theta_{13} \end{pmatrix}$$

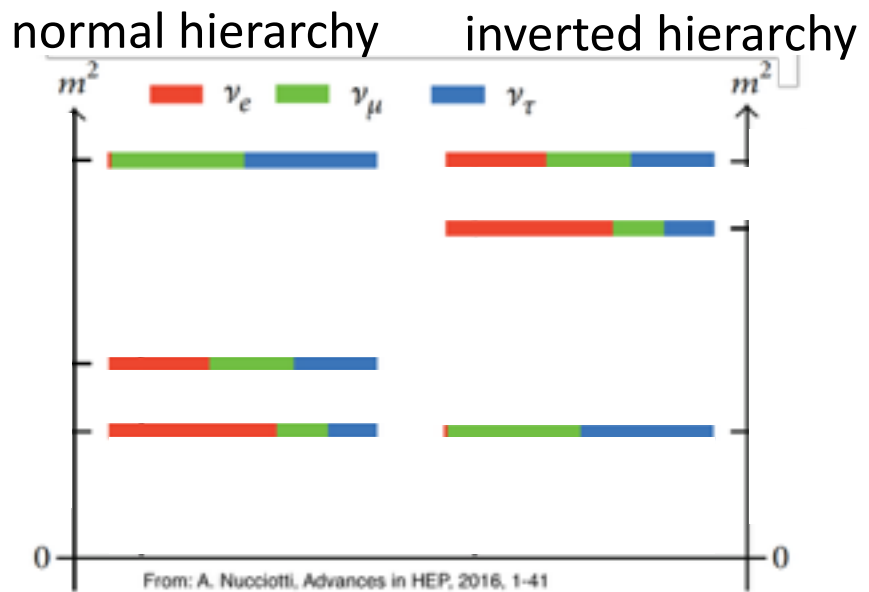
“atmospheric” mixing angle

$$\begin{pmatrix} \cos \theta_{12} & \sin \theta_{12} & 0 \\ -\sin \theta_{12} & \cos \theta_{12} & 0 \\ 0 & 0 & 1 \end{pmatrix}$$

$$\begin{pmatrix} 1 & 0 & 0 \\ 0 & e^{i\frac{\alpha_{21}}{2}} & 0 \\ 0 & 0 & e^{i\frac{\alpha_{31}}{2}} \end{pmatrix}$$

LARGE mixing angles

$$\theta_{23} \approx 45^\circ, \theta_{13} \approx 9^\circ, \theta_{12} \approx 34^\circ$$



The PMNS matrix elements

Oscillation experiments depend on PNMS matrix and mass differences:

“solar” mixing angle

$$\begin{pmatrix} 1 & 0 & 0 \\ 0 & \cos \theta_{23} & \sin \theta_{23} \\ 0 & -\sin \theta_{23} & \cos \theta_{23} \end{pmatrix}$$

$$\begin{pmatrix} \cos \theta_{13} & 0 & \sin \theta_{13} e^{-i\delta_{CP}} \\ 0 & 1 & 0 \\ -\sin \theta_{13} e^{i\delta_{CP}} & 0 & \cos \theta_{13} \end{pmatrix}$$

“atmospheric” mixing angle

$$\begin{pmatrix} \cos \theta_{12} & \sin \theta_{12} & 0 \\ -\sin \theta_{12} & \cos \theta_{12} & 0 \\ 0 & 0 & 1 \end{pmatrix}$$

$$\begin{pmatrix} 1 & 0 & 0 \\ 0 & e^{i\frac{\alpha_{21}}{2}} & 0 \\ 0 & 0 & e^{i\frac{\alpha_{31}}{2}} \end{pmatrix}$$

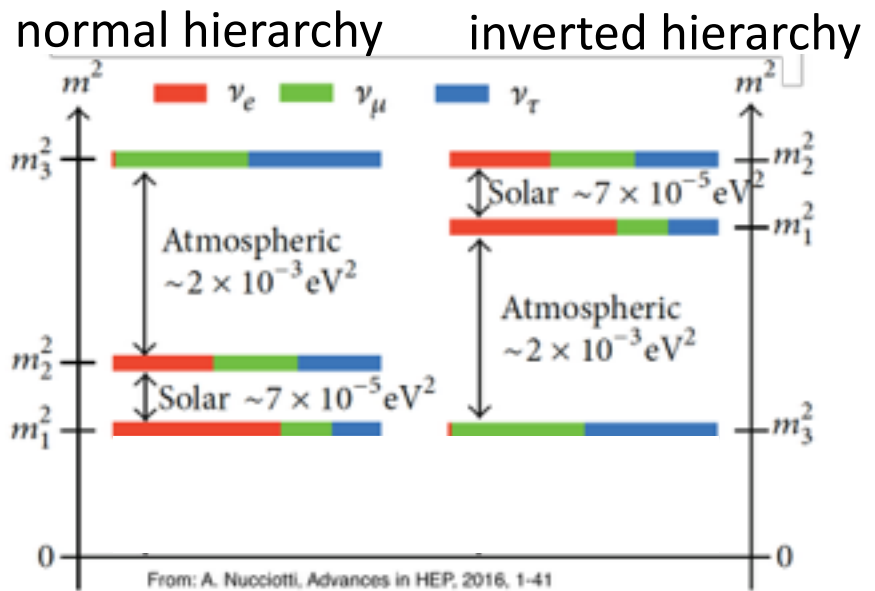
LARGE mixing angles

TINY mass differences

$$\theta_{23} \approx 45^\circ, \theta_{13} \approx 9^\circ, \theta_{12} \approx 34^\circ$$

$$\Delta m_{21}^2 = m_2^2 - m_1^2 \approx 8 \times 10^{-5} \text{ eV}^2$$

$$|\Delta m_{32}^2| = m_3^2 - m_2^2 \approx 2.5 \times 10^{-3} \text{ eV}^2$$



The PMNS matrix elements

Oscillation experiments depend on PNMS matrix and mass terms

Oscillation have no sensitivity
to Majorana phases

“solar” mixing angle

$$\begin{pmatrix} 1 & 0 & 0 \\ 0 & \cos \theta_{23} & \sin \theta_{23} \\ 0 & -\sin \theta_{23} & \cos \theta_{23} \end{pmatrix}$$

$$\begin{pmatrix} \cos \theta_{13} & 0 & \sin \theta_{13} e^{-i\delta_{CP}} \\ 0 & 1 & 0 \\ -\sin \theta_{13} e^{i\delta_{CP}} & 0 & \cos \theta_{13} \end{pmatrix}$$

“atmospheric” mixing angle

$$\begin{pmatrix} \cos \theta_{12} & \sin \theta_{12} & 0 \\ -\sin \theta_{12} & \cos \theta_{12} & 0 \\ 0 & 0 & 1 \end{pmatrix}$$

$$\begin{pmatrix} 1 & 0 & 0 \\ 0 & e^{i\frac{\alpha_{21}}{2}} & 0 \\ 0 & 0 & e^{i\frac{\alpha_{31}}{2}} \end{pmatrix}$$

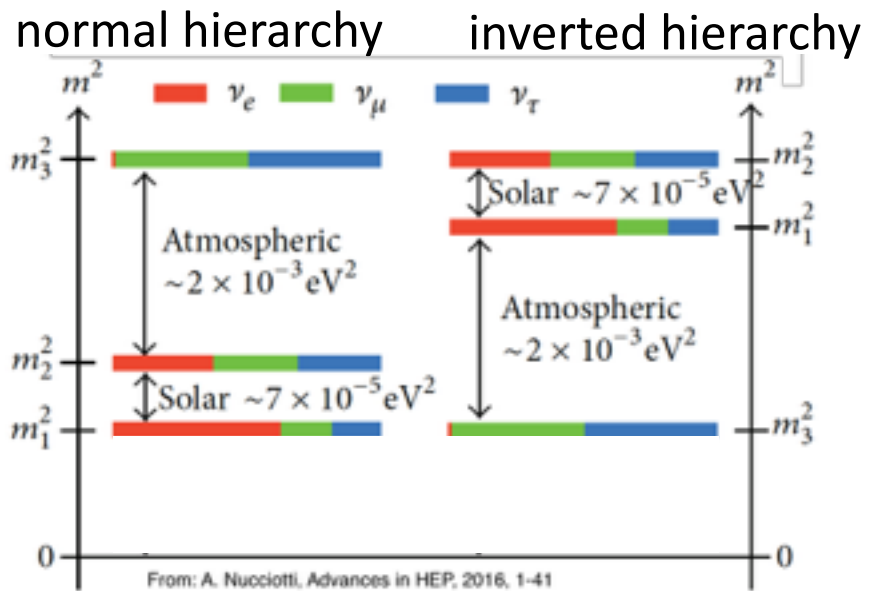
LARGE mixing angles

TINY mass differences

$$\theta_{23} \approx 45^\circ, \theta_{13} \approx 9^\circ, \theta_{12} \approx 34^\circ$$

$$\Delta m_{21}^2 = m_2^2 - m_1^2 \approx 8 \times 10^{-5} \text{ eV}^2$$

$$|\Delta m_{32}^2| = m_3^2 - m_2^2 \approx 2.5 \times 10^{-3} \text{ eV}^2$$



The PMNS matrix elements

Oscillation experiments depend on PNMS matrix and mass

Oscillation have no sensitivity
to Majorana phases

“solar” mixing angle

$$\begin{pmatrix} 1 & 0 & 0 \\ 0 & \cos \theta_{23} & \sin \theta_{23} \\ 0 & -\sin \theta_{23} & \cos \theta_{23} \end{pmatrix}$$

$$\begin{pmatrix} \cos \theta_{13} & 0 & \sin \theta_{13} e^{-i\delta_{CP}} \\ 0 & 1 & 0 \\ -\sin \theta_{13} e^{i\delta_{CP}} & 0 & \cos \theta_{13} \end{pmatrix}$$

“atmospheric” mixing angle

$$\begin{pmatrix} \cos \theta_{12} & \sin \theta_{12} & 0 \\ -\sin \theta_{12} & \cos \theta_{12} & 0 \\ 0 & 0 & 1 \end{pmatrix}$$

$$\begin{pmatrix} 1 & 0 & 0 \\ 0 & e^{i\frac{\alpha_{21}}{2}} & 0 \\ 0 & 0 & e^{i\frac{\alpha_{31}}{2}} \end{pmatrix}$$

LARGE mixing angles

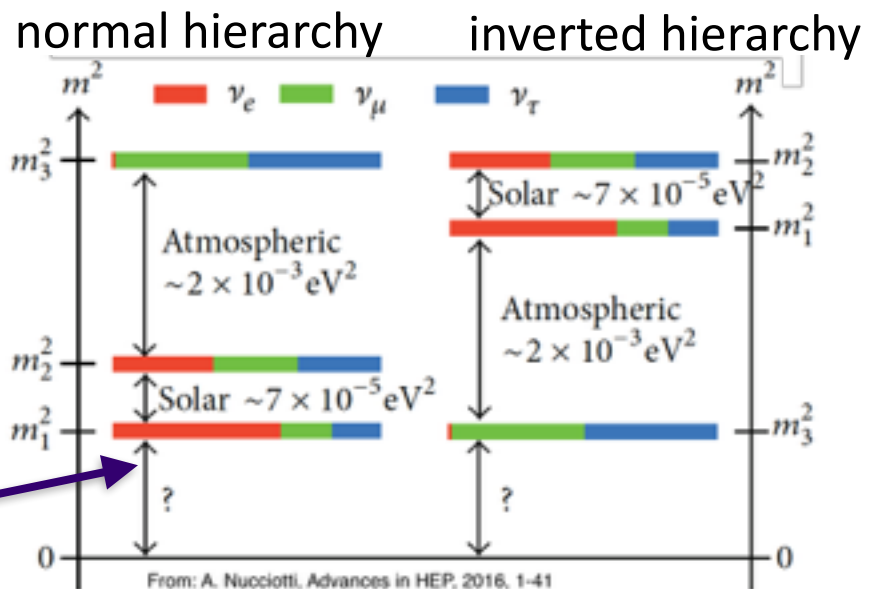
TINY mass differences

$$\theta_{23} \approx 45^\circ, \theta_{13} \approx 9^\circ, \theta_{12} \approx 34^\circ$$

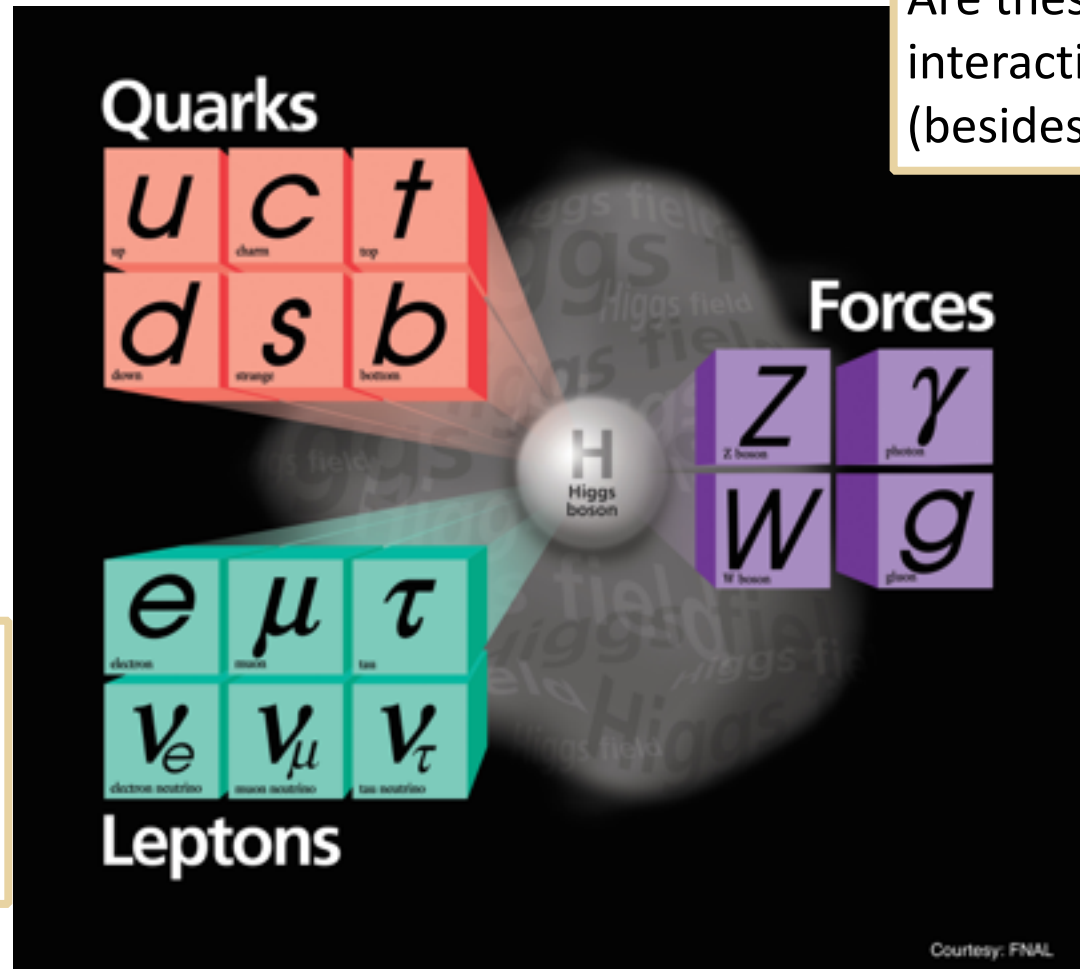
$$\Delta m_{21}^2 = m_2^2 - m_1^2 \approx 8 \times 10^{-5} \text{ eV}^2$$

$$|\Delta m_{32}^2| = m_3^2 - m_2^2 \approx 2.5 \times 10^{-3} \text{ eV}^2$$

No sensitivity to absolute mass scale



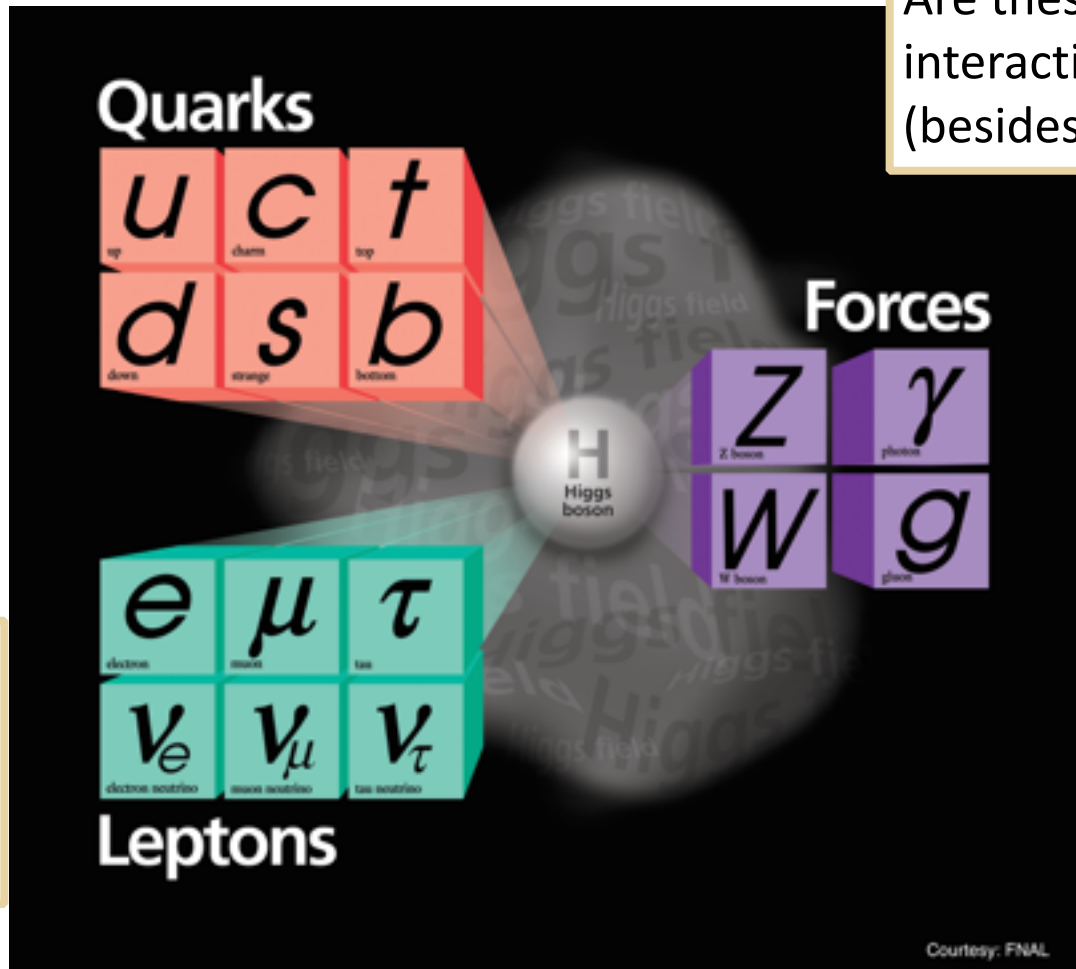
The Standard Model of Particle Physics in one picture



What are the neutrino masses?
How do neutrinos obtain mass?

Are these the only interactions in nature (besides gravity)?

The Standard Model of Particle Physics in one picture



What are the neutrino masses?
How do neutrinos obtain mass?

Are these the only interactions in nature (besides gravity)?

Beta decay electron spectrum

With neutrino mixing and nuclear recoil for T_{nuc} :

$$\frac{dN}{dE_e} = \frac{G_F^2 m_e^5 \cos^2 \theta_C}{2\pi^3 \hbar^7} |M_{\text{nuc}}|^2 F(Z, E_e) p_e E_e \sum_i |U_{ei}|^2 (E_{\max} - E_e) \\ \times \sqrt{(E_{\max} - E_e)^2 - m_{\nu i}^2} \cdot \Theta(E_{\max} - E_e - m_{\nu i})$$

For unresolved neutrino mass splitting:

$$m(\nu_e) = \sqrt{\sum_i |U_{e,i}|^2 m_i^2}$$

Spectrum of certain nuclei can be used
to search for chirality flipping interactions

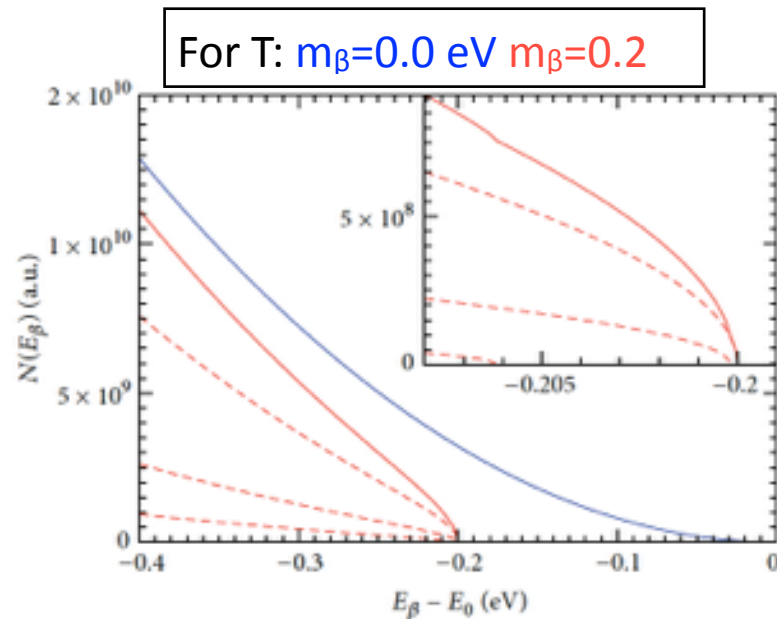
Beta decay electron spectrum

With neutrino mixing and nuclear recoil for T_{nuc} :

$$\frac{dN}{dE_e} = \frac{G_F^2 m_e^5 \cos^2 \theta_C}{2\pi^3 \hbar^7} |M_{\text{nuc}}|^2 F(Z, E_e) p_e E_e \sum_i |U_{ei}|^2 (E_{\max} - E_e) \\ \times \sqrt{(E_{\max} - E_e)^2 - m_{\nu i}^2} \cdot \Theta(E_{\max} - E_e - m_{\nu i})$$

For unresolved neutrino mass splitting:

$$m(\nu_e) = \sqrt{\sum_i |U_{e,i}|^2 m_i^2}$$



Nucciotti, Advances in High Energy Physics, Vol. 2016, 9153024

Spectrum of certain nuclei can be used
to search for chirality flipping interactions

Beta decay electron spectrum

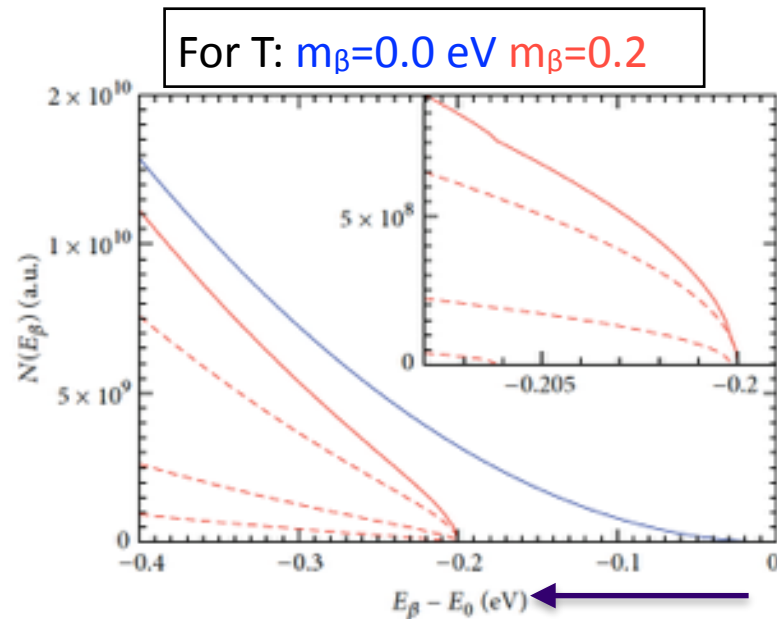
With neutrino mixing and nuclear recoil for T_{nuc} :

$$\frac{dN}{dE_e} = \frac{G_F^2 m_e^5 \cos^2 \theta_C}{2\pi^3 \hbar^7} |M_{\text{nuc}}|^2 F(Z, E_e) p_e E_e \sum_i |U_{ei}|^2 (E_{\max} - E_e) \\ \times \sqrt{(E_{\max} - E_e)^2 - m_{\nu i}^2} \cdot \Theta(E_{\max} - E_e - m_{\nu i})$$

For unresolved neutrino mass splitting:

$$m(\nu_e) = \sqrt{\sum_i |U_{e,i}|^2 m_i^2}$$

$$BR \approx \left(\frac{\delta E}{E_0} \right)^3$$



Spectrum of certain nuclei can be used to search for chirality flipping interactions

Beta decay electron spectrum

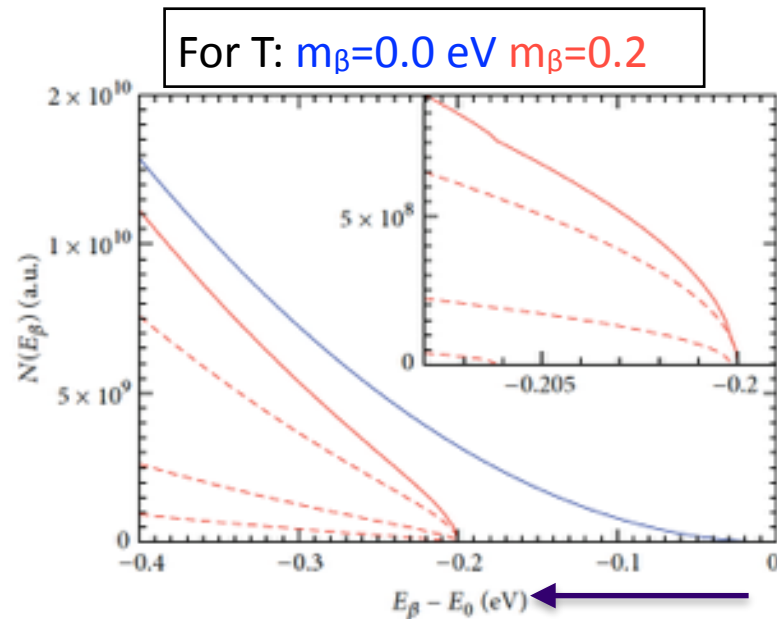
With neutrino mixing and nuclear recoil for T_{nuc} :

$$\frac{dN}{dE_e} = \frac{G_F^2 m_e^5 \cos^2 \theta_C}{2\pi^3 \hbar^7} |M_{\text{nuc}}|^2 F(Z, E_e) p_e E_e \sum_i |U_{ei}|^2 (E_{\max} - E_e) \\ \times \sqrt{(E_{\max} - E_e)^2 - m_{\nu i}^2} \cdot \Theta(E_{\max} - E_e - m_{\nu i})$$

For unresolved neutrino mass splitting:

$$m(\nu_e) = \sqrt{\sum_i |U_{e,i}|^2 m_i^2}$$

$$BR \approx \left(\frac{\delta E}{E_0} \right)^3$$



Nucciotti, Advances in High Energy Physics, Vol. 2016, 9153024

Tritium

$$Q(T_A) = 18.59201(7) \text{ keV}$$

Super allowed transition

$$T_{1/2} = 12.32 \text{ y}$$

$$BR(1\text{eV}) = 2 \times 10^{-13}$$

Spectrum of certain nuclei can be used to search for chirality flipping interactions

Myers et al, PRL 114, 013033, 2015

M. Fertl

PSI 10/18/2016

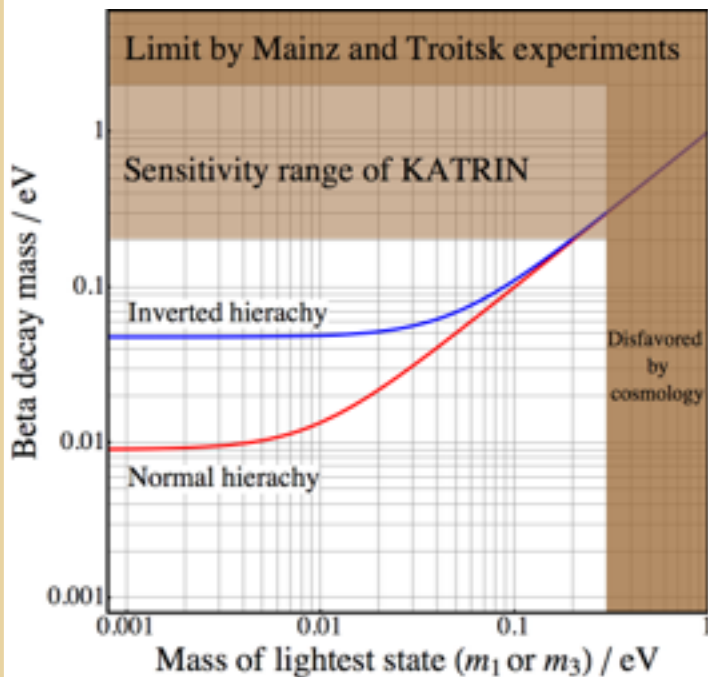
UNIVERSITY of WASHINGTON

22

Anti-electron neutrino mass limits from tritium beta decay experiments

$T_2 \beta^-$ decay kinematics
Super allowed transition

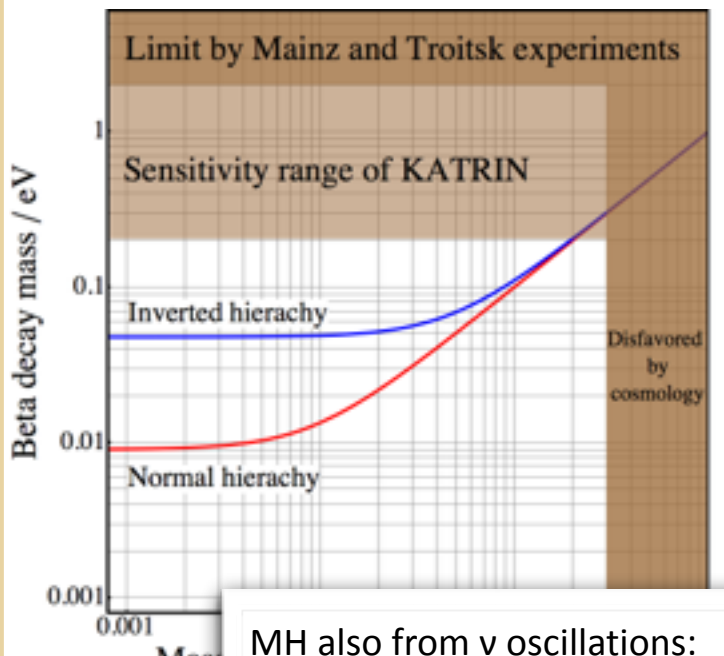
$$T_{1/2} = 12.32 \text{ y}$$
$$\text{BR (1eV)} = 2 \times 10^{-13}$$



Anti-electron neutrino mass limits from tritium beta decay experiments

$T_2 \beta^-$ decay kinematics
Super allowed transition

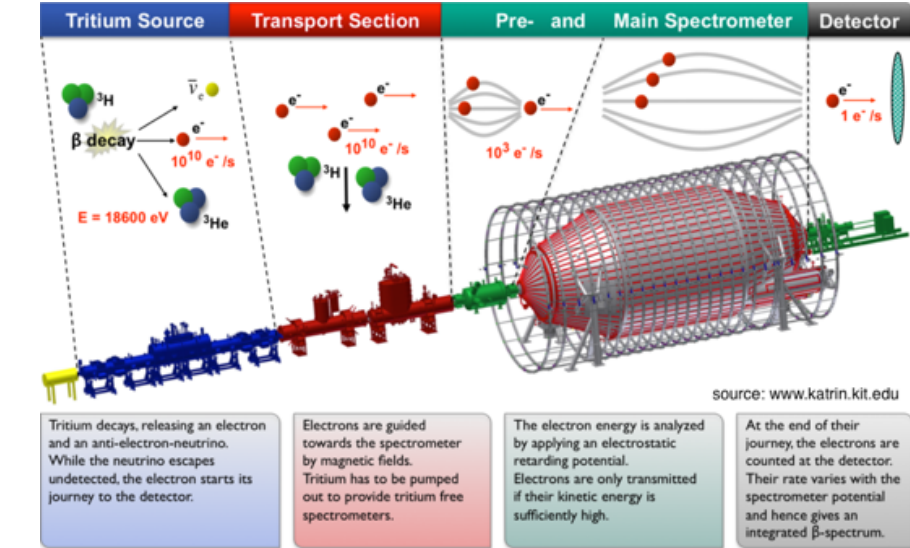
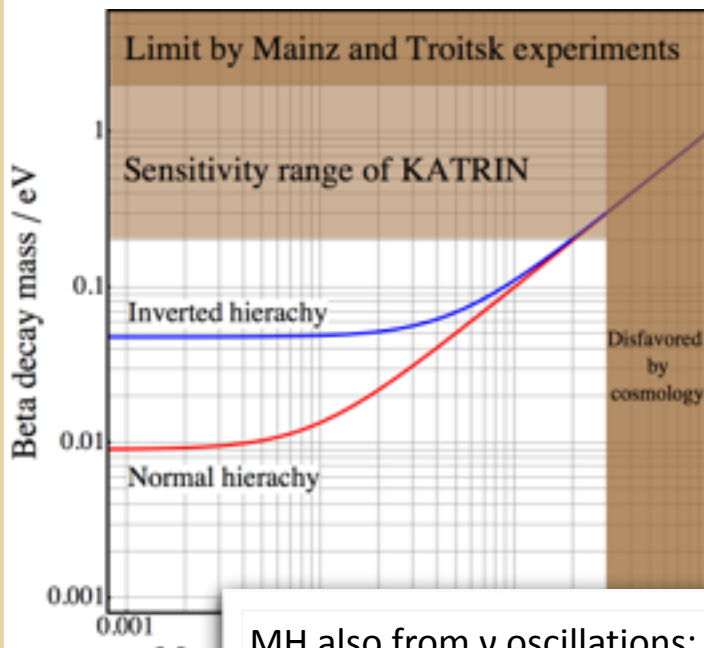
$$T_{1/2} = 12.32 \text{ y}$$
$$\text{BR (1eV)} = 2 \times 10^{-13}$$



Anti-electron neutrino mass limits from tritium beta decay experiments

$T_2 \beta^-$ decay kinematics
Super allowed transition

$$T_{1/2} = 12.32 \text{ y}$$
$$\text{BR (1eV)} = 2 \times 10^{-13}$$



- Window less gaseous T_2 source (10^{11} Bq)
- MAC-E filter technique scales like area
- Column density limited, T_2 final states
- Sensitivity: $< 200 \text{ meV}$ (90% CL)

First light in October 2016!

Highest precision measurements ...

... often follow A. Schawlow's advice:

“Never measure anything but frequency”



Highest precision measurements ...

... often follow A. Schawlow's advice:

“Never measure anything but frequency”



Hydrogen 1S-2S

$$\sigma = 4.2 \cdot 10^{-15}$$

Hänsch et al., 2011

Electron g-factor

$$\sigma = 2.8 \cdot 10^{-13}$$

Gabrielse et al., 2008

G. Gabrielse, Mon 11:00

Electron mass in u

$$\sigma = 2.9 \cdot 10^{-11}$$

Sturm et al., 2014

K. Blaum, Tue 11:00

Highest precision measurements ...

... often follow A. Schawlow's advice:

"Never measure anything but frequency"



Hydrogen 1S-2S
 $\sigma = 4.2 \cdot 10^{-15}$

Hänsch et al., 2011

Electron g-factor
 $\sigma = 2.8 \cdot 10^{-13}$

Gabrielse et al., 2008

Electron mass in u
 $\sigma = 2.9 \cdot 10^{-11}$

Sturm et al., 2014

G. Gabrielse, Mon 11:00

K. Blaum, Tue 11:00

New frequency based measurements also for:

Anti-electron neutrino mass

New chirality flipping interactions?

The cyclotron frequency in a nutshell

Feb. 20, 1934.

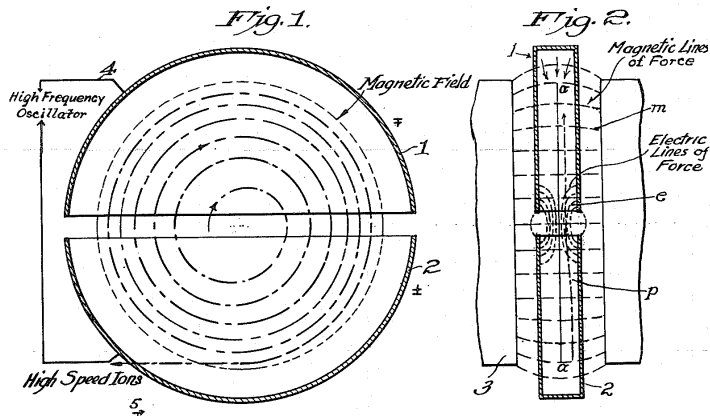
E. O. LAWRENCE

1,948,384

METHOD AND APPARATUS FOR THE ACCELERATION OF IONS

Filed Jan. 26, 1932

2 Sheets-Sheet 1



The cyclotron frequency in a nutshell

Feb. 20, 1934.

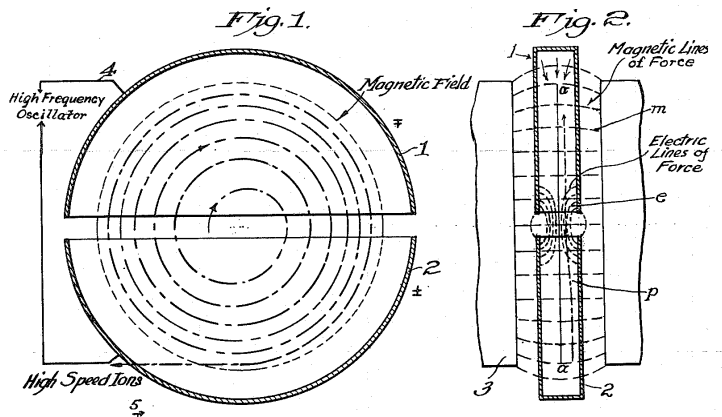
E. O. LAWRENCE

1,948,384

METHOD AND APPARATUS FOR THE ACCELERATION OF IONS

Filed Jan. 26, 1932

2 Sheets-Sheet 1



Cyclotron motion:

The cyclotron frequency in a nutshell

Feb. 20, 1934.

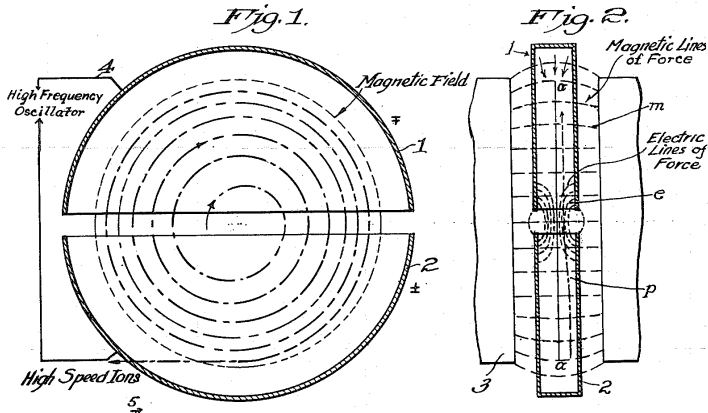
E. O. LAWRENCE

1,948,384

METHOD AND APPARATUS FOR THE ACCELERATION OF IONS

Filed Jan. 26, 1932

2 Sheets-Sheet 1



Cyclotron motion:

- Only charged particles

The cyclotron frequency in a nutshell

Feb. 20, 1934.

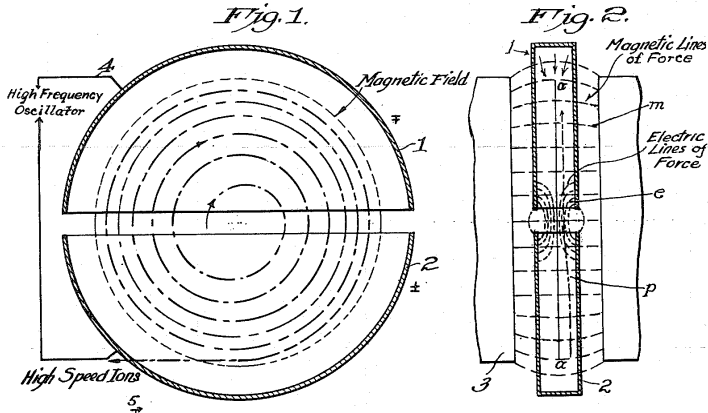
E. O. LAWRENCE

1,948,384

METHOD AND APPARATUS FOR THE ACCELERATION OF IONS

Filed Jan. 26, 1932

2 Sheets-Sheet 1



Cyclotron motion:

- Only charged particles
- In non relativistic limit a ratio of precisely measured constants

$$f_{c,0} = \frac{1}{2\pi} \frac{eB}{m_e}$$

The cyclotron frequency in a nutshell

Feb. 20, 1934.

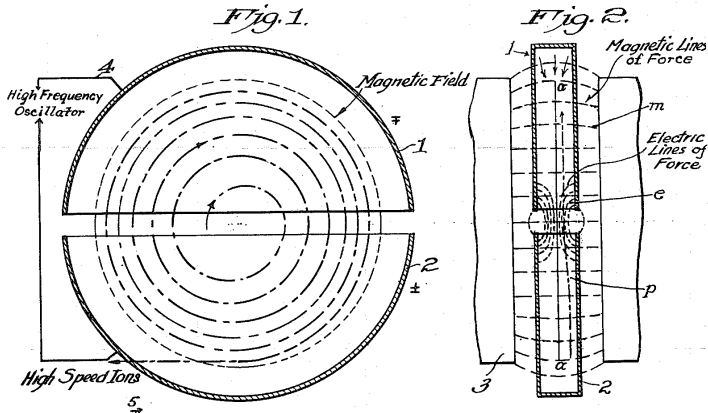
E. O. LAWRENCE

1,948,384

METHOD AND APPARATUS FOR THE ACCELERATION OF IONS

Filed Jan. 26, 1932

2 Sheets-Sheet 1



Cyclotron motion:

- Only charged particles
- In non relativistic limit a ratio of precisely measured constants
- Energy dependent (Lorentz factor)

$$f_{c,0} = \frac{1}{2\pi} \frac{eB}{m_e}$$

$$f_c = \frac{f_{c,0}}{\gamma} = \frac{1}{2\pi} \frac{eB}{m_e + E_{\text{kin}}/c^2}$$

The cyclotron frequency in a nutshell

Feb. 20, 1934.

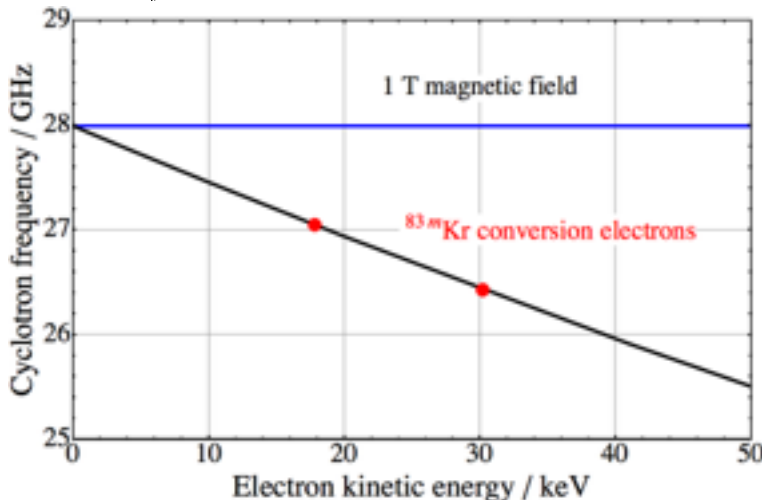
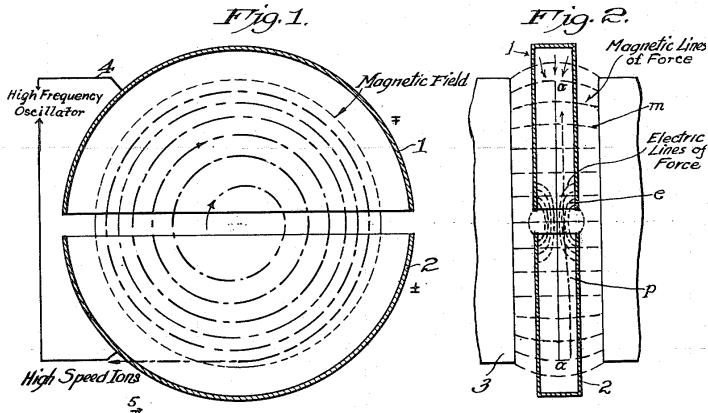
E. O. LAWRENCE

1,948,384

METHOD AND APPARATUS FOR THE ACCELERATION OF IONS

Filed Jan. 26, 1932

2 Sheets-Sheet 1



Cyclotron motion:

- Only charged particles
- In non relativistic limit a ratio of precisely measured constants

$$f_{c,0} = \frac{1}{2\pi} \frac{eB}{m_e}$$

- Energy dependent (Lorentz factor)

$$f_c = \frac{f_{c,0}}{\gamma} = \frac{1}{2\pi} \frac{eB}{m_e + E_{\text{kin}}/c^2}$$

The cyclotron frequency in a nutshell

Feb. 20, 1934.

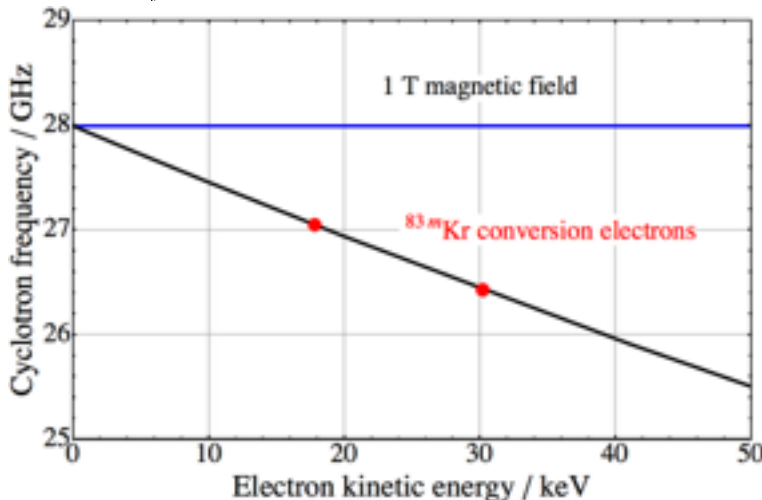
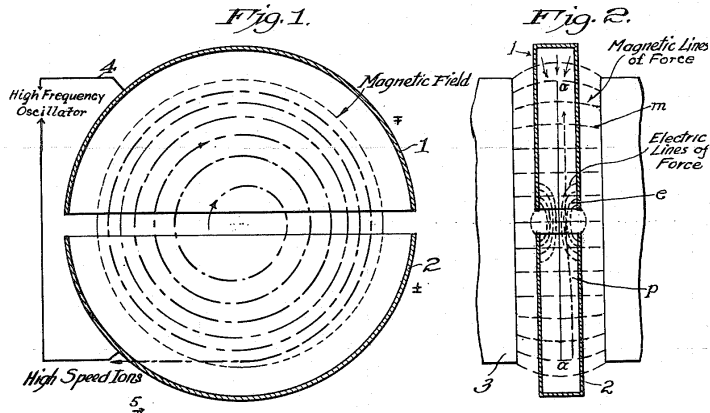
E. O. LAWRENCE

1,948,384

METHOD AND APPARATUS FOR THE ACCELERATION OF IONS

Filed Jan. 26, 1932

2 Sheets-Sheet 1



Cyclotron motion:

- Only charged particles
- In non relativistic limit a ratio of precisely measured constants

$$f_{c,0} = \frac{1}{2\pi} \frac{eB}{m_e}$$

- Energy dependent (Lorentz factor)

$$f_c = \frac{f_{c,0}}{\gamma} = \frac{1}{2\pi} \frac{eB}{m_e + E_{\text{kin}}/c^2}$$



Limits the cyclotron
as accelerator

The cyclotron frequency in a nutshell

Feb. 20, 1934.

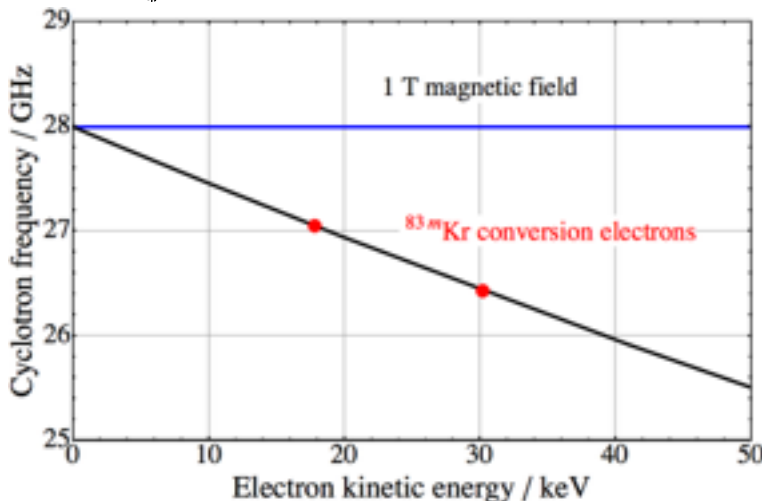
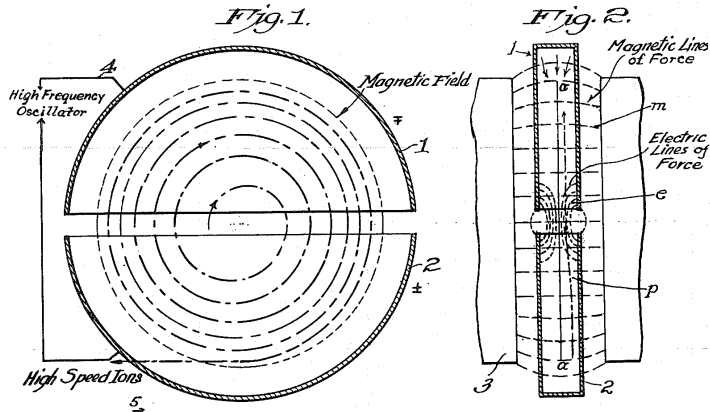
E. O. LAWRENCE

1,948,384

METHOD AND APPARATUS FOR THE ACCELERATION OF IONS

Filed Jan. 26, 1932

2 Sheets-Sheet 1



Cyclotron motion:

- Only charged particles
- In non relativistic limit a ratio of precisely measured constants

$$f_{c,0} = \frac{1}{2\pi} \frac{eB}{m_e}$$

- Energy dependent (Lorentz factor)

$$f_c = \frac{f_{c,0}}{\gamma} = \frac{1}{2\pi} \frac{eB}{m_e + E_{kin}/c^2}$$

Limits the cyclotron
as accelerator

Measurement of
kinetic energy!

Axial motion: side band generation

Harmonic magnetic bottle introduces a degeneracy between kinetic energy and pitch angle!

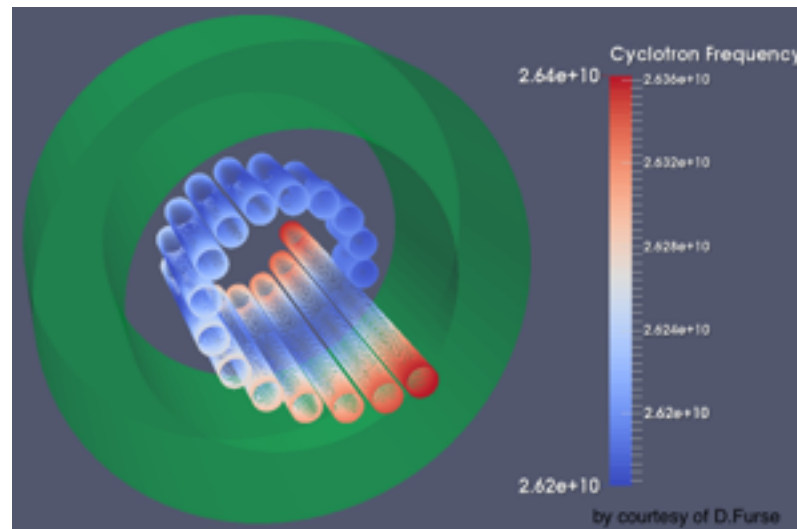
$$f_c = \frac{eB}{m + E_{\text{kin}}/c^2} \left(1 + \frac{\cot^2 \theta}{2} \right)$$

Axial motion: side band generation

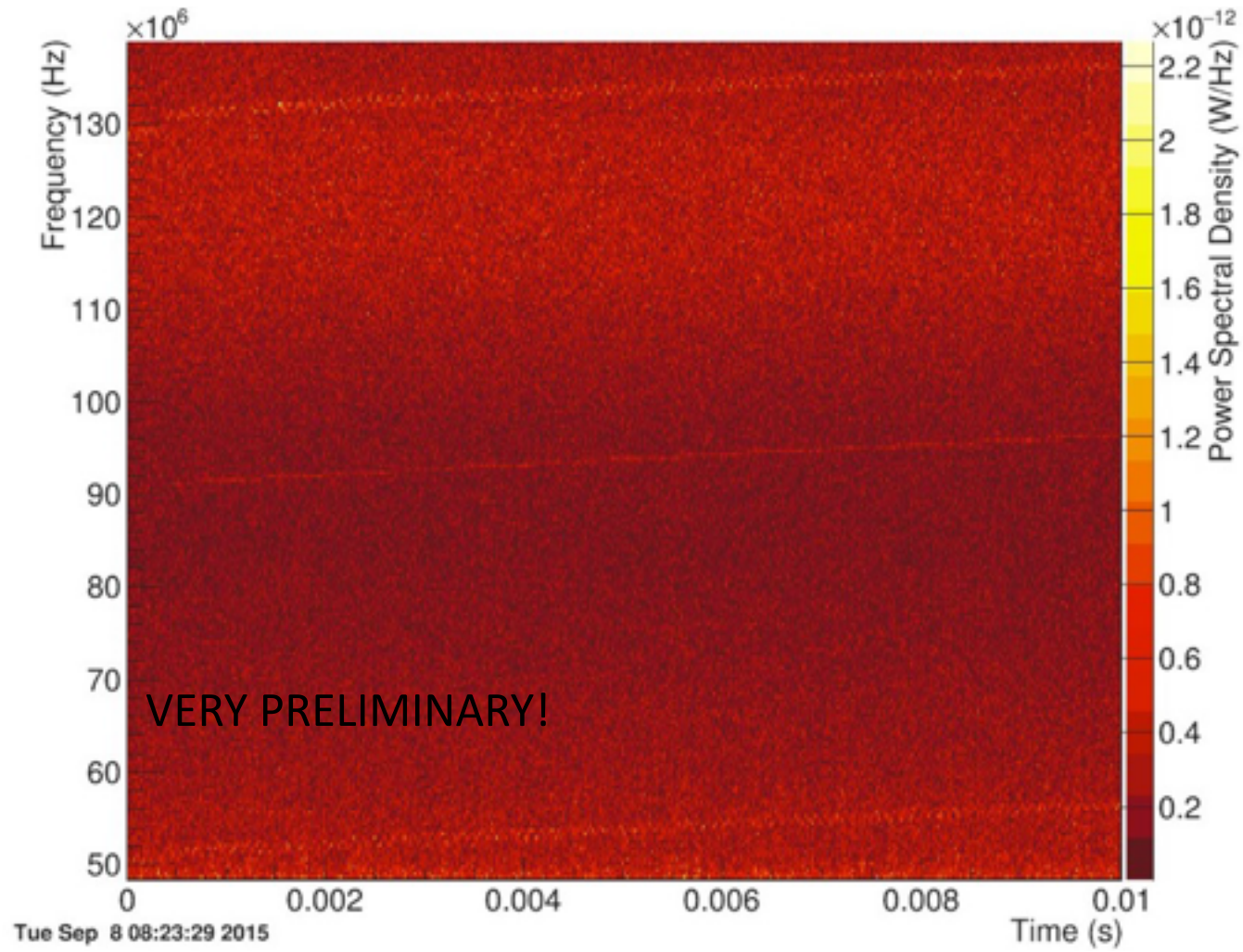
Harmonic magnetic bottle introduces a degeneracy between kinetic energy and pitch angle!

$$f_c = \frac{eB}{m + E_{\text{kin}}/c^2} \left(1 + \frac{\cot^2 \theta}{2} \right)$$

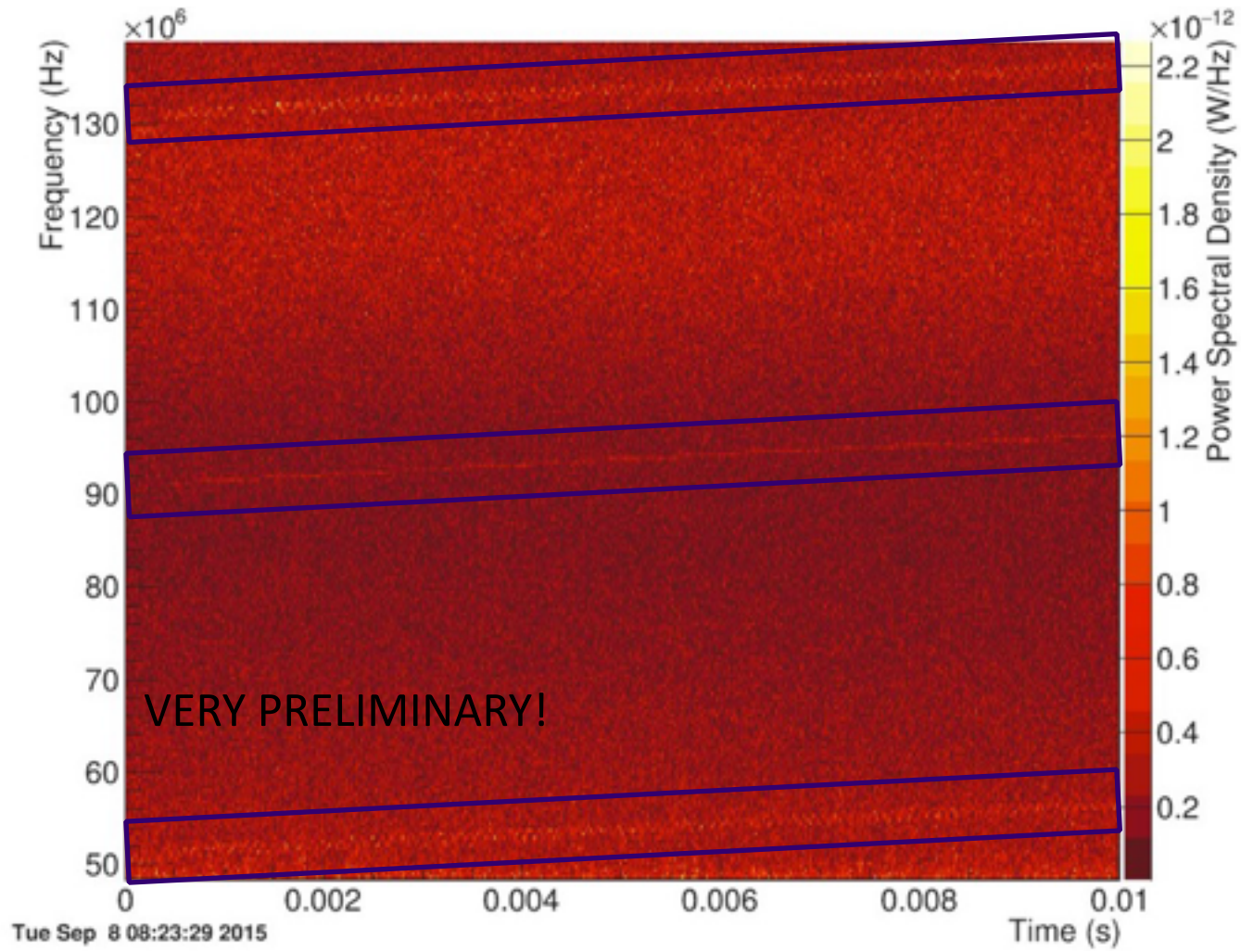
Axial electron motion → Modulation of cyclotron frequency → Side band generation



Axial motion: side band generation

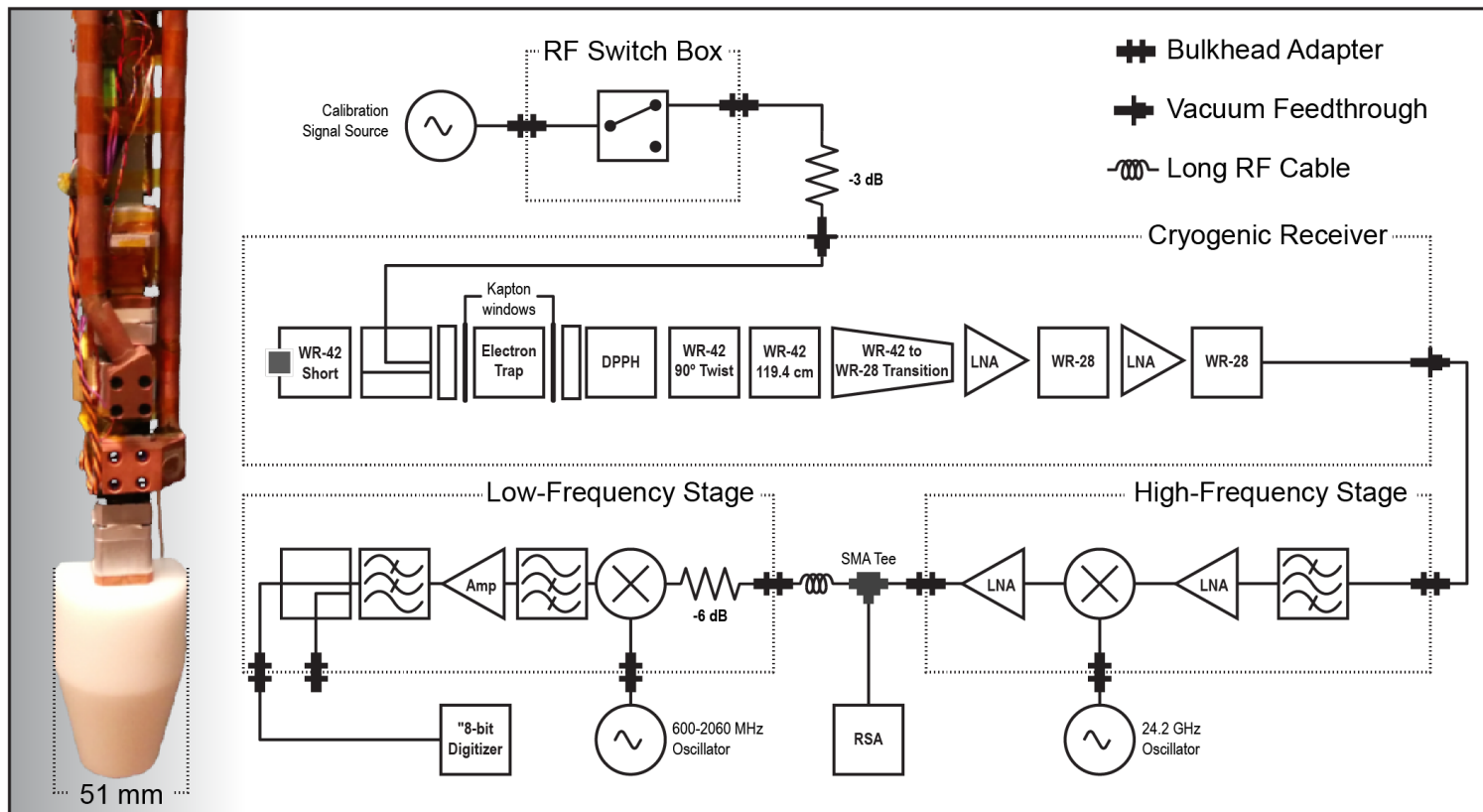


Axial motion: side band generation

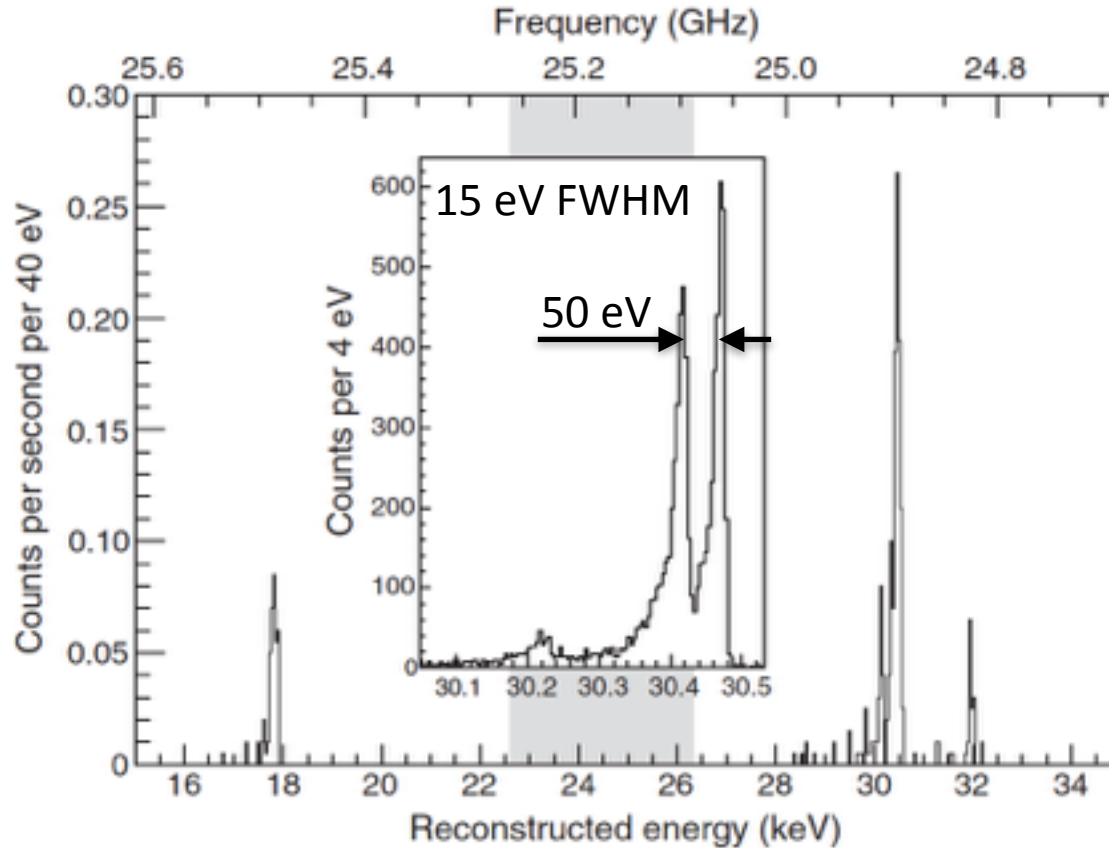


The microwave detector

- Cryogenic preamplifiers (50K physical temp.)
- Double stage frequency mixing (24.2 GHz, 0.6 GHz to 1.2 GHz)

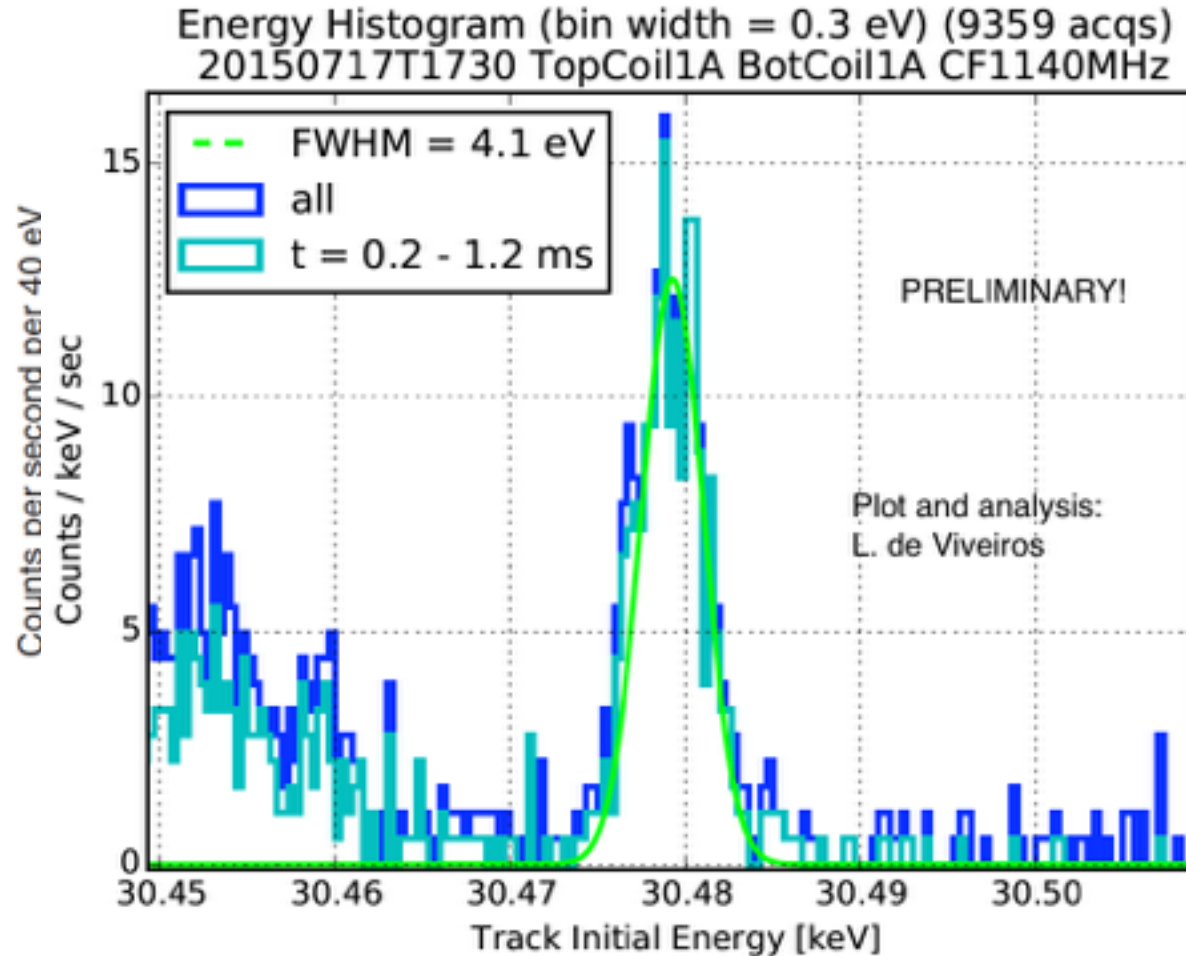


A cyclotron radiation emission spectrum of ^{83m}Kr conversion electrons

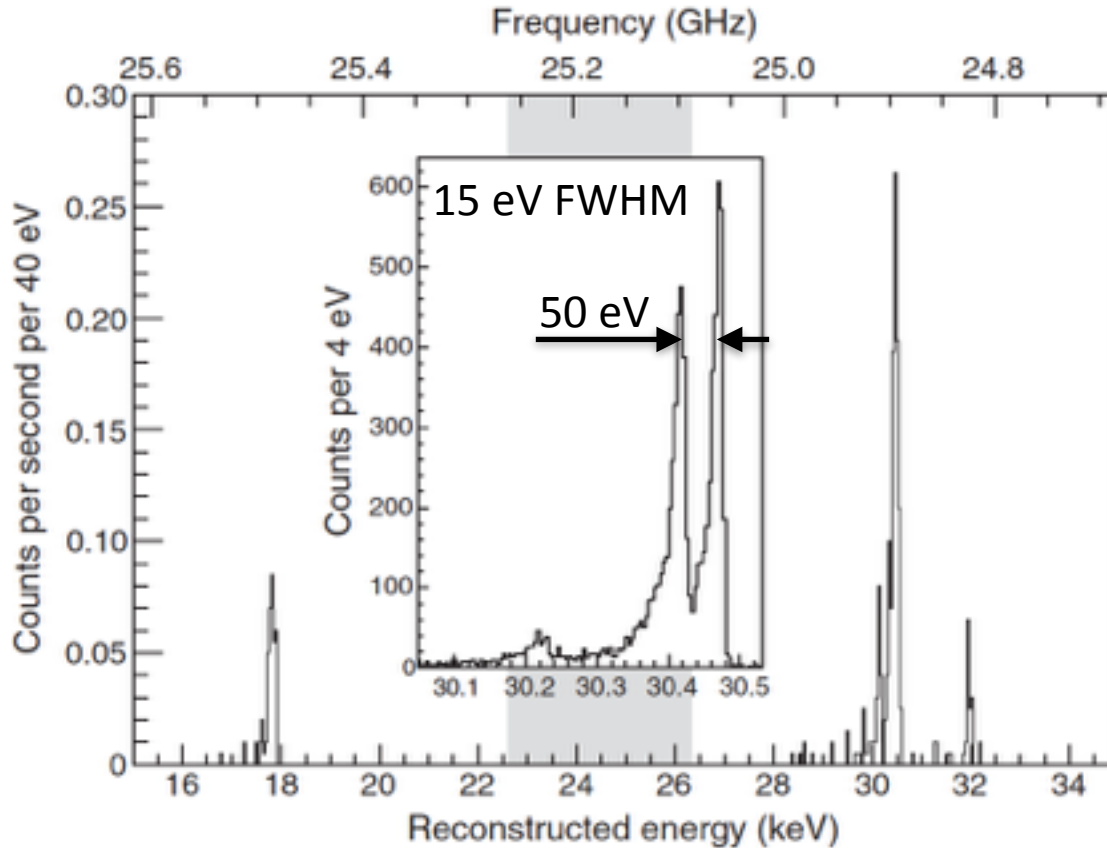


Asner et al., Physical Review Letters, 114, 162501 (2015)

A cyclotron radiation emission spectrum of ^{83m}Kr conversion electrons



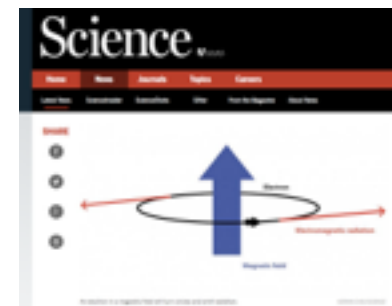
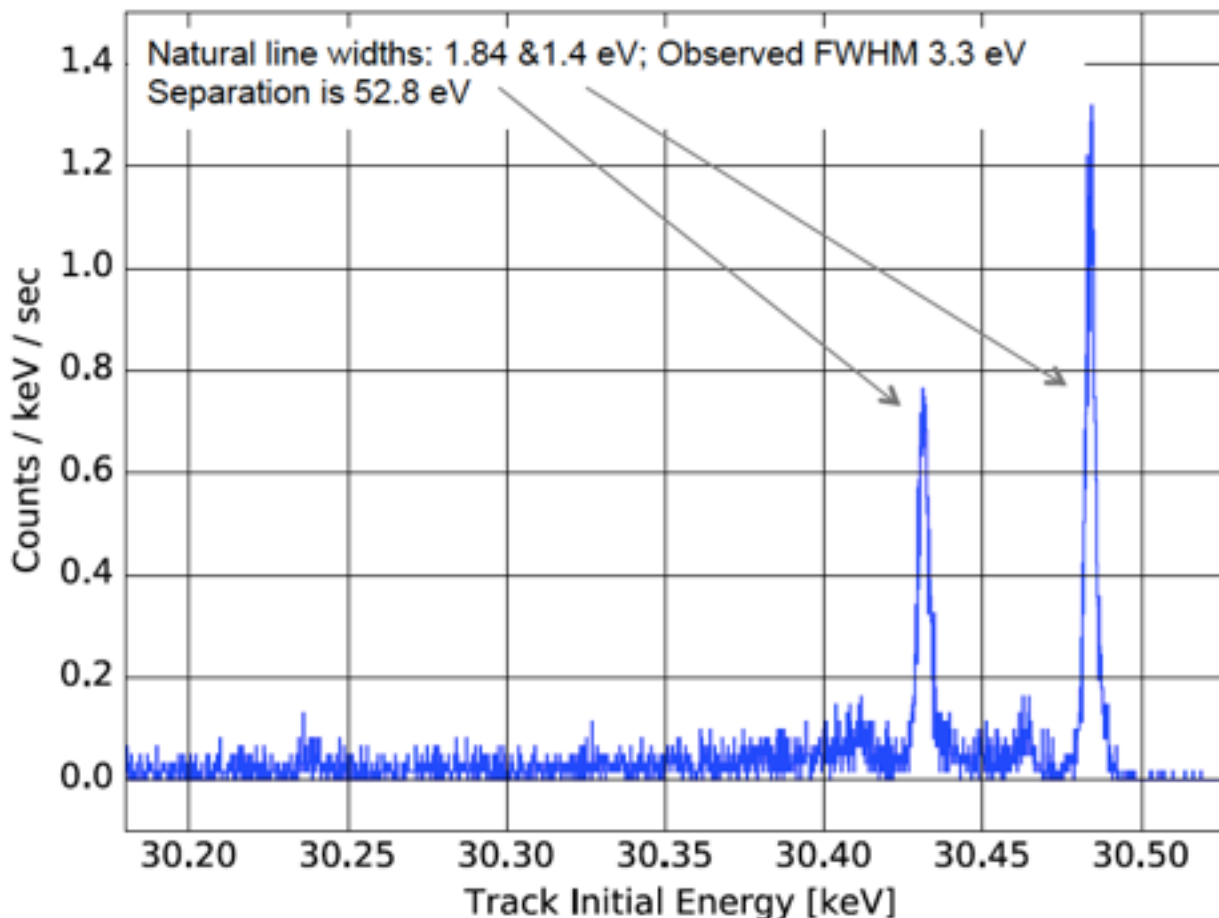
CRES spectrum of ^{83m}Kr conversion electrons

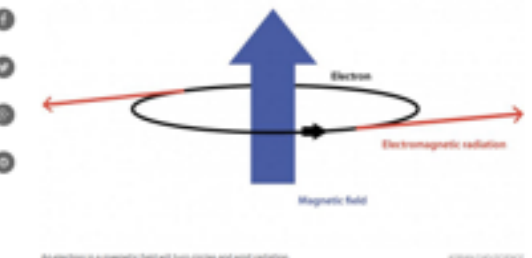


Asner et al., Physical Review Letters, 114, 162501 (2015)

CRES spectrum of ^{83m}Kr conversion electrons

Region of interest near the 30.4 keV lines
(bins are 0.5 eV wide)





Viewpoint

Cyclotron Radiation from One Electron

Patrick Huber*Center for Neutrino Physics, Virginia Polytechnic Institute and State University, Blacksburg, VA 24061, USA*

Published April 20, 2015

An electron's energy can be determined with high accuracy by detecting the radiation it emits when moving in a magnetic field.

Office of
Science[Programs](#)[Laboratories](#)[User Facilities](#)[Universities](#)[Funding Opportunities](#)[News](#)[About](#)

You are here: SC Home > Programs > NP Home > Science Highlights > 2015 > Project 8 Detects Individual Electrons by their Cyclotron Radiation

Nuclear Physics (NP)

[NP Home](#)

November 2015

Project 8 Detects Individual Electrons by their Cyclotron Radiation

New electron spectroscopy technique may lead to an improved neutrino mass determination.

QUICK STUDY

Ben Monroe is an assistant professor of physics at the University of California, Santa Barbara.



Single-electron cyclotron radiation

Benjamin Monroe

Experiments that track the radiation emitted by a lone electron orbiting a magnetic field may, in time, reveal the effects of neutrino mass.

In: *Physics Today* 69(1), 70 (2016)

НОВОСТИ

[Главная / Новости науки](#)

Циклотронное излучение открывает новые возможности для

29.04.15 | [Физика](#), [Игорь Иванов](#) | [Комментарии \(17\)](#)**facebook**[Sign Up](#)

Física de Materiais - UFU

June 23, 2015 · [@](#)Journal Club [@](#)

O Journal Club da próxima sexta-feira, 26 de Junho, às 11:30 no Anfiteatro do Bloco 1X, será apresentado pelo Prof. Ricardo Kagimura. Segue a referência:

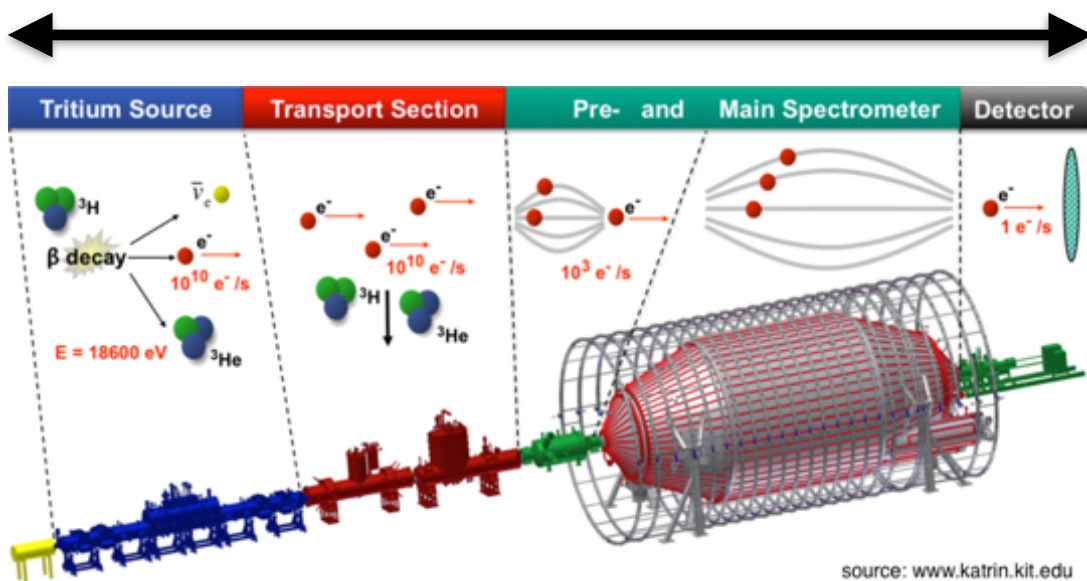
[Single-Electron Detection and Spectroscopy via Relativistic Cyclotron Radiation](#)

D. M. Asner et al.

[Phys. Rev. Lett. 114, 162501 \(2015\)](#)

Electrostatic spectrometer with magnetic adiabatic conversion (MAC-E) technique

70 m long, 10 m diameter vacuum tank



Tritium decays, releasing an electron and an anti-electron-neutrino. While the neutrino escapes undetected, the electron starts its journey to the detector.

Electrons are guided towards the spectrometer by magnetic fields. Tritium has to be pumped out to provide tritium free spectrometers.

The electron energy is analyzed by applying an electrostatic retarding potential. Electrons are only transmitted if their kinetic energy is sufficiently high.

At the end of their journey, the electrons are counted at the detector. Their rate varies with the spectrometer potential and hence gives an integrated β -spectrum.

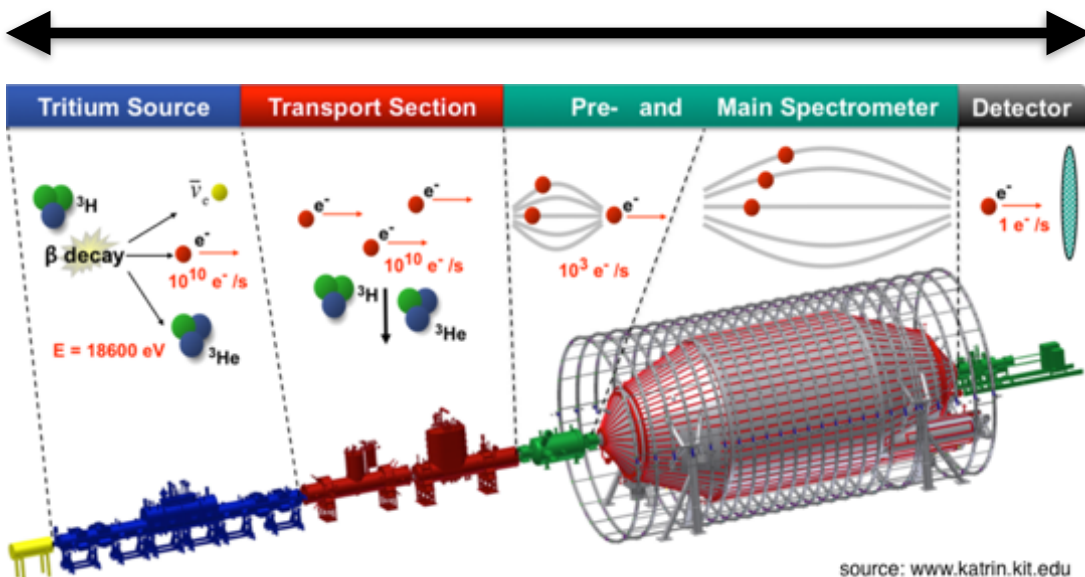
- Window less gaseous tritium source (10^{10} Bq)
- Molecular T_2
- Anticipated mass sensitivity: $< 200 \text{ meV}$ (90% CL)
- Resolution scales like the area of the analyzing plane

source: www.katrin.kit.edu

First light in October 2016, tritium operation starting in early 2017!

Electrostatic spectrometer with magnetic adiabatic conversion (MAC-E) technique

70 m long, 10 m diameter vacuum tank



Tritium decays, releasing an electron and an anti-electron-neutrino. While the neutrino escapes undetected, the electron starts its journey to the detector.

Electrons are guided towards the spectrometer by magnetic fields. Tritium has to be pumped out to provide tritium free spectrometers.

The electron energy is analyzed by applying an electrostatic retarding potential. Electrons are only transmitted if their kinetic energy is sufficiently high.

source: www.katrin.kit.edu
At the end of their journey, the electrons are counted at the detector. Their rate varies with the spectrometer potential and hence gives an integrated β -spectrum.

- Window less gaseous tritium source (10^{10} Bq)
- Molecular T_2
- Anticipated mass sensitivity: $< 200 \text{ meV (90\% CL)}$
- Resolution scales like the area of the analyzing plane

New technique needed for independent confirmation or to scale beyond MAC-E sensitivity

First light in October 2016, tritium operation starting in early 2017!

KATRIN: MAC-E-TOF

Neutrino mass sensitivity by MAC-E-Filter based time-of-flight spectroscopy with the example of KATRIN

Nicholas Steinbrink^{1,3}, Volker Hennen¹, Eric L Martin², R G Hamish Robertson², Michael Zacher¹ and Christian Weinheimer¹

New Journal of Physics 15 (2013) 113020 (29pp)

Received 6 August 2013

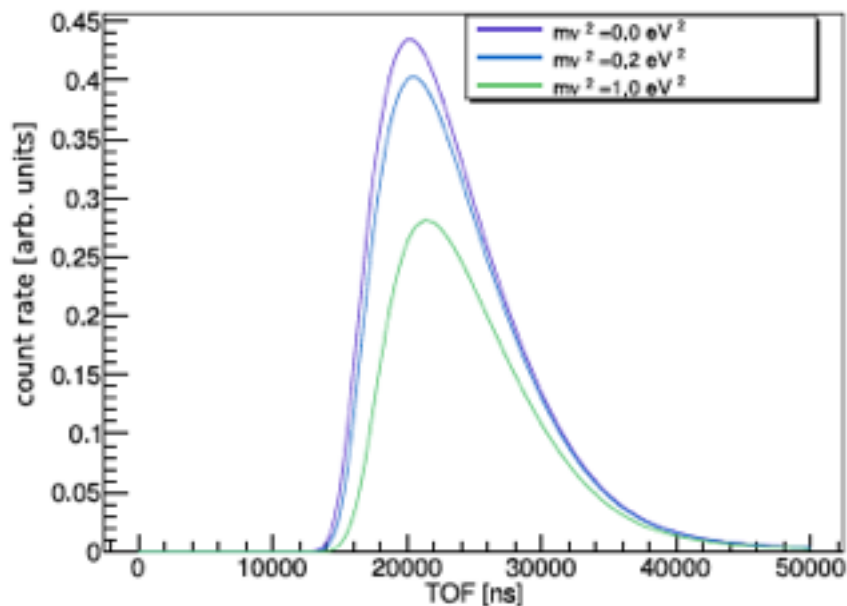


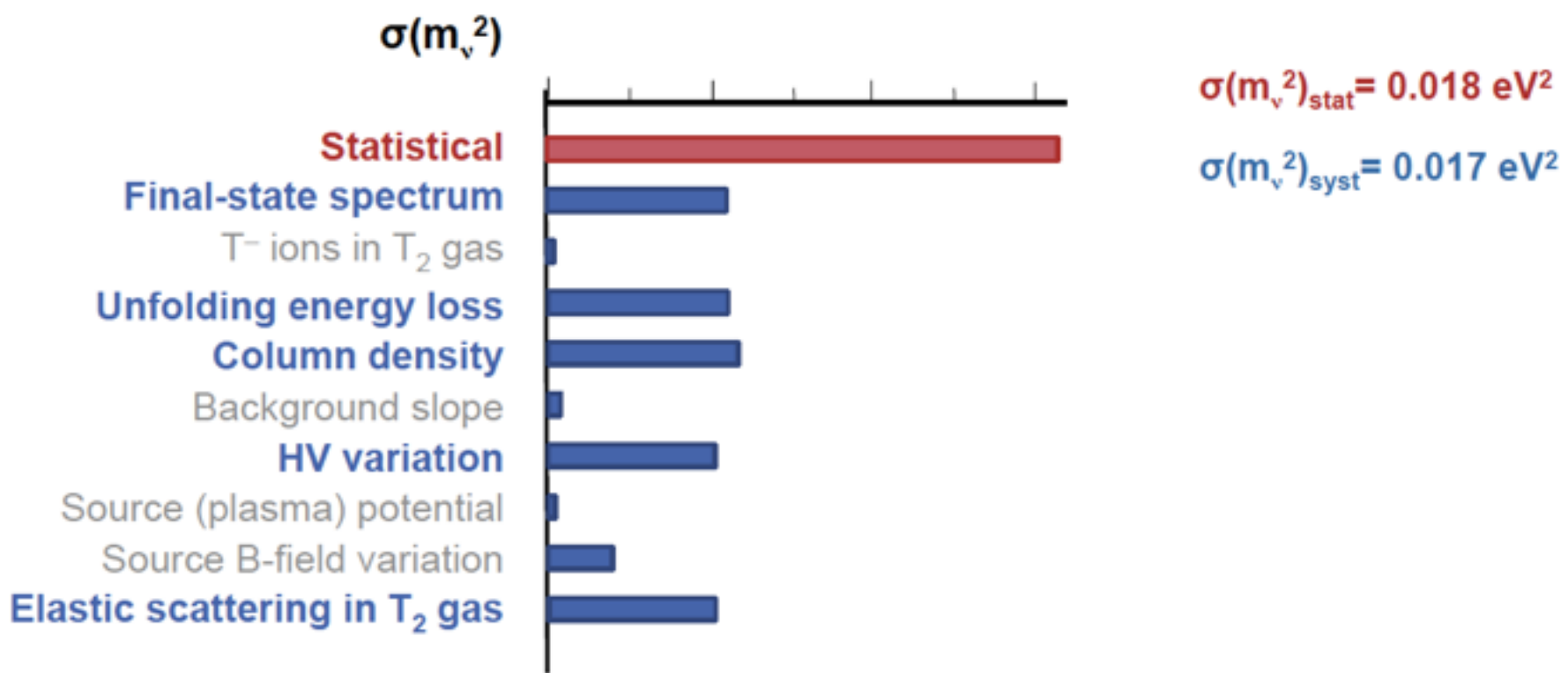
Figure 6. Effects on the TOF spectrum for different neutrino masses at a high retarding potential (18 570 eV) with endpoint $E_0 = 18\,574.0\,\text{eV}$. The scaling of the y-axis is arbitrary.

But requires individual electron tagging!

as a function of the measurement interval below the endpoint E_0 (difference between lowest retarding potential and the endpoint E_0 using $E_0 = 18.575\,\text{keV}$). Compared with the reference value of KATRIN, $\sigma_{\text{stat}}(m_{\nu_e}^2) = 0.018\,\text{eV}^2/c^4$ (see figure 13 curve (b) for measurement interval

of 30 eV), a statistical improvement of up to a factor 5 is possible in the optimal case (figure 13 (1)), equivalent to a factor of more than 2 in statistical sensitivity of m_{ν_e} . It can be shown (compare the difference in figure 13 between curves (b) and (c) w.r.t. point (2)) that this improvement factor is essentially not caused by neglecting the background but by intrinsic advantages of the method itself. A total improvement factor needs to take the systematics

The sensitivity reach of KATRIN



Kathrin Valerius, HEPHY Colloquium, Vienna, Jan 2016

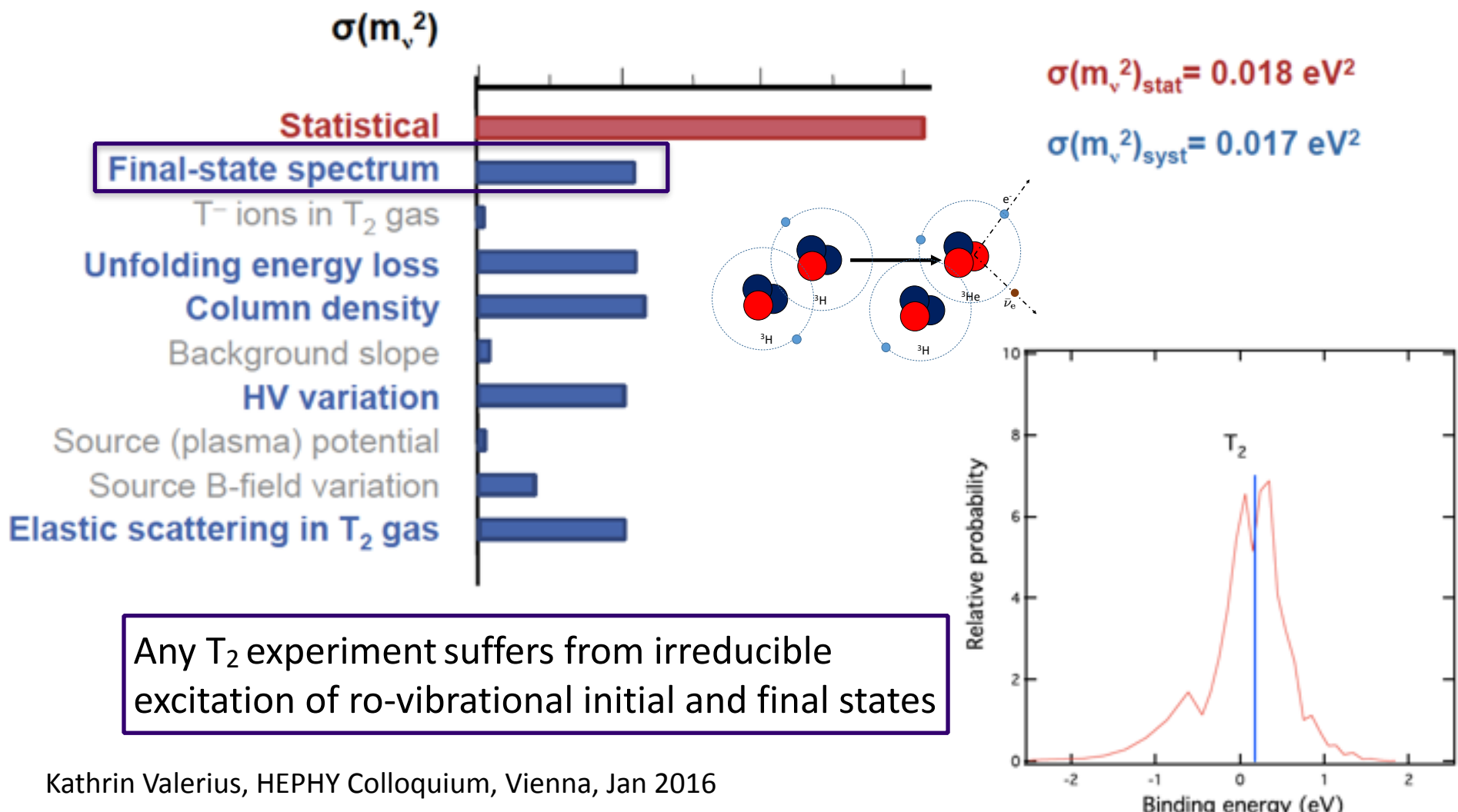
M. Fertl

Lexington 09/30/2016

UNIVERSITY of WASHINGTON

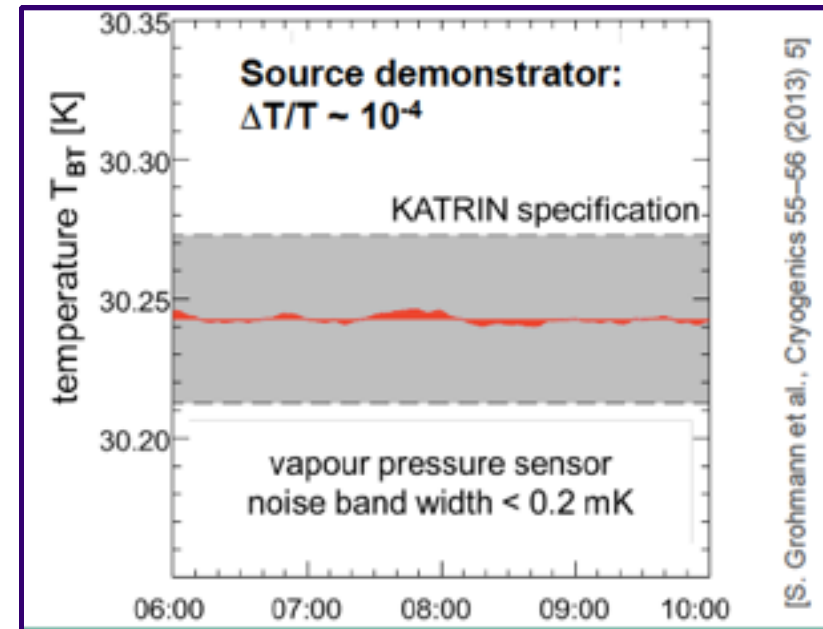
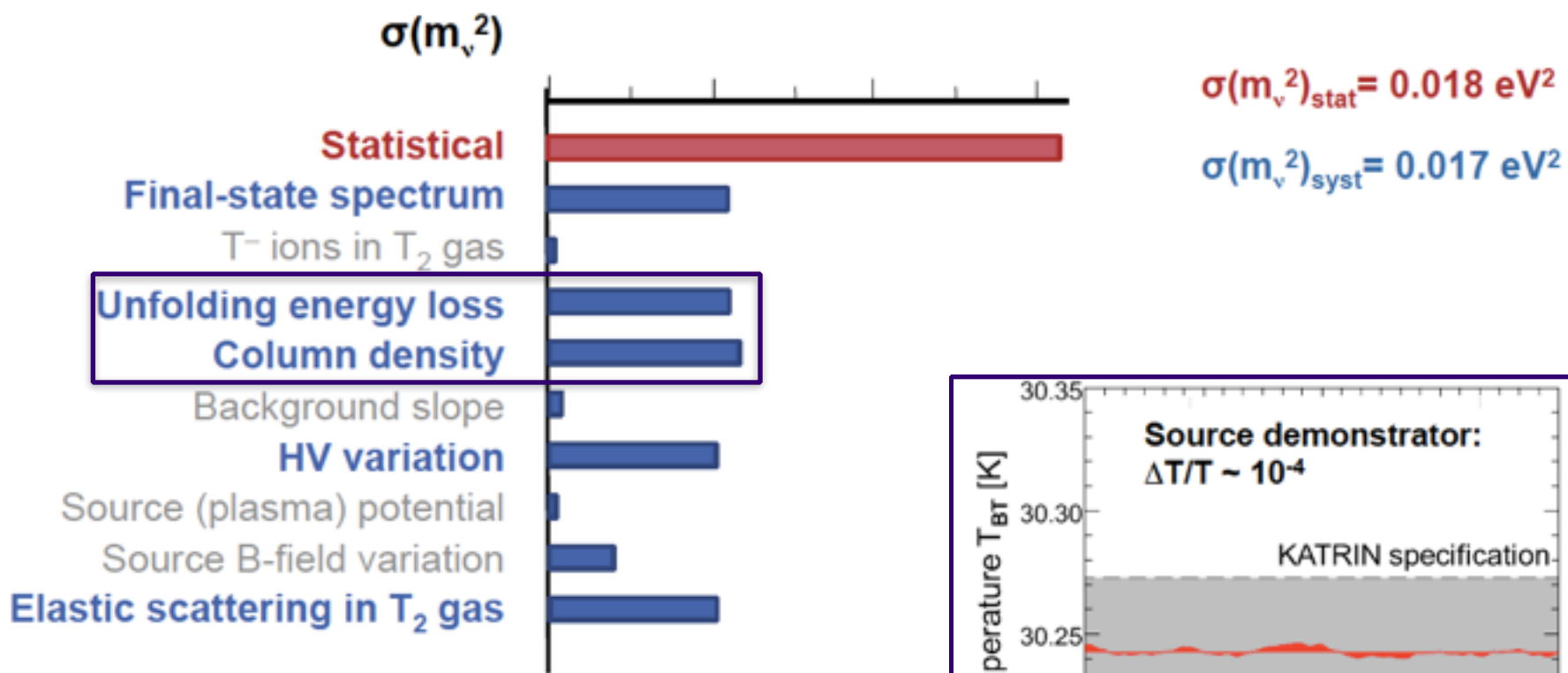
33

The sensitivity reach of KATRIN



Kathrin Valerius, HEPHY Colloquium, Vienna, Jan 2016

The sensitivity reach of KATRIN



Kathrin Valerius, HEPHY Colloquium, Vienna, Jan 2016

M. Fertl

Lexington 09/30/2016

UNIVERSITY of WASHINGTON

The sensitivity reach of KATRIN

